Assessment of NDE and Condition Monitoring Technologies for Defect Detection in Non-Metallic Pipe – Task 1 Report: Literature Review

EWI Project No. 59408GTH

March 31, 2022

Tom McGaughy
Sr. Technology Leader
Structural Integrity
EWI

Co-Authors

Roger Spencer, EWI
Lindsey Lindamood, EWI
Mark Lozev, NDE4Zero, LLC

EWI®
We Manufacture Innovation

Table of Contents

List of Figures

Executive Summary

This project was initiated in late October 2021 to evaluate several commercially available nondestructive examination (NDE) methods and techniques for detecting, characterizing, and sizing features, anomalies, and flaws in spoolable composite pipe (SCP) and reinforced thermoplastic pipe (RTP). The program scope of work is built on extensive laboratory-based inspection trials on numerous SCP and RTP pipe samples provided by several non-metallic pipe manufacturers as well as pipe samples removed from field service. The pipe sample matrix includes new, virgin pipe straight from the production line as well as virgin pipe that has intentionally induced damage or flaws to simulate expected field damage, and pipe removed from service containing an array of wear and tear features common to oil and gas field service operations. The controlled laboratory NDE inspections will allow for careful experimentation and evaluation of current state-of-the-art NDE methods and provide independent validation of NDE results.

This report documents work completed under Task 1 to survey recent published literature describing related research on the development and implementation of various NDE technologies on composite and polymer materials. The objective of this literature review was to identify recent advances in NDE methods, sensors or data analysis and signal processing that may be valuable for inclusion in this program. This report fulfills the deliverable objective of Task 1 under the project scope of work.

This review was carried out over four months leading to a collection of more than 200 abstracts with more than 70 papers and technical reports selected for review by the EWI project team. The focus of the review concentrated on inspection methods that included computed tomography (CT), ultrasonic testing (UT), microwave and thermography techniques where they were used on polymer or composite materials similar to those used in SCP and RTP pipe, whether they were monolithic or multi-material combinations.

Literature that specifically addressed inspection of SCP or RTP pipe was very limited. This implies that little to no research has been performed to date on these specific types of pipes, or at least very little has been publicly disseminated from any studies on NDE characteristics of these types of pipes. Regardless, numerous papers and reports did offer useful insight that will be considered in the development of the inspection procedures to be used in this program. The results of the literature review strongly indicate that there will be a need for multiple NDT methods to fully detect and characterize anomalies and damage in SCP and RTP pipe. The multi-layered structural composition of these pipes combined with the variety of types of damage and anomalies that can occur will likely require multiple NDE methods to be used to fully interrogate and quantify damage through an entire RTP or SCP pipe system. This report highlights specific attributes of various NDE methods that may have specific advantage for inspecting certain layers or regions of RTP and SCP pipe. These attributes will be investigated in the project tasks to be completed in 2022 and 2023.

Abbreviated Terms

ACUT	air coupled UT
AE	acoustic emission
AIRT	active infrared thermography
BF	butt fusion
CFRP	carbon fiber reinforced polymers
CR	computed radiography
CT	computed tomography
DDF	dynamic depth focusing
DOT	Department of Transportation
DR	digital radiography
DT	destructive testing
EF	electrofusion
FBH	flat bottom holes
FMC	full matrix capture
G	gain
GFRP	glass fiber reinforced polymer
GRE	glass reinforced epoxy
HAZ	heat affected zone
HDPE	high-density polyethylene
ID	inner diameter
IFOV	instantaneous field of view
IR	infrared
LOF	lack of fusion
LT	lock-in thermography
MW	microwave
MWIR	mid wave infrared radiation
NDE	nondestructive evaluation
NDT	nondestructive testing
NEdT	noise equivalent differential temperature
NMP	non-metallic pipe
OD	outer diameter
PAUT	phased array UT
PC	principal components
PCA	principal component analysis
PHMSA	Pipeline and Hazardous Materials Safety Administration
POD	probability of detection
PP	polypropylene
PSP	plastic-steel-plastic
PT	pulse thermography

PTFE	polytetrafluoroethylene
PWI	plane wave imaging
QC	quality control
RT	radiographic testing
RTP	reinforced thermoplastic pipe
S-	sectorial
SAR	synthetic aperture radar
SCP	spoolable composite pipe
SDH	side drilled holes
SF	saddle fusion
SNR	signal noise ratio
TFM	total focusing method
TOFD	time-of-flight diffraction
TRL	transmit-receive longitudinal
UHF	ultra-high frequency
UT	ultrasonic test
UWB	ultrawide band

1.0 Introduction

This report documents work completed under Task 1 to survey recent published literature describing related research on the development and implementation of various nondestructive examination (NDE) technologies on composite and polymer materials. The objective of this literature review is to identify recent advances in NDE methods, sensors or data analysis and signal processing that may be valuable for inclusion in this program. This report fulfills the deliverable objective of Task 1 under the project scope of work.

This project was initiated in late October 2021 to evaluate several commercially available NDE techniques for detecting, characterizing, and sizing features, anomalies, and flaws in spoolable composite pipe (SCP) and reinforced thermoplastic pipe (RTP). Project funding is provided by the U.S. Department of Transportation (DOT) Pipeline and Hazardous Materials Safety Administration (PHMSA) under Agreement No.: 693JK32110010POTA with in-kind support from ExxonMobil, Baker Hughes, Shawcor, and key contributions from NDE4Zero LLC as a subcontractor.

2.0 Background

Use of SCP and RTP is increasing in many onshore and offshore oil and gas applications such as in gathering lines, subsea flexibles, jumpers, water injection lines and risers. This is being driven by increased availability of SCP and RTP having greater temperature and pressure operating limits, and larger pipe sizes that can increase the economics of non-metallic pipe as a viable alternative to traditional steel pipe. To safely utilize these pipes in more aggressive environments and as a potential replacement for applications where steel pipe has been widely used, limitations in inspection and condition monitoring techniques and knowledge of damage modes and tolerance limits must be addressed.

While SCP and RTP manufacturers have a good history of producing quality products that have served the industry well for many years, increasing use of and implementation of these types of pipes in more demanding applications will require more rigorous engineering knowledge of and methods for quantifying the condition of these pipes and predicting their serviceability limits. However, limited capability currently exists for NDE of these pipes either as a manufacturing quality control (QC) tool or to assess in-service condition. This presents a significant gap to the development and implementation of robust engineering assessment methodologies and limits expanding use of these types of non-metallic pipe (NMP). Completion of this research effort will provide a critical foundation for the development of robust safety and integrity assessment methods for NMP. This project is focused on addressing defect and anomaly detection technologies as input to determining maximum operating pressure and predicting service life limits.

Description of SCP and RTP Pipe

Both SCP and RTP pipe are composite pipe in that they are produced using different materials that are layered within the wall of the pipe. They are manufactured in long continuous lengths that are spooled for transport and storage. SCP and RTP pipe can be produced in continuous lengths up to 5,000 feet or more. They typically have three distinct layers characterized by an inner liner designed for fluid or gas flow and containment, a reinforcing layer that wraps around the inner liner that forms the primary resistance to stresses due to pipeline pressurization, and an outer jacket that protects the reinforcement layer from abrasion and wear during pipeline installation, ultraviolet rays (if the pipeline is left exposed on the ground), and potential damage due to typical service conditions (i.e., isolate the reinforcement from water, rock impingement, soil-corrosion interactions, etc.). The outer jacket also protects the reinforcement and inner liner at locations where metallic connectors are installed onto the pipe.

Both types of pipes typically have a high-density polyethylene (HDPE) inner liner and outer jacket, although depending on design service conditions other inner liners such as nylon or polyamide can be used for higher temperature or corrosive service conditions. SCP pipes have a reinforcement layer made of glass fibers encased in a thermosetting epoxy resin matrix with the reinforcement layer bonded directly to the inner liner using an adhesive. Thus, the reinforcement layer is structurally connected to the inner liner. RTP pipes may have several types of reinforcement ranging from glass fiber strands wound over the inner layer with no resin matrix, or they may use thin steel strips or tape, steel wire or other composite fiber windings. The reinforcement layer in RTP pipe is unbonded and therefore the inner layer and reinforcement layer can slide relative to each other depending on loading conditions.

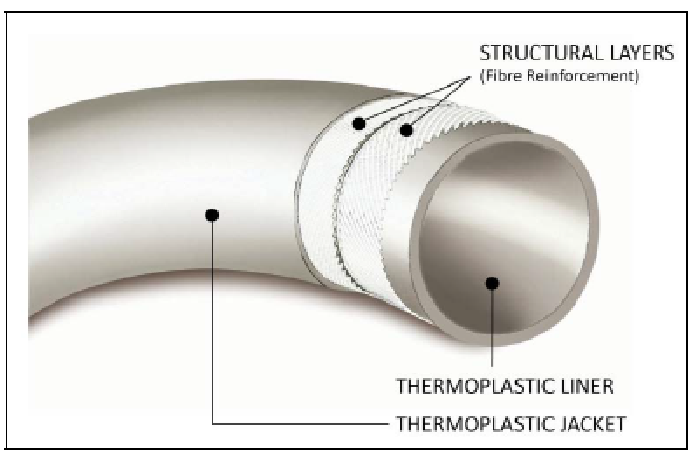

Figure 1. General construction of SCP and RTP pipe (from Tatarov & Gareau 2014)

Figure 2. Image of the FlexFlow SCP pipe construction (Courtesy Shawcor website)

The SCP and RTP pipes evaluated in this program have a design temperature and maximum allowable operating pressure of at least 180°F and 2200 psi, respectively. They can be manufactured in pipe diameters of NPS 2 in. to NPS 8 in.

Typical Applications of SCP and RTP:

- High-pressure water injection pipelines
- Water transport and distribution
- Effluent water disposal
- Temporary surface lines
- Oil and gas flow- and gathering lines
- (Domestic) Gas pipelines
- Multi-phase pipelines
- Well intervention
- Landing/export lines

(a) Reeled pipe ready for installation **(b) A connector joining two spools of pipe**

Figure 3. Spoolable pipe in the field (from CAPP 2017)

<u>Outline of Project Scope</u>

The program scope of work is built on extensive laboratory-based inspection trials on numerous SCP and RTP pipe samples provided by several non-metallic pipe manufacturers as well as on pipe samples removed from field service. The pipe sample matrix includes new, virgin pipe straight from the production line as well as virgin pipe that has intentionally induced damage or flaws to simulate expected field damage, and pipe removed from service containing an array of wear and tear features common to oil and gas field service operations. The controlled laboratory NDE inspections will allow for careful experimentation and evaluation of current state-of-the-art NDE methods with independent validation of NDE results.

The inspection methods to be used in this program include:

- Computed Tomography (CT)
  - Used as the referee method combined with selective destructive sectioning
- Ultrasonic test (UT) method and techniques
  - Air-coupled technique
  - Conventional single element technique
  - Time-of-flight diffraction (TOFD) technique
  - Phased array UT (PAUT) technique
  - Full matrix capture/total focusing method (FMC/TFM) technique
- Microwave
- Thermography method and techniques
  - Flash thermography technique
  - Equivalent wave thermography technique

The pipe matrix for the program includes virgin pipe straight from the production line and virgin pipe with intentional damage provided by each pipe manufacturer contributing to the program, and field-used pipe from one or more operators. Inspection activities will characterize anomalies and damage to the outer jacket, reinforcement layer, inner liner and the interface between pipe and connector. The type of features, anomalies, and damage to be examined in the program include:

- Punctures
- Tears or cracks
- Gouges
- Kinks
- Crush damage (ovality anomalies and damage to inner liner and reinforcement)
- Overloading of the reinforcement, including reinforcement failure
- Disbonding or delamination of SCP reinforcement and inner liner layers
- Pipe damage at connectors (i.e., cracks, gouges, tears, over compression of the pipe during installation, etc.)
- Inner liner erosion

Expected outcomes from this effort include:

1. Understanding the capability of current NDE tools for quantifying the condition of SCP and RTP pipe, including detection, characterization, and sizing accuracy.
2. Development of a best practice guide for implementing selected NDE methods as an in-plant pipe manufacturing quality assurance – quality control tool.
3. Better understanding of the NDE tools and methodologies that would be needed for field in-service inspection of SCP and RTP pipe.

The initial activity in this program is a survey of publicly available technical literature from recent research on the development and application of various NDE methods for inspecting a wide range of polymer and composite materials. Potential insights gained from these corollary research initiatives may offer value to this program in fine-tuning the inspection methodologies, sensors, and data analysis approaches to be used in the upcoming laboratory NDE trials.

This report documents the activities and findings of that literature review task.

3.0 Objectives

Overall program objectives include:

1) Evaluate selected NDE methods for detecting and sizing pipe body and pipe-to-connector defects, damage, and anomalies in SCP and RTP pipes.
2) Develop NDE inspection guidelines for new SCP and RTP pipe production QC methods and identify requirements for in-service field inspection.
3) Characterize inner liner erosion performance and NDE detection of in-service erosion damage.

4.0 Literature Review Process

Numerous sources were used to identify and collect relevant research papers, project reports, and other public-domain materials describing development and application of various NDE methods for inspecting a range of polymer and composite materials. Sources included: two large electronic databases that contain more than 40 million global abstracts for materials science and engineering publications, the PHMSA website to gather publicly available published reports and other project files for related NDE projects funded by PHMSA, and EWI's collection of published papers, journal articles and other publicly disseminated materials – published by EWI and other journal and conference sponsoring organizations such as ASME, ASNT, etc. under EWI authorship.

This effort extended over four months leading to a collection of more than 200 abstracts with more than 70 papers and technical reports selected for review by the EWI project team. The focus of the review was concentrated on the inspection methods to be used in this program (various CT, UT, microwave and thermography techniques) where they were used on polymer or composite materials similar to those used in SCP and RTP pipe, whether they were monolithic or multi-material combinations. Literature that specifically addressed inspection of SCP or RTP pipe was very limited. This implies that little to no research has been performed to date on these specific types of pipes, or at least very little has been publicly disseminated from any studies on NDE characteristics of these types of pipes. Regardless, numerous papers and reports did offer useful insight that will be considered in the development of the inspection procedures to be used in this program.

5.0 Brief Overview of NDE Methods of Interest to this Program

For readers unfamiliar with NDE techniques, this section provides a very basic description of the underlying principles employed in the NDE methods and techniques to be used in this program along with a list of advantages and disadvantages of each technique. Readers having more in-depth NDE knowledge may wish to move to Section 6.

The Objective of NDE Test Methods and Techniques

Nondestructive testing (NDT) involves the application of NDE methods and techniques to quantify the condition of a material or component without destroying, cutting, or otherwise physically altering the object being investigated. Thus, NDT/NDE testing uses noninvasive techniques to determine the physical condition of a component or structure or to quantitatively measure certain physical characteristics of an object. A wide variety of NDE methods exist, but the most common use ultrasound, radiography, eddy current, thermal and acoustic emission methods, supplemented by less sophisticated methods such as visual and dye penetrant testing, which can only characterize surface features.

A basic description of the underlying principles of the NDE techniques to be used in this program follows.

Principles of X-Ray Computed Tomography (CT) Methods

Computed tomography is a radiographic NDT technique used to locate and size internal features of a part in three dimensions. CT scanning was first developed and deployed in the medical field in the 1970's. Since then, it has evolved for use in numerous industrial applications, including NDT/NDE testing of materials. CT methods use x-rays to penetrate an object from which the density of the material at any location can be measured. Defects, anomalies, and other features cause a local change in material density, which changes how the x-rays are absorbed as they pass through those features.

A CT scan consists of a large number of 2D scans or images taken through the material, which when merged together form a 3D picture of the internal structure. Once these images have been reconstructed using sophisticated computerized methods, the structure of the part can be viewed through "virtual slices" taken through the object in any direction, allowing the internal structure, features, and flaws to be visualized and measured.

Principle of Ultrasonic Test (UT) Methods

While several approaches for implementing UT inspection exist, they are all based on the principle of exciting high frequency sound waves (i.e., ultrasound waves) into the material or part to be inspected. An ultrasonic wave is a mechanical vibration or pressure wave similar to audible sound, but with a much higher vibration frequency. For NDT purposes, the range is usually from 1 MHz to 30 MHz.

Special sensors called transducers or probes generate the ultrasonic sound wave and impart the wave into the couplant and testing material or directly into the material. The ultrasound wave moves along and through the material and is reflected when the wave hits a surface, such as the back edge of the component, or a defect embedded somewhere in the material. These features cause the sound wave to change direction and/or speed or intensity, and sensors placed on the test part can detect these changes in the sound wave propagation. Depending on the test requirements, these waves can be highly directional and focused on a small spot or in a thin line or limited to a very short distance. Thus, UT test techniques can be specifically tailored for characterizing the condition of a component based on what features are being sought or for the type of material and/or geometry of the part being inspected.

Principle of Thermography Test Method

Thermography NDE methods are based on the principle of generating a rapid heating of the surface of the material or part being inspected to produce a moving “thermal wave” in the material. This is often called infrared (IR) thermography. As the temperature of the part is increased, it gives off electromagnetic radiation – thermal radiant heating – which all heated objects will do.

Infrared thermography is the process of using a thermal imager to detect radiation (heat) coming from an object, converting it to temperature and displaying an image of the temperature distribution. Images of the detected temperature distribution are called thermograms, and they make it possible to see heat-producing objects invisible to the naked eye. Physical defects and anomalies in the inspected part localize the heat allowing for detecting and sizing of these features.

Principle of Microwave Test Method

Similar to thermography methods, microwave inspection involves the generation of electromagnetic waves into a part, but at the microwave frequency realm. In microwave testing, the microwaves move through and interact with the part based on the dielectric properties of the material. Defects and anomalies cause the microwave to be reflected based on the size, location, and orientation of these features. Special sensors can monitor how the microwaves are influenced by these features in the part and allow determination of defect size among other physical characteristics.

A list of advantages and disadvantages of these NDE methods and techniques is given below. Consideration of these advantages and disadvantages are important when planning NDE trials and defining the inspection protocols that should be used.

X-ray computed tomography (CT):

Advantages:
- Detection of small flaws
- 3D viewing of parts and components
- Accurate measurements of internal flaws and part features
- Data files for measurement and retention purposes

Disadvantages:
- Slow
- Limited part size and geometry
- Requires access to both sides of pipe
- High equipment cost
- Large data file sizes
- Not portable for field use

Ultrasonic testing (Air Coupled)

Advantages:
- No couplant needed
- Good inspection speed
- Scan data files can be easily obtained

Disadvantages:
- Low portability
- Pitch-catch probe arrangement required
- Fixturing required to accurately align probes
- Dead zones at inner diameter (ID) and outer diameter (OD) surface

Ultrasonic testing (Conventional – single element)

Advantages:
- Widely used
- Equipment readily available
- Relatively low equipment cost
- Portable
- Good inspection speed
- Good resolution

Disadvantages:
- Couplant needed
- Typically used for manual scanning with no data file

Ultrasonic testing (Time-of-flight-diffraction (TOFD))

Advantages:
- Widely used primarily for weld inspection

- Equipment readily available
- Relatively low equipment cost
- Good inspection speed
- Good resolution
- Data file acquisition possible if encoded scanner is used

Disadvantages:
- Couplant needed
- Not good for near (OD) surface detection
- Pitch-catch probe arrangement required
- Fixturing required to accurately align probes

Ultrasonic testing (Linear phased array)

Advantages:
- Widely used
- Equipment readily available
- Portable
- Good inspection speed
- Good resolution
- Electronic beam scanning, steering, and focusing
- Data file acquisition possible if encoded scanner is used.

Disadvantages:
- Couplant needed
- Equipment cost approx. 5x higher than conventional UT
- Electronic beam scanning, steering, and focusing in one plane only

Ultrasonic testing (2D matrix phased array)

Advantages:
- Equipment availability somewhat limited
- Portable
- Good inspection speed
- Good resolution
- Electronic beam scanning, steering, and focusing in multiple planes
- Data file acquisition possible if encoded scanner is used.

Disadvantages:
- Couplant needed
- Equipment cost approx. 8x higher than conventional UT

Ultrasonic testing (Full matrix capture/total focusing method - plane wave imaging)

Advantages:
- Equipment availability somewhat limited
- Portable

- Good penetration in non-metallic materials
- Good inspection speed
- Good resolution
- Focusing at the receiver
- Data file acquisition possible if encoded scanner is used

Disadvantages:
- Couplant needed
- Equipment cost approx. 8x higher than conventional UT

Thermography

Advantages:
- Good inspection speed
- Data images or videos for record retention
- Detection of subsurface changes in thermal conductivity
- Measure emissivity variations at the surface
- Can be non-contact method
- Inspection area is limited by camera (large areas can be inspected at once)
- Sensitive to delamination

Disadvantages:
- Emissivity differences can affect detection and repeatability
- Environmental factors such as temperature and humidity could affect results.
- Sensitive to surface reflections
- Defect size detection limited by special resolution of lens and distance from target
- Heat source may be directional – limited for use with flat surfaces

Microwave

Advantages:
- Good inspection speed
- Contact with component not necessary
- Portable
- Capable of detecting thickness of individual layers
- Good detection of impact damage
- Non-contact

Disadvantages:
- Microwaves do not penetrate conductors or graphite composites
- Defect detection is orientation dependent

6.0 Key Findings from Literature

Highlights of relevant NDE research and notable findings from the literature review are summarized below. Some details and sources of literature reviewed are not included in this discussion. However, the most pertinent findings are discussed along with summaries of related research efforts that have particular relevance to this program. The discussion is organized by material type and includes key points found about the target NDE inspection methodologies in this program, which includes various UT methods, followed by microwave and thermography.

Overview of NDE Methods and Materials

More than 70 individual published papers and technical reports were collected for this review. A sizeable body of research exists for inspection of monolithic HDPE pipe and associated fusion welds, with limited research material available for inspection of SCP and RTP pipe. Inspection methods for monolithic HDPE pipe has relevance to this program considering that most SCP and RTP pipe has an inner liner and outer jacket consisting of monolithic HDPE. Several research papers were collected that describe developments for NDE inspection of various composite panels. A variety of composite materials and matrices are included. This research could help inform inspection practices that may be useful for SCP and RTP reinforcement layers and for inspecting through either the inner liner or outer jacket to interrogate the reinforcement layer. In addition, many of the research papers on NDE of composite materials address detection of damage similar to that expected in SCP and RTP pipe. For example, reinforcement filament or fiber damage and disbondment between the reinforcement and inner liner are likely to have similar characteristics to damage and disbondment in a wide assortment of other composite and multi-layered materials.

Collectively, this body of literature does provide some insights as well as limitations that are likely to be encountered in this program as NDE methods are applied to the inspection of SCP and RTP pipe.

The collected literature base describes research covering the following NDE techniques and materials or applications.

1. HDPE pipe and fusion welds (electrofusion, butt fusion and saddle fusion joints)
    a. NDE methods: UT and PAUT, TOFD, FMC/TFM techniques
2. SCP and RTP pipe
3. Filament-wound glass reinforced epoxy pipe
    a. NDE Method: UT
4. Adhesively bonded couplings
    a. NDE method: UT

5. Carbon fiber reinforced polymers
    a. NDE methods: UT and microwave
6. Glass fiber reinforced polymer (GFRP) panels
    a. NDE methods: UT and air coupled UT (ACUT) technique; IR and active infrared thermography (AIRT) technique
7. Filament wound glass epoxy composite pipe
    a. NDE method: ACUT

Key findings based on material or application are summarized below.

<u>Key Findings from Recent Research on HDPE</u>

Over the last 15+ years, ultrasonic inspections of simple high-density polyethylene (HDPE) pipe used in the gas distribution industry have advanced with a focus on evaluation of the pipe base material, electrofusion (EF) lap, butt fusion (BF), and saddle fusion (SF) joints (welds). Much of this research centered around phased array ultrasonic testing (PAUT), which was pioneered and used with promising success during an open trial to detect and visualize defects in electrofusion lap joints in HDPE as reported by Lozev et al. 2005. Figure 4 shows fused and unfused areas in EF joints that were part of this study.

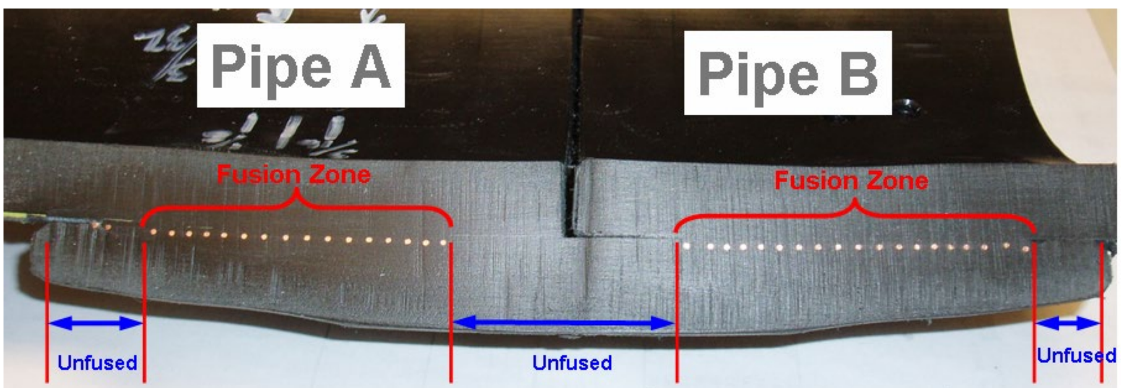

Figure 4. Fusion Zones of Typical EF Joint

To minimize the effects of beam skew and velocity variations in the joint, a linear PA probe was used. Several PAUT probes were used in a pulse-echo mode to transmit and receive high-frequency longitudinal waves in the joints. Electronic scanning and focusing, using PAUT principles to obtain B-scans and sectorial (S-) scans, were deployed to ensure complete weld volume inspection, even in the presence of unpredictable beam skew. The use of dynamic depth focusing (DDF) minimizes the noise due to the EF joint structure, improves the imaging of the flaws and allows easier interpretation of the scan results. Artificial flaws were implanted in the welds using Kapton® tape, aluminum and steel foils, pipe compound and light dirt. These features were detected using 7.5- and 5-MHz PA ultrasonic probes. Test samples were destructively sectioned to validate the PAUT results. Figure 5 shows the PAUT setup while Figure 6 illustrates the effectiveness of PAUT for imaging a joint containing intentional dirt to produce incomplete fusion.

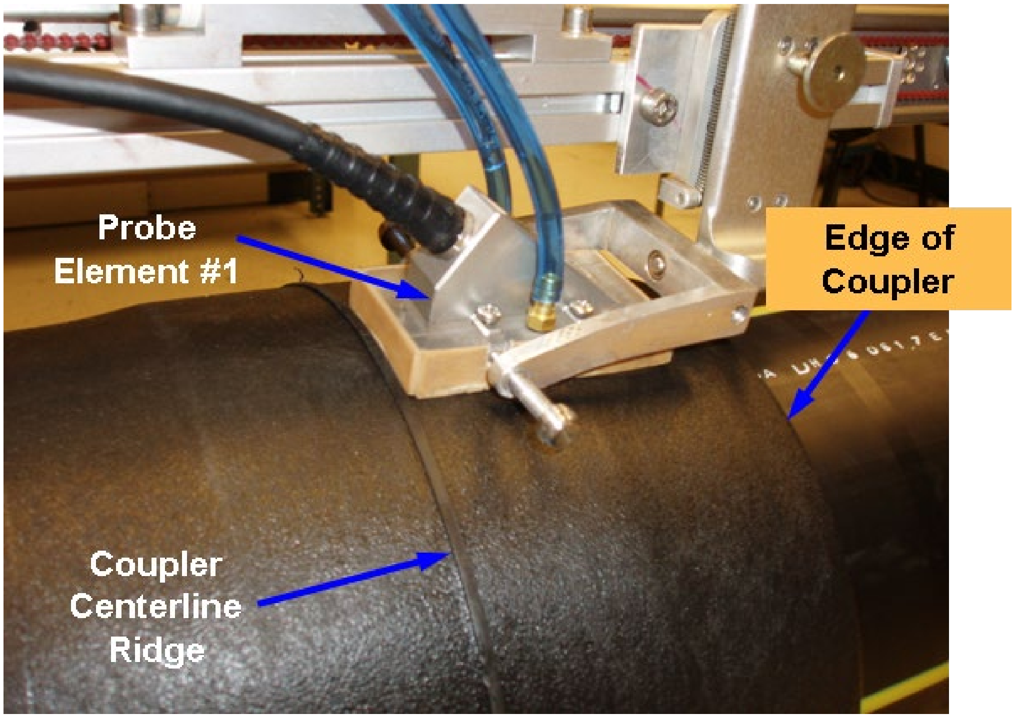

Figure 5. PAUT Inspection Setup

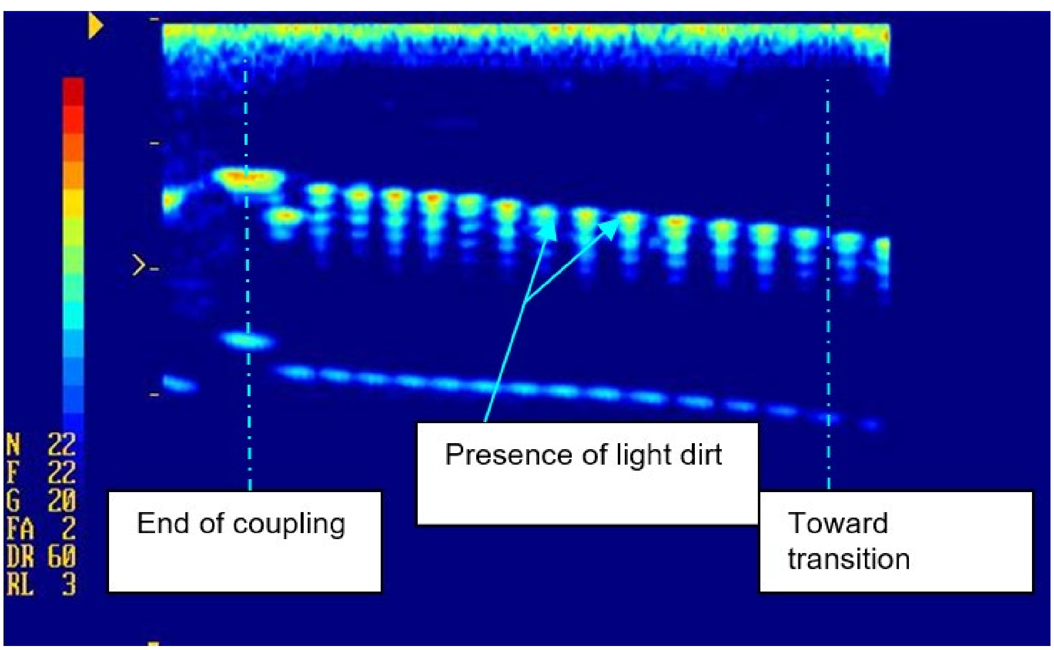

Figure 6. PAUT Images of Detected Implanted/Seeded Light Dirt

Test samples were destructively sectioned and good agreement between PA and destructive testing (DT) was achieved. However, it was found that simulated flaws in the welds such as oil contamination, angular misalignment of the joint and poor joint quality associated with no joint edge scraping or cleaning of the pipe surface were not detectable with PA technology. Ultrasonic measurements of the flaw size in the longitudinal direction of the pipe were achieved with reasonable accuracy but in the circumferential direction, sizing was not possible without encoders.

The phased array technique has been specifically optimized for the reliable detection of lack of fusion, lack of penetration and voids in HDPE electrofusion joints as described by Caravaca et al. 2007. An ultrasonic prototype was developed to provide inspection of electrofusion couplers. Also, an ultrasonic method was developed to determine whether the weld heating cycle was applied correctly to the electrofusion joint. The results of the extensive laboratory experiments and the field application of a prototype system were presented.

Ultrasonic modeling and simulations were conducted to support advanced engineering applications of PAUT for inspection of HDPE BF and SF joints as reported by Lozev and Spencer 2007, and Lozev and Spencer 2008. Ultrasonic simulation and virtual optimization work was based on a two-step, semi-analytical approach using a software package for processing, imaging, and simulating ultrasonic data. Figure 7 provides a schematic of the setup approach.

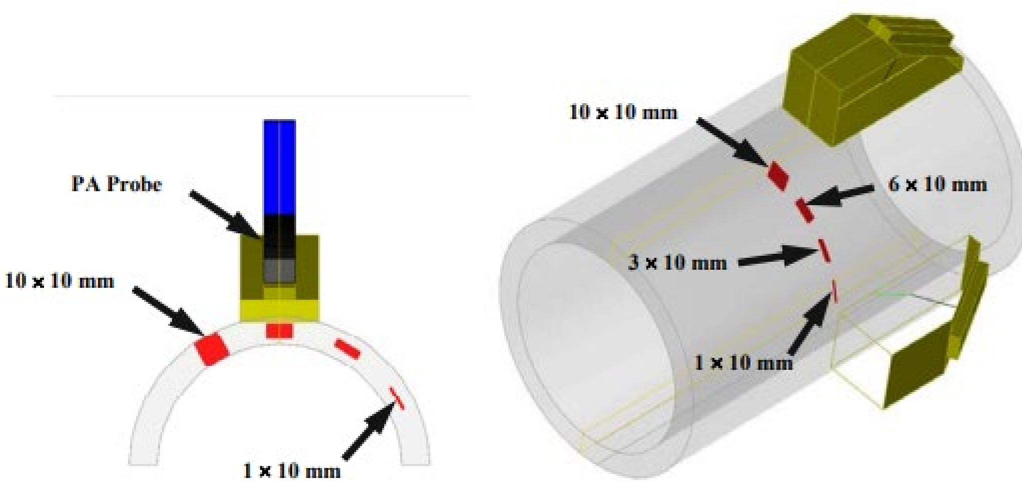

Figure 7. PAUT BF Interaction Model

The simulation results were successfully validated using an optimized PAUT procedure during an open trial on PE BF joints with implanted and natural flaws. Figure 8 shows pipe cross-sectional views indicating the type and location of some flaws.

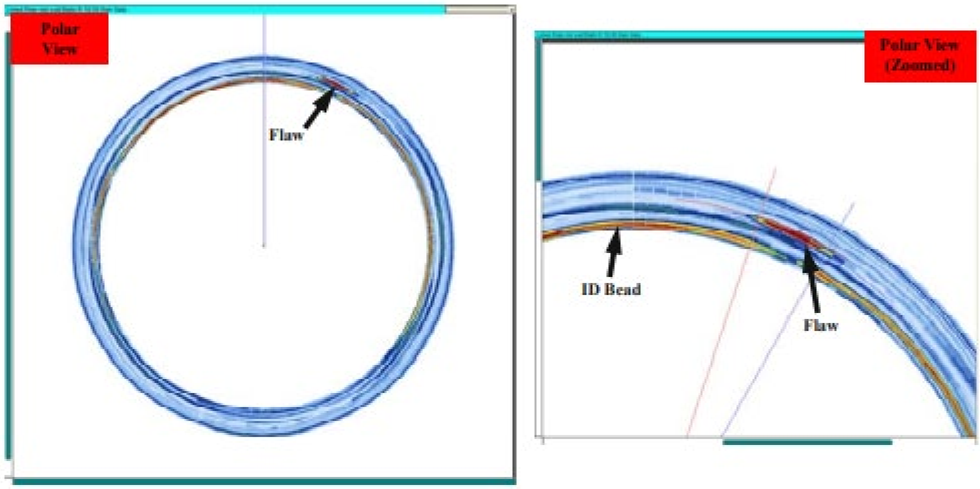

Figure 8. PAUT Polar View Imaging of Flaw in BF joint

The detection and sizing capabilities of current state-of-the-art phased-array PAUT techniques were defined for NDE of EF, BF, and SF joints in HDPE gas distribution pipelines as reported by Lozev et al. 2008. Figure 9 illustrates some of the PAUT techniques used in this study.

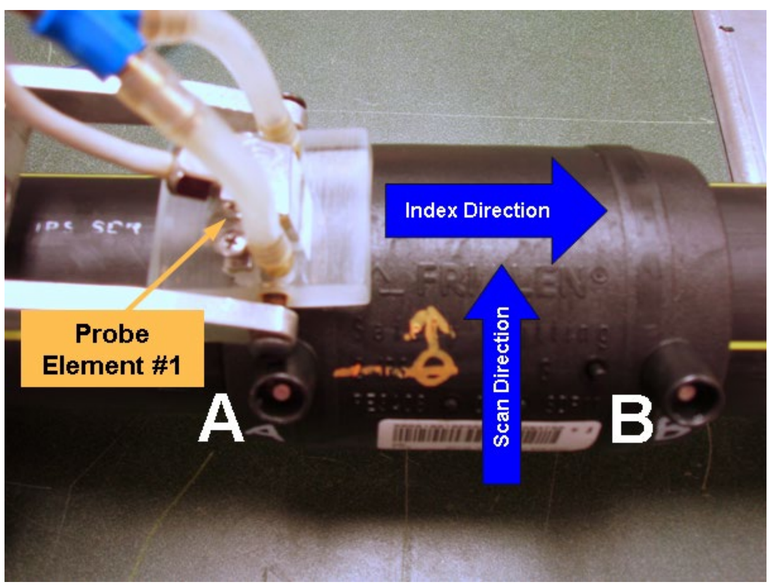

a)

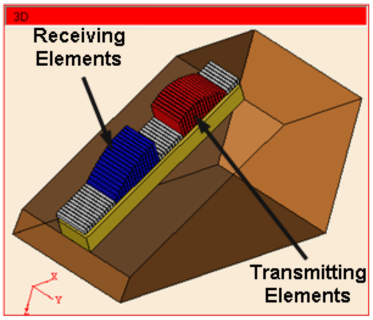

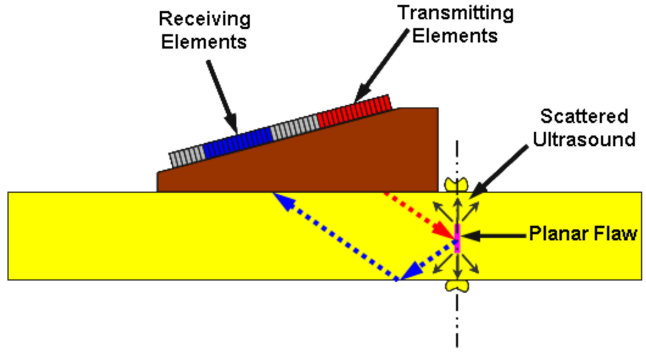

b)

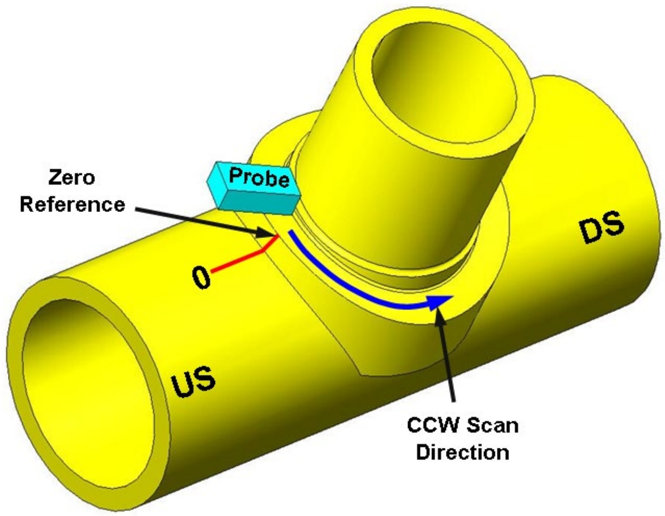

c)

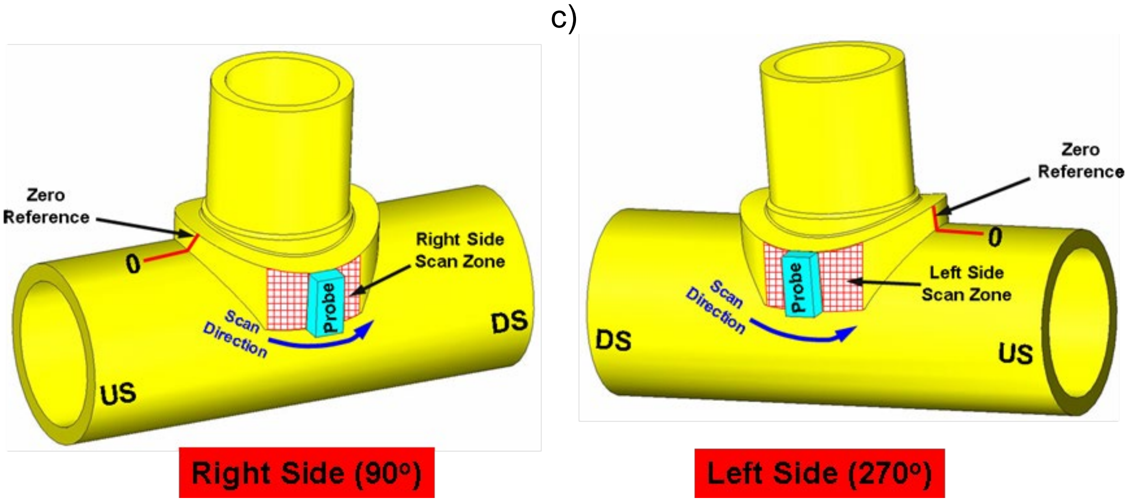

d)

Figure 9. PAUT Techniques: a) Focused and Steered Normal Beam for horizontal/parallel Planar flaw detection; b) Tandem for Vertical Planar Flaw Detection; c) Focused and Steered Normal Beam for Planar horizontal/parallel flaw detection in SF joints from the rim; d) Focused and Steered Normal Beam for Vertical Planar flaw detection SF joints from the side.

PAUT flat bottom hole calibration approaches and scans illustrating several types of flaws in EF weld joints are shown in Figure 10 and Figure 11.

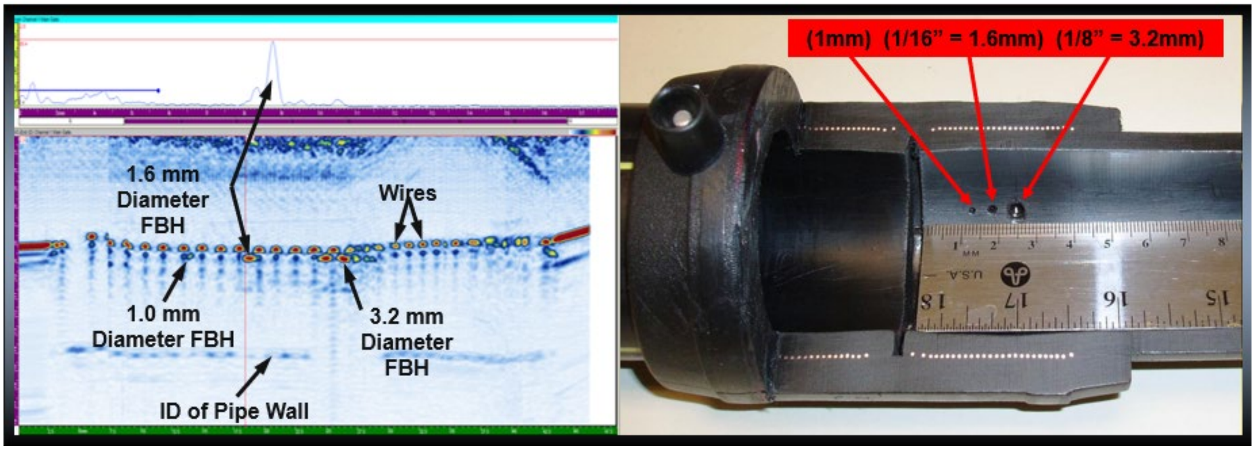

Figure 10. PAUT EF Imaging of Calibration Flat Bottom Holes

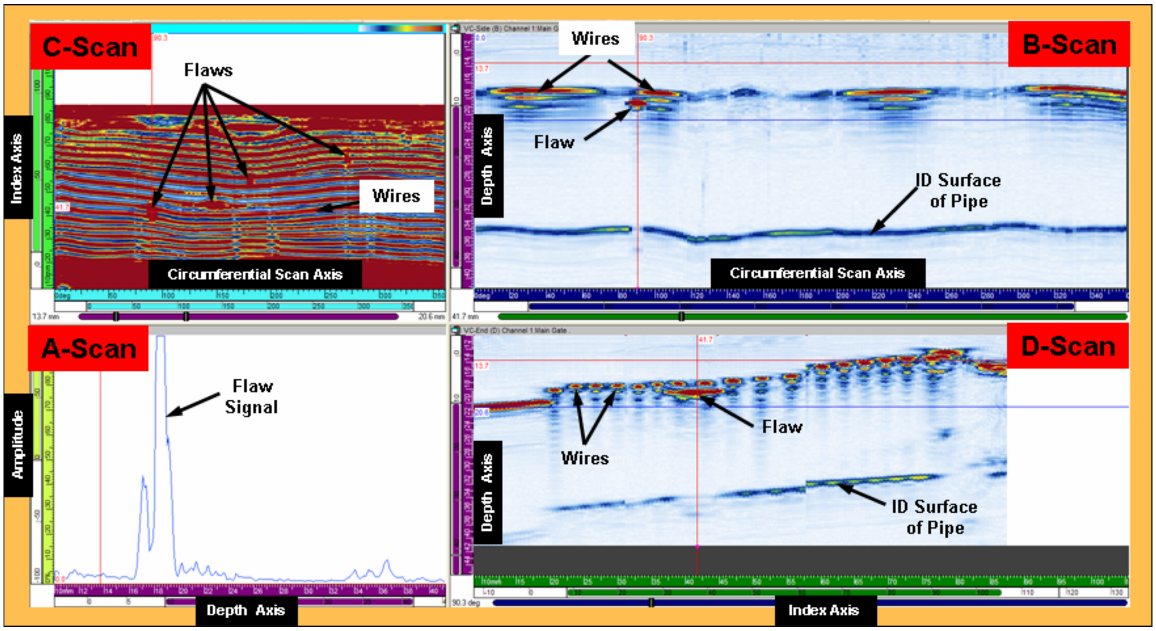

a)

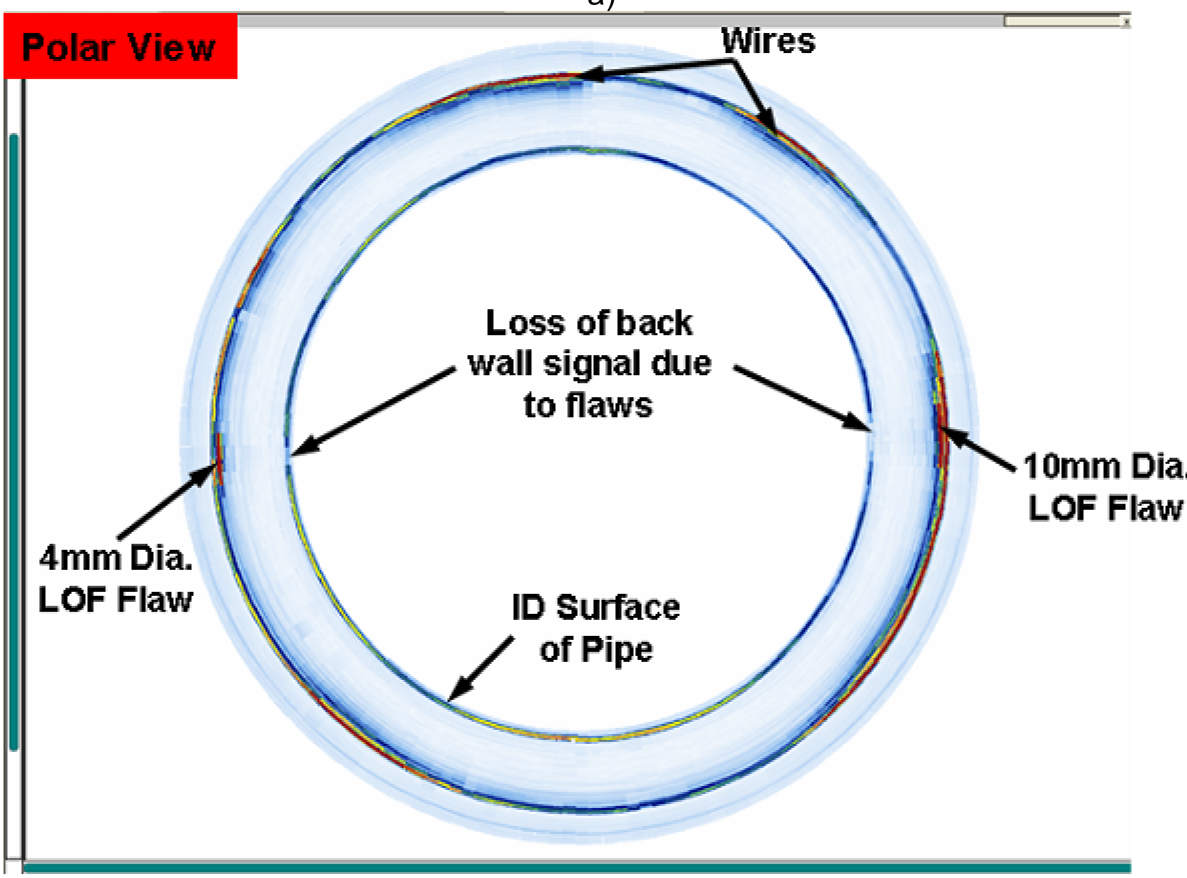

b)

Figure 11. PAUT EF Data Displays of LOF: a) – A, B, C, D-scans; b) – polar view

PA procedures were then optimized, and the performance validated in the laboratory and in the field. Artificial defects consisting of aluminum disks with various diameters were implanted in the joints of polyethylene pipes to simulate lack of fusion (LOF). Blind tests of EF joints by multiple UT operators were performed for a probability of detection (POD) and sizing study.

Detection performance with 90% POD and 95% confidence of $\mathbf{a_{90/95}}$ = 5.5 mm was demonstrated. "$\mathbf{a_{90/95}}$" is the most quoted detection performance parameter in the literature. It means that 90% of the defect with this size will be detected and this is true in 95% of the inspections under similar conditions (equipment, operators, environment etc.). Sizing length error better than 10 mm at -95% LUS was achieved. "-95% LUS" is referred as "95% lower limit against under-sizing".

PAUT detection performance and sizing length error is shown in Figure 12.

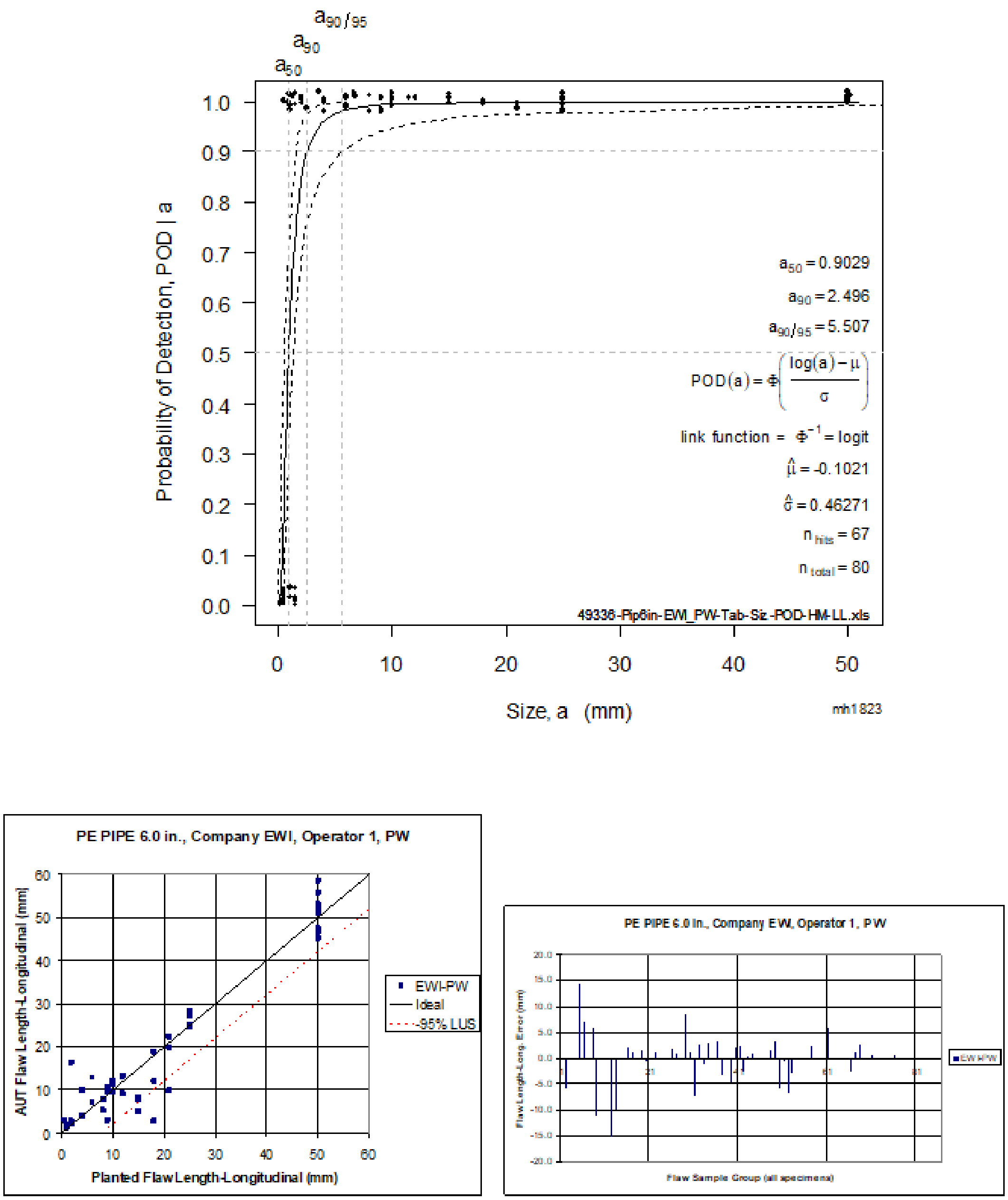

Figure 12. PAUT detection performance and sizing length error

Typically lack of proper heating creates weak/cold EF joints with inadequate fused area, which is often considered as a weld flaw (defect). PAUT technology can image and measure the vertical height of the heat affected zone (HAZ) because of the differences of acoustical impedances in the base material of the fitting and in the cross-linked HAZ area. A D-Scan view was used to determine the vertical height of the HAZ. PAUT measurements were verified destructively by cross sectioning and visualizing the HAZ height using an EWI patented technique. D-scan views of two joint cross-sections are shown in Figure 13.

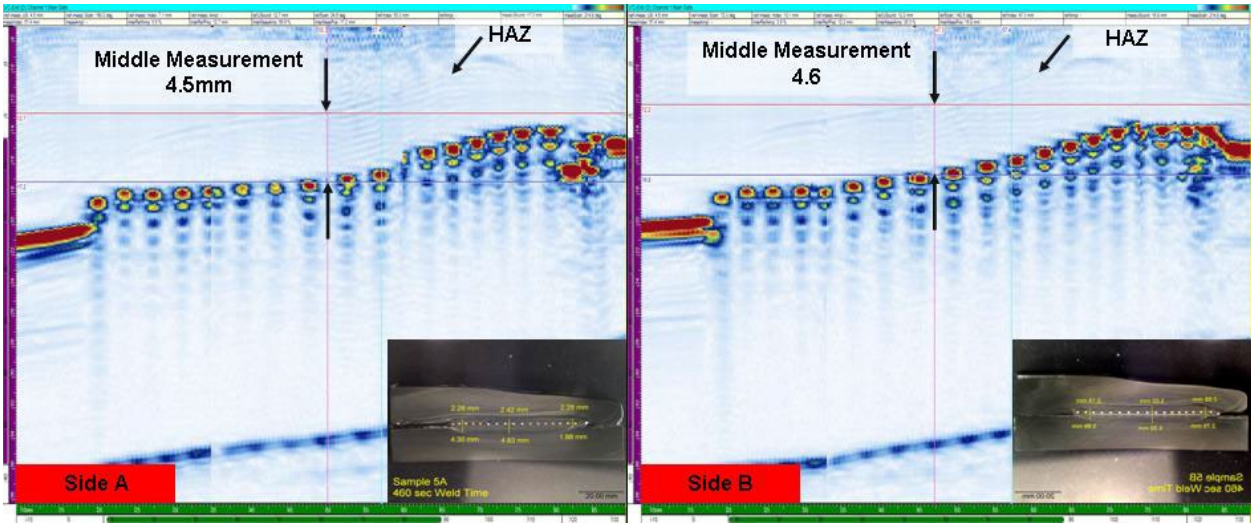

Figure 13. D-Scan view and cross sections of joint heated at 460 Sec.

A linear correlation between cross sectioning results and PAUT predictions for vertical height of HAZ were also found. The results are shown in Figure 14. It was confirmed that D-Scan view can be used to accurately determine the vertical height of the HAZ and access EF joint quality.

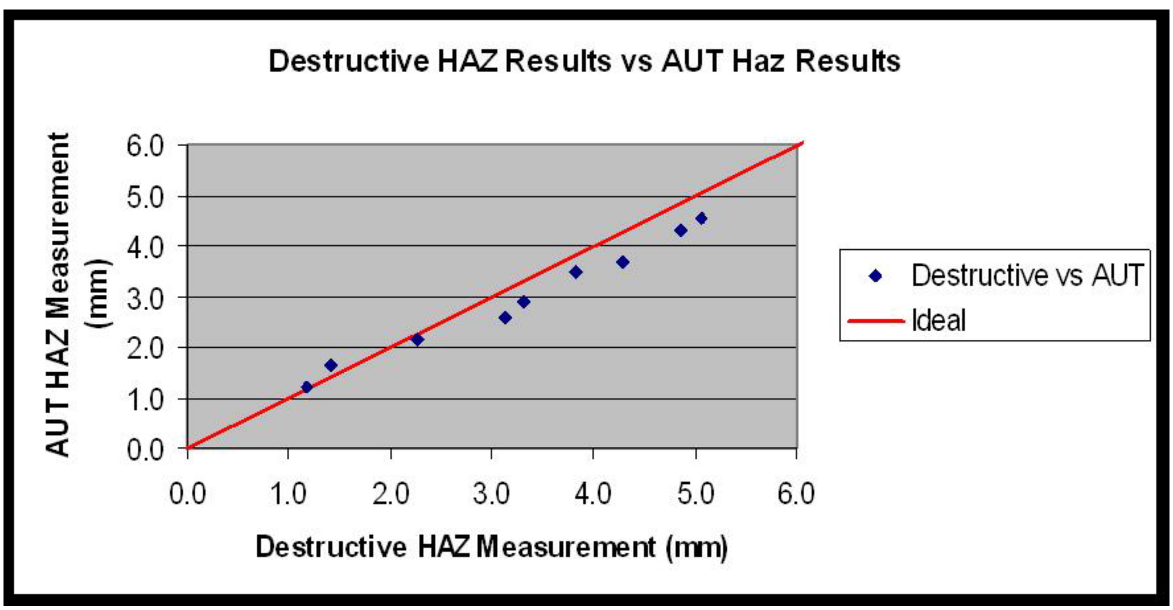

Figure 14. Correlation between cross sectioning results and PAUT predictions for the vertical height of EF HAZ

An inspection system was developed with capability of detecting lack of fusion defects greater than 6-mm circumferential length with a 2 mm through wall height within HDPE pipework using phased array technology as described in MacLennan et al. 2012. This paper provided useful insights with respect to challenges overcome during the development for manufacturing representative test blocks. PAUT results are compared with radiographs in Figure 15 illustrating the detection capability of PAUT.

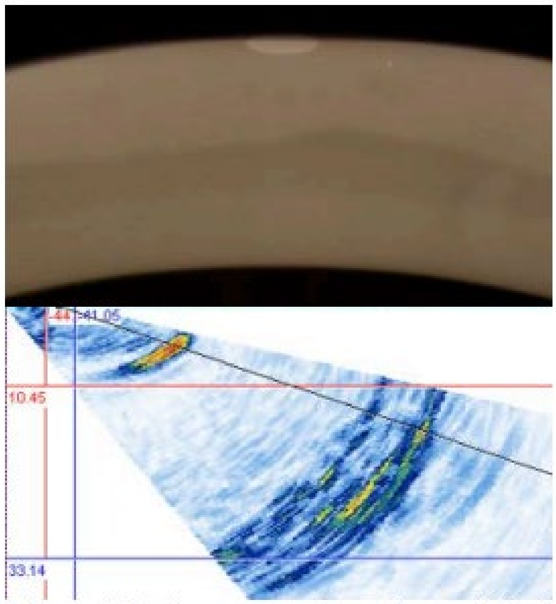

(Top) Radiograph showing a near surface reflector within the pie and (bottom) its specular response

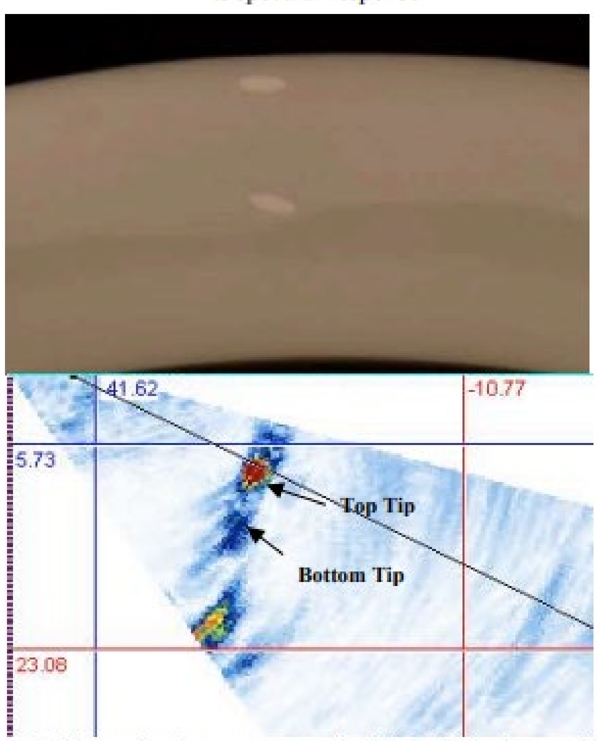

(Top) Radiograph of two targets embedded within the test block (Bottom) Edges of target resolved using tip diffraction.

Figure 15. Correlation between Radiography and PAUT

Pettigrew 2014 describes a large-scale pipeline NDE validation program that was undertaken to evaluate the use of ultrasonic TOFD complimented by PAUT for volumetric inspection of BF welds. In addition, PAUT was used for the volumetric inspection of EF welds during the same program. Figure 16 below provides images for some of the inspection set-ups.

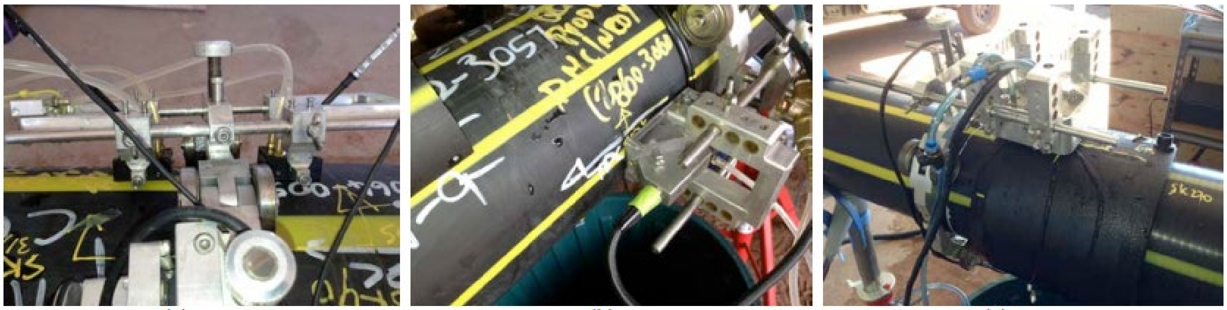

(a) (b) (c)

Figure 3. Inspection set-up for (a) TOFD of butt fusion welds, (b) PAUT of butt fusion welds, and (c) PAUT of electrofusion welds.

Figure 16. TOFD and PAUT inspection set-ups from Pettigrew 2014

Figure 17 compares some of the BF PAUT and TOFD inspection results from the Pettigrew 2014 study.

Figure 18 (a), (b), (c) and (d) show several inspection images for various defects in EF joints in HDPE as part of the Pettigrew 2014 study. These results illustrate good ability to detect wire misalignment in the EF coupler, surface scratches on the pipe and volumetric features such as defects produced by sunscreen contamination in the joint and pipe misalignment in the coupler. Considering that the wires in the EF couplers are embedded, this suggests that PAUT should be promising for inspecting SCP and RTP reinforcement layers. The ability shown by Pettigrew to detect surface scratches and volumetric features also suggest UT may be effective at finding similar features in SCP and RTP pipe. However, development and optimization of inspection procedures specific to SCP and RTP pipe are anticipated.

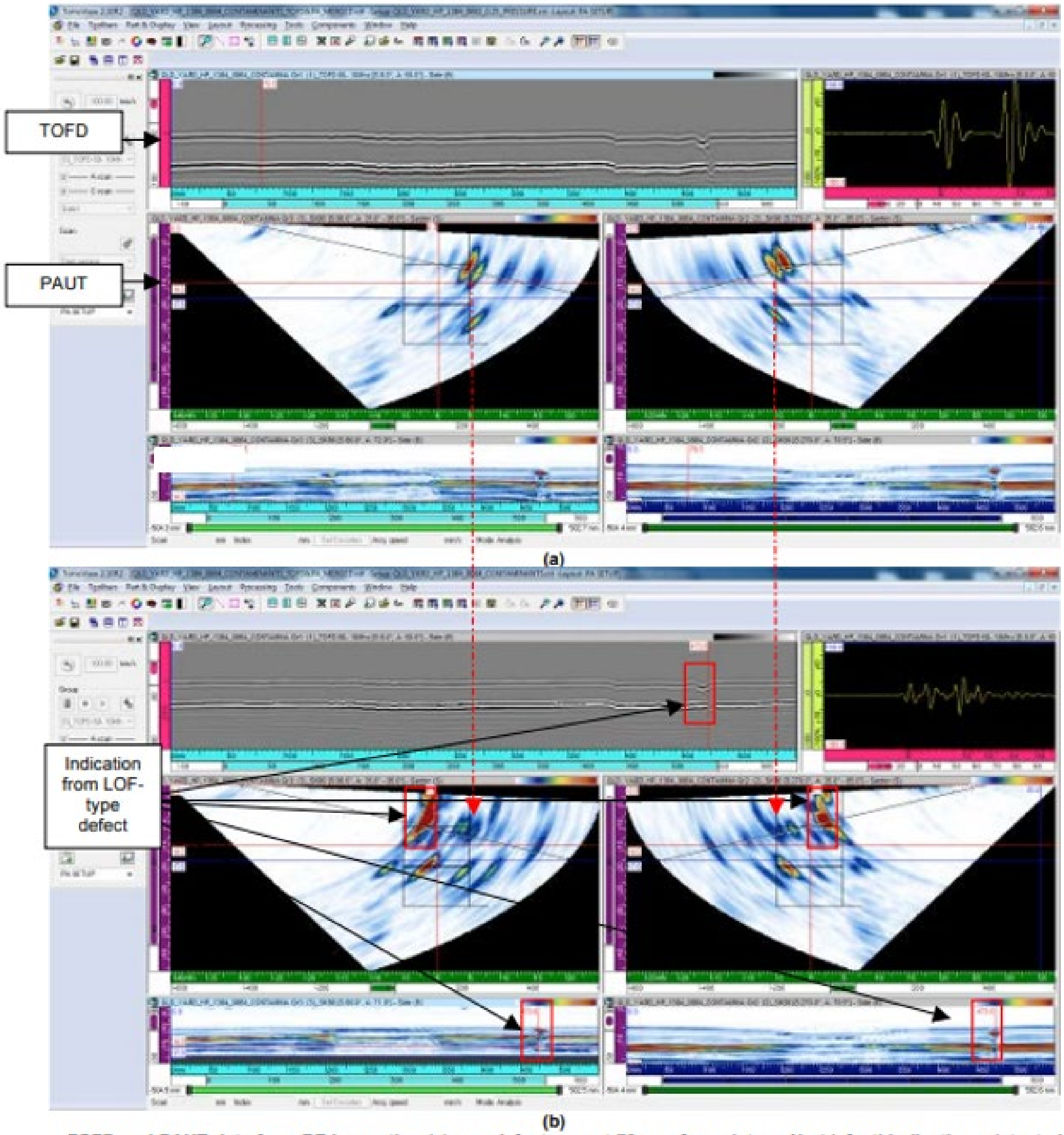

TOFD and PAUT data from BF inspection (a) non-defect area at 79 mm from datum. No 'defect' indications detected on the TOFD or PAUT scan and (b) LOF region from 465 to 480 mm from datum. Defect indications detected on the TOFD and PAUT scan. Note the reduction in amplitude of the corner trap signal on the PAUT data due the LOF reducing the energy through the weld (dashed lines).

Figure 17. BF PAUT and TOFD Inspection Results

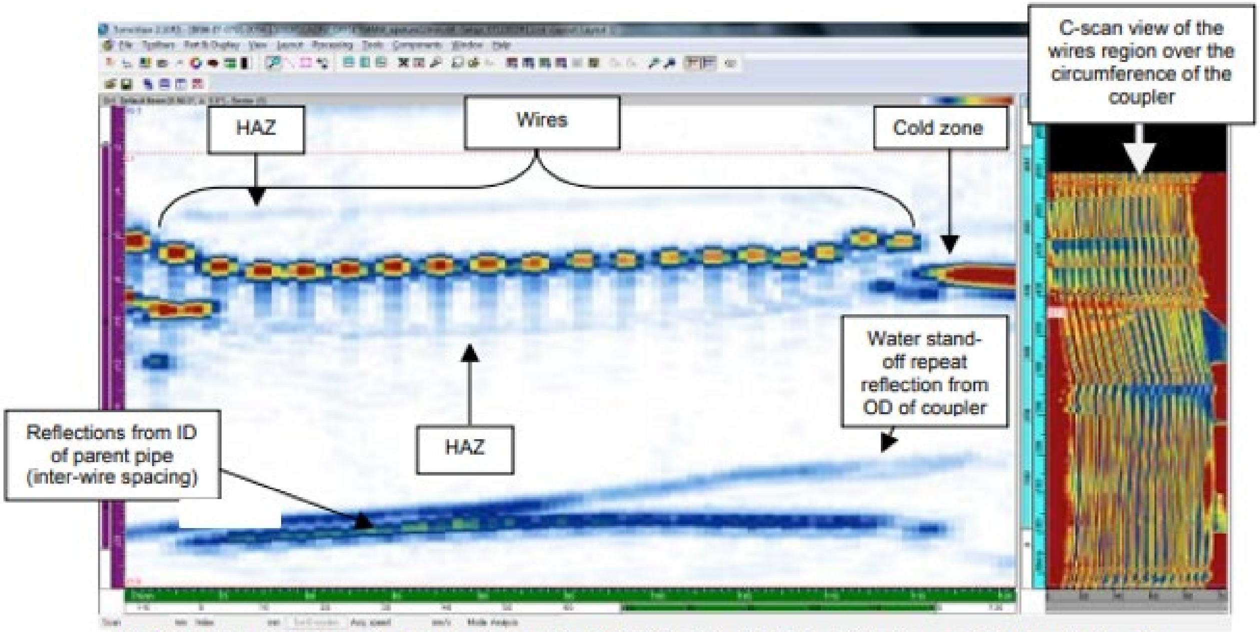

PAUT data from EF inspection (a) ductile weld (no LOF defects) with HAZ visible above and below wired region.

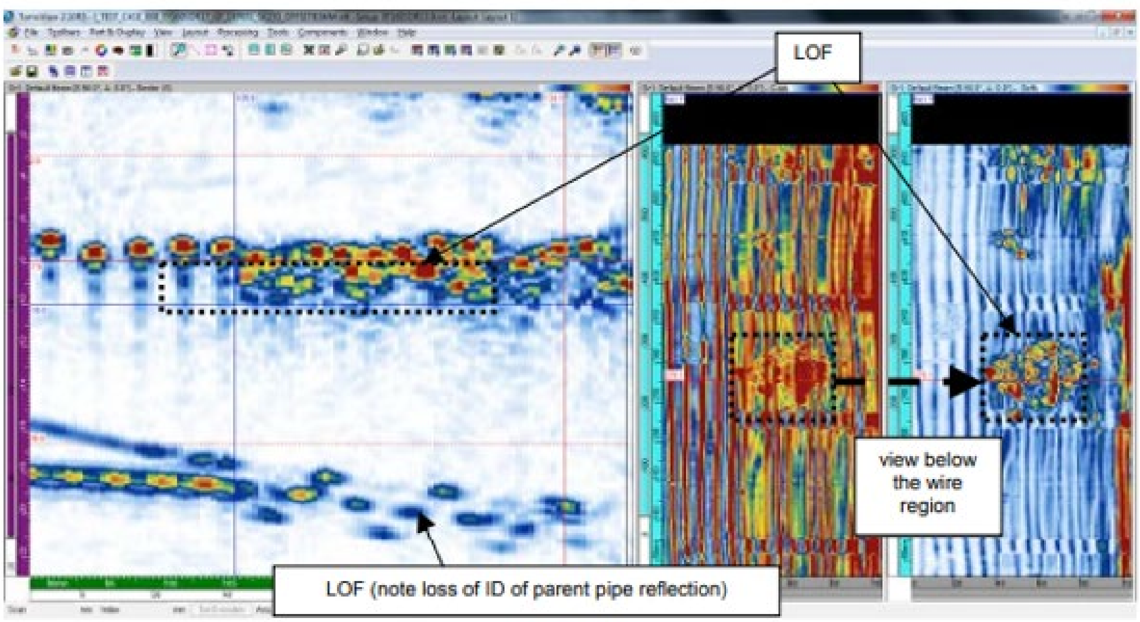

PAUT data from EF inspection: sunscreen contamination.

(a)

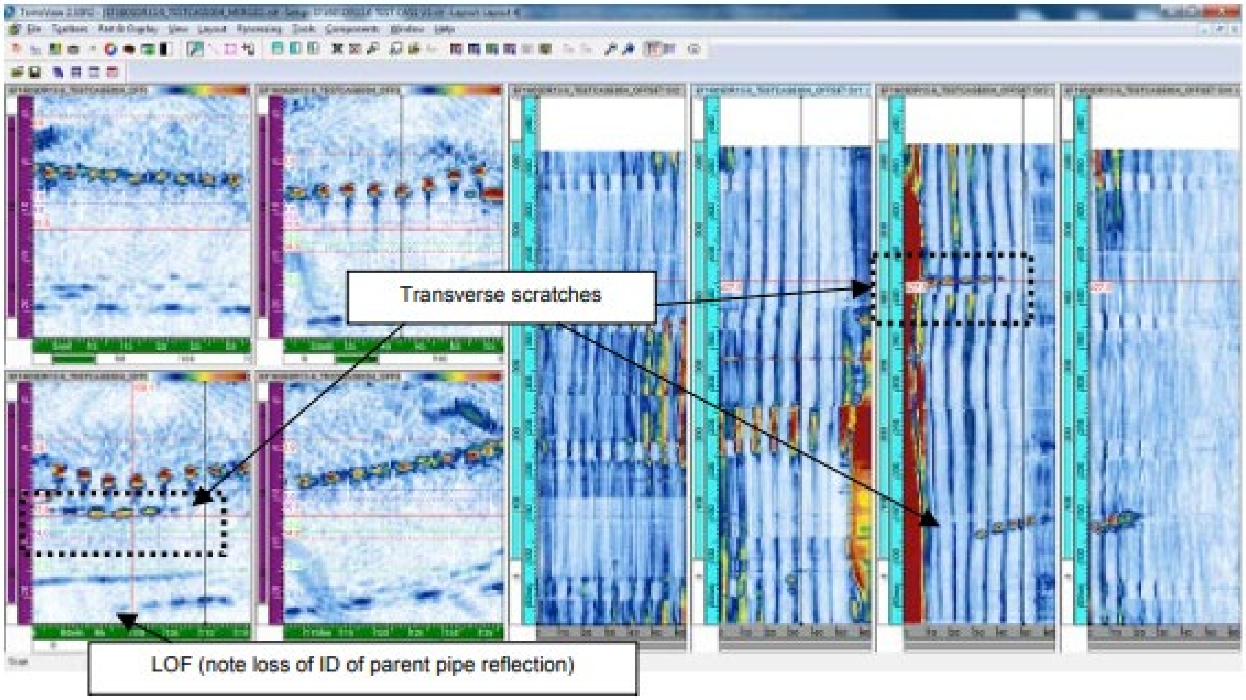

PAUT data from EF inspection: detection of transverse scratches on parent pipe.

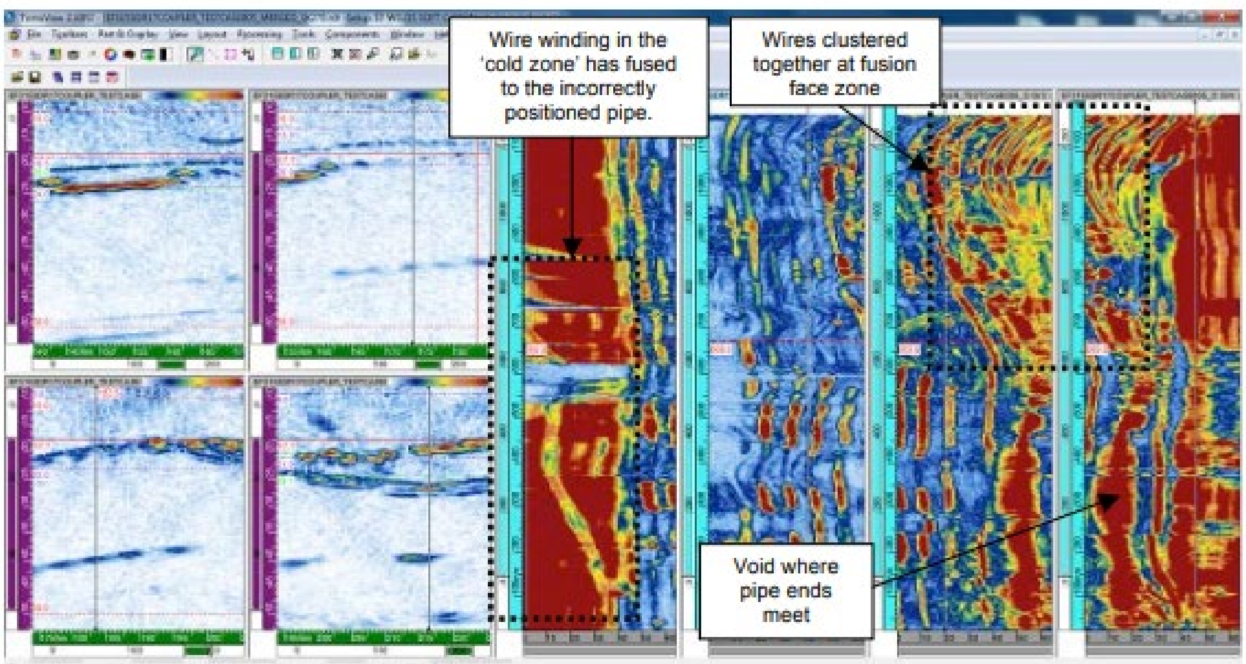

PAUT data from EF inspection: mispositioned pipe in coupler.

(b)

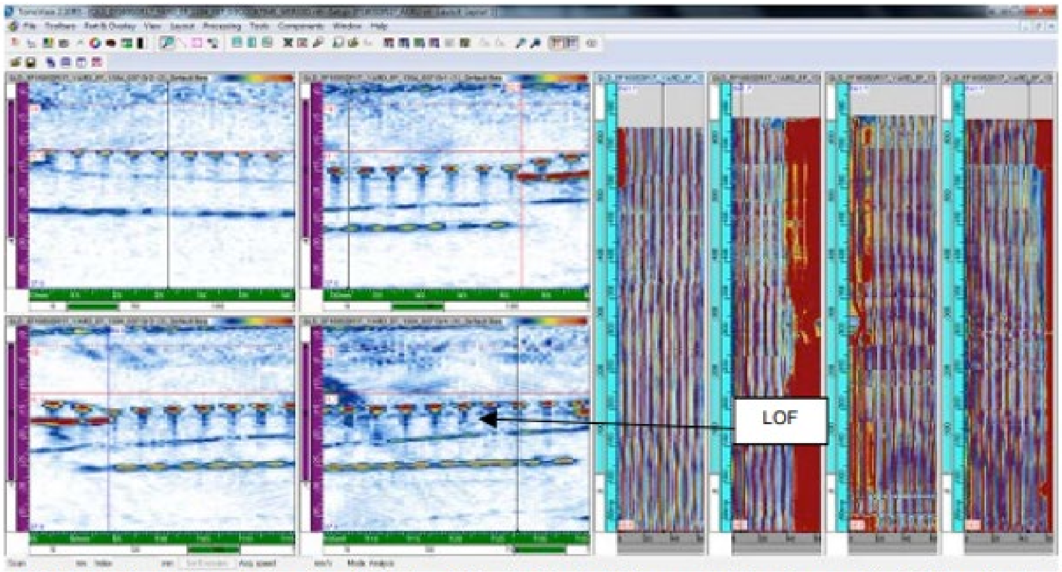

PAUT data from EF inspection: insufficient cook time leading to LOF represented as low amplitude inter-wire signal at the interface.

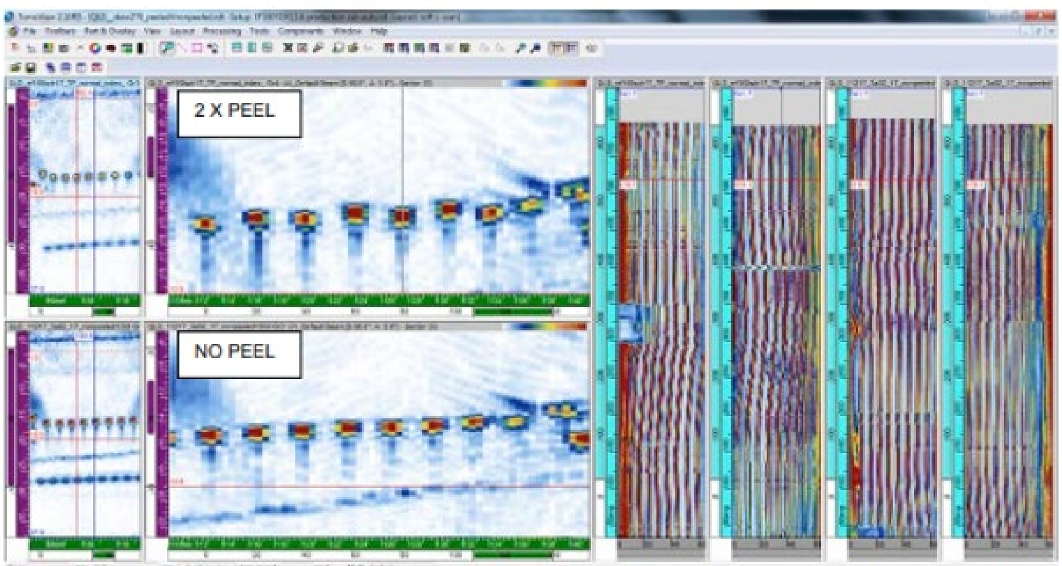

PAUT data from EF inspection: peeled vs. non-peeled comparison. Wire Uniformity (amplitude response and throughwall depth positioning) with the non-peel. Peeled; displacement of wires relating to the pitch of the peeling.

(c)

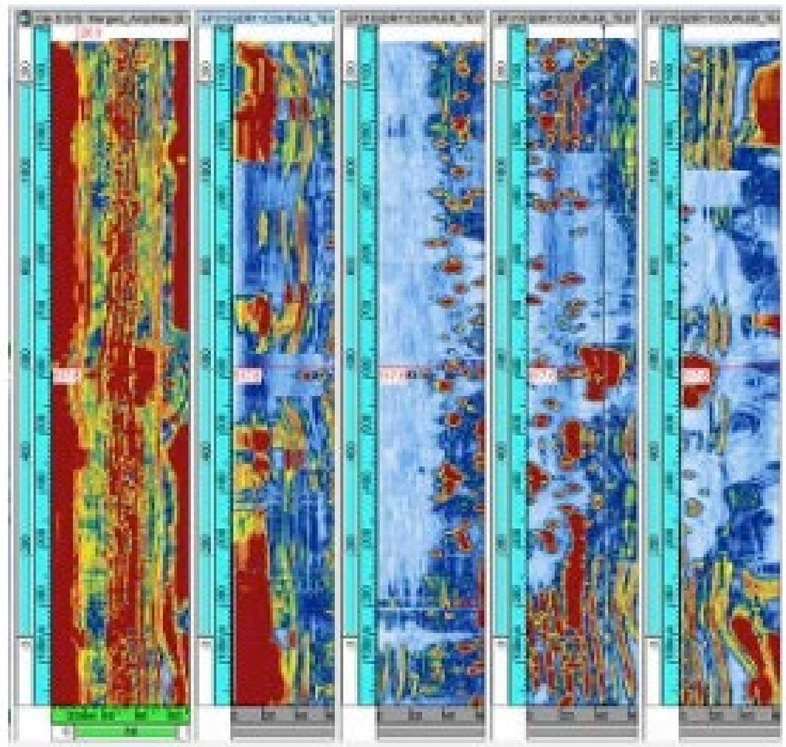

. PAUT data from EF inspection; void and air bubble mapping around circumference of the coupler.

(d)

Figure 18. (a). Scans showing incomplete fusion from sunscreen contamination in the joint (b). Scans showing scratches and misalignment of the pipe in the coupler (c). Scans showing effect of heat time and peeling in the joint (d). Scans showing effect of voids and air bubbles

A PAUT system capable of inspecting BF and EF joints in polyethylene pipes of diameters between 90 and 800 mm was described in Troughton et al. 2012, and Hagglund et al. 2014. These two different types of weld joints having different geometrical structures and fusion zones that vary in location, orientation, and size were examined with results reported in these papers. Several individual techniques were applied to fully cover the weld fusion zones. These techniques were configured in a simple and easily deployable system. The PAUT system utilized membrane water wedges for overcoming some of the problems related to the acoustic properties in plastic pipes. The details of the system were described, and its capabilities evaluated. Case studies showing on-site inspection work are presented, providing confidence in the inspection results. A set of linear, sector, and creeping wave scans from this work are shown in Figure 19.

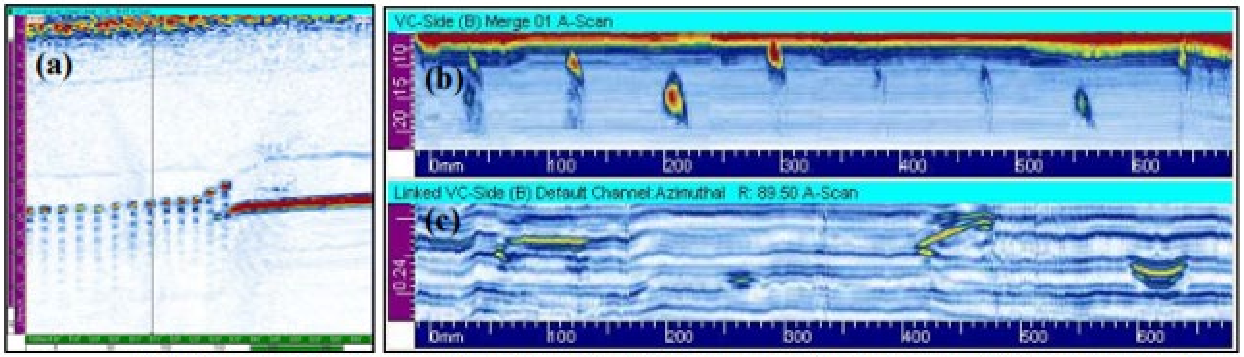

(a) Linear electronic scan for EF joints. (b) Sector scan for BF joints. (c) Creeping wave scan for BF joints.

Figure 19. EF and BF PAUT Results from large diameter PE pipes

PAUT has been applied for investigation of the integrity of thick HDPE BF joints and mitered joints in Searfass et al. 2015. The scanning technique utilized a PAUT phased array pitch-catch scanning method and longitudinal, transmit-receive (TRL), matrix probes operating in a pitch-catch configuration that provides full volumetric coverage of the fusion zone for the detection of inclusions and surface-breaking defects. The transmitting and receiving probes were placed adjacent to one another to scan the pipe using refracted longitudinal waves with a half path focusing method. Empirical results supported by numerical CIVA modeling were presented to demonstrate capabilities of this technique for detection of voids and inclusions. Additionally, the effects of temperature on focalization and the proper countermeasures were discussed. The ability of the developed PAUT technique to detect a 2.7-mm defect anywhere in the BF zone of a straight or mitered joint was demonstrated. Figure 20 shows an example of the PAUT TRL response for a surface breaking flaw on the inside diameter surface.

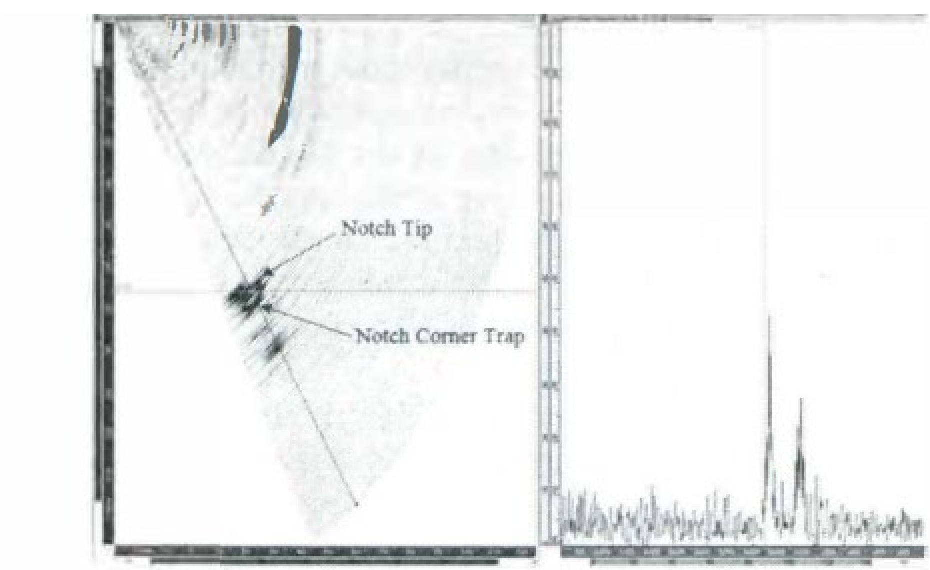

Figure 20. Indication of a 2.7-mm inner diameter surface breaking defect using PAUT

A useful review of nondestructive examination technology for HDPE pipe and examples of PAUT results for EF and BF joints inspected per ASME Code Case N755 have been published by Kim et al. 2016 and Zheng et al. 2018. Figure 21 illustrates some of the results for an EF joint in HDPE having a variety of flaws or anomalies as well as for sound pipe having no indications.

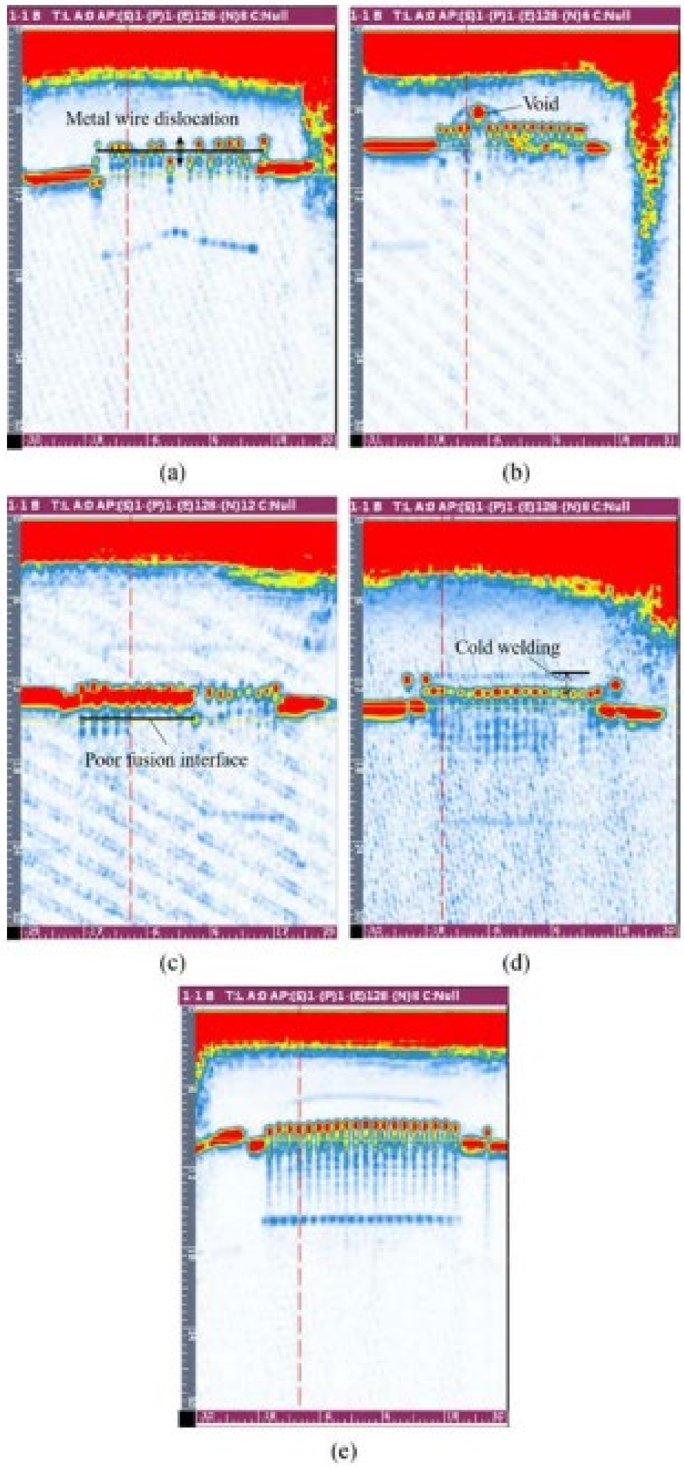

Figure 21. Typical PAUT results in an EF joint (a) metal wire dislocation, (b) void (c) poor fusion (d) cold weld (e) normal

Evaluation of the effect of 32-128 elements PAUT aperture on the detection of parent material inhomogeneities and planar flaws created using implanted stainless steel disks in HDPE BF joints using 2-MHz matrix probes and a transmit-receive longitudinal (TRL) technique was presented in Crawford et al. 2017. True-state information on parent material and joints with attempted fine particulate contamination and cold fusion/lack of fusion defects were obtained using RT or high-resolution CT examination and destructive testing for validation. The true-state data was successfully reconciled with PAUT data. Figure 22 provides a set of results documenting the aperture effect on the signal-to-noise ratio (SNR).

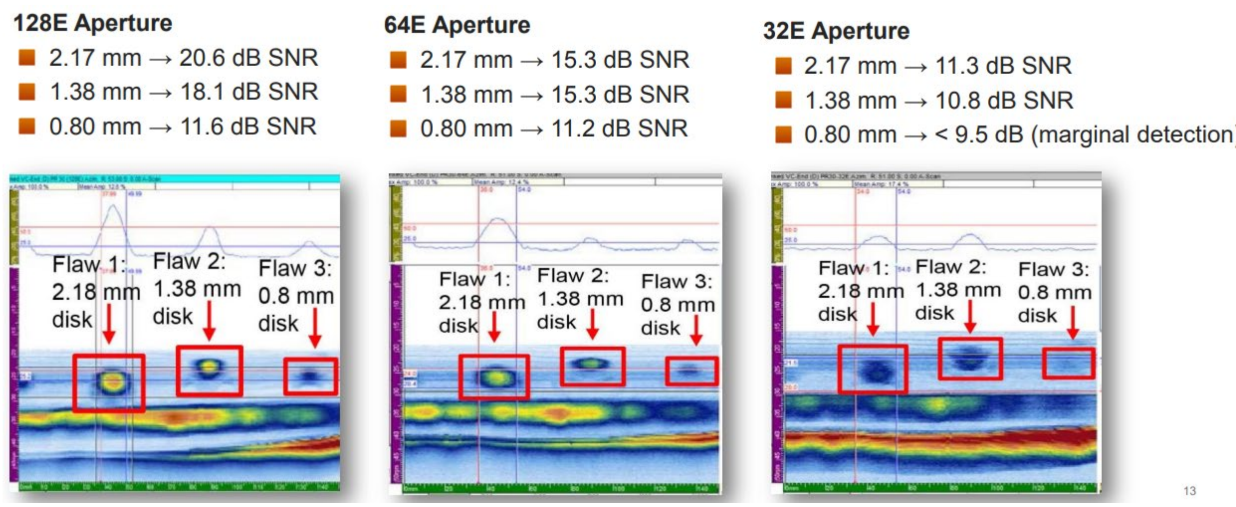

Figure 22. Aperture Effect on PAUT TRL Technique Capability

HDPE parent material and welds flaws were identified and NDE techniques have been reviewed in Egerton 2018. This work included modeling of ultrasonic array inspection of HDPE parent material, EF, and BF pipe joints of cooling water pipework with improvements of PAUT procedures proposed.

The relationship between acoustic attenuation and dispersion of longitudinal waves using normal focused and steered beam in HDPE was obtained by numerical field simulation (Qin et al. 2019). The linear relation between peak offset and propagation distance was studied. An improved delay law was proposed to increase the intensity of the ultrasonic field. This improved delay law was compared with the conventional one by numerical simulation of the ultrasonic field and PAUT experiments, which showed that the improved delay law could increase the image sensitivity. Figure 23 illustrates the effect of the improved delay law using A-scans.

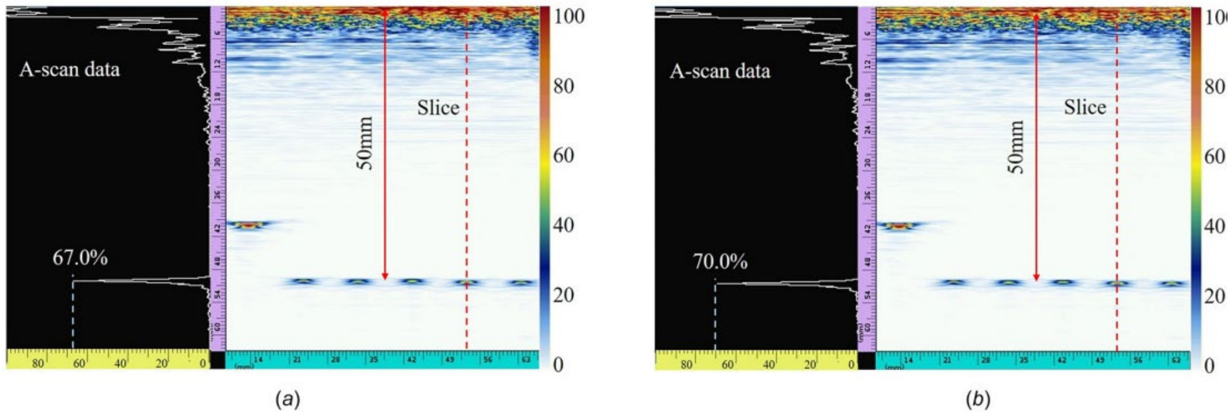

Inspection result ($F = 50$ mm, $\theta = 0$ deg, $N_a = 32$, and gain = 51 dB): (*a*) conventional delay law and (*b*) improved delay

Figure 23. PAUT conventional and improved delay laws

The use of TOFD for enhancement of HDPE pipe BF butt joints inspection for oil and gas and nuclear safety related cooling water applications was reported in Smith et al. 2019. Figure 24 provides an example of the TOFD enhancement for lack of fusion and porosity defects in a pipeline.

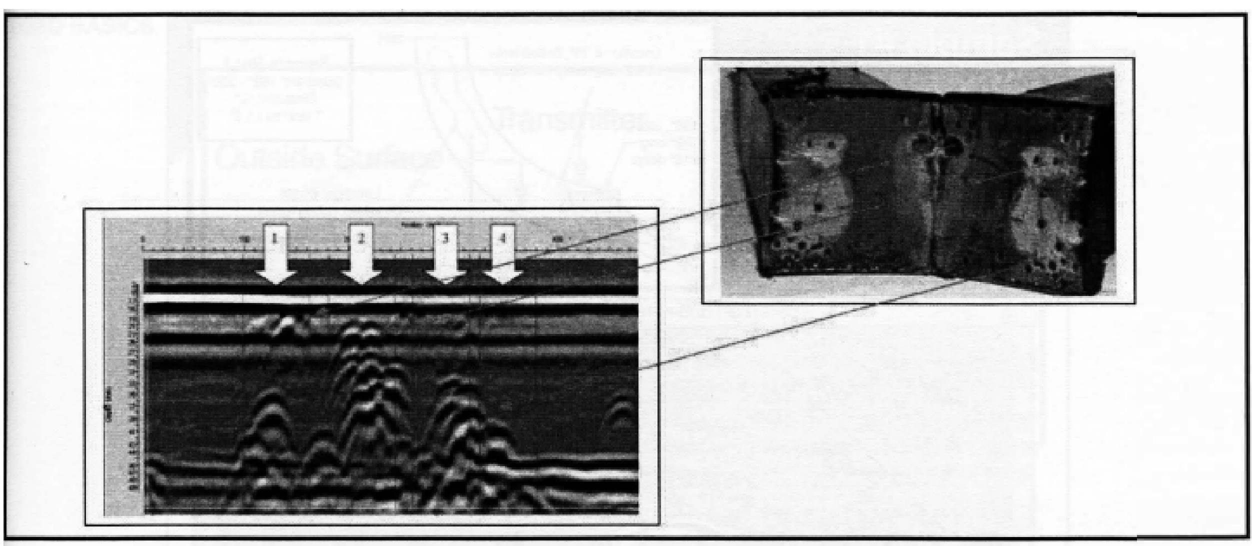

Figure 24. TOFD enhancement of HDPE in pipe BF butt joints showing lack of fusion and porosity

Optimization of HDPE ultrasonic inspections was discussed with a summary of ASME Section V Article 4, and mandatory Appendix X requirements for all ultrasonic techniques required for examination of fusion joints of HDPE pipes by Reverdi 2020. The code specifies that all classical parameters related to calibration checks, sensitivity settings, sizing method, and scan plan be provided, and that the examination coverage should include the fusion face ± 8 millimeters (0.3 inches) on each side of the weld joint. Imaging examples of optimized TOFD and PAUT (with and without wedge) procedures were included. A no-wedge configuration allows detection of all the defects without any wedge echoes. Despite being at normal incidence, the no-wedge configuration allows detection of the top side drilled holes (SDH). The high attenuation leads to lower frequency content and the pitch of the probe becomes quite small compared to the wavelength. The configuration thus does not generate any grating lobes. Figure 25 provides an example of a no-wedge imaging result.

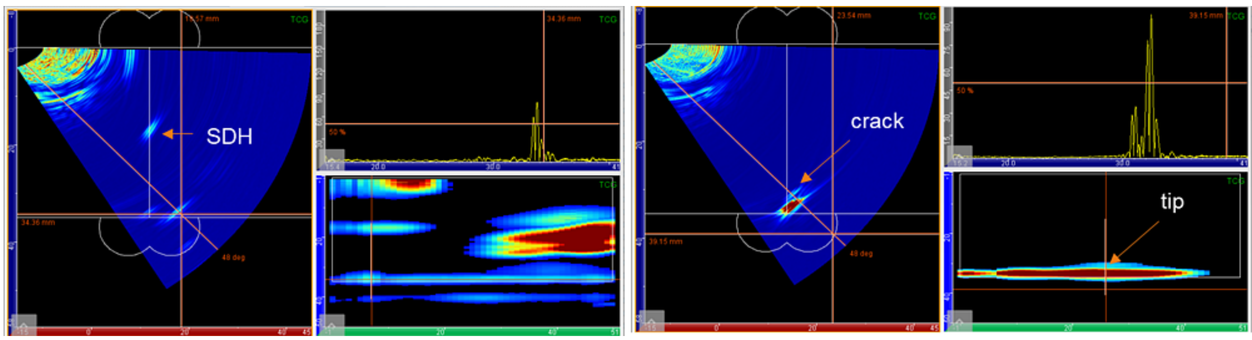

Figure 25. PAUT no-wedge configuration imaging

A new TFM technique called plane wave imaging (PWI) has been introduced. While the classical TFM reconstruction process uses the full elements of the probe, the FMC excitation of only one element may not be enough while inspecting thick and attenuative materials. Instead of firing the element one by one, during PWI process the system performs a sectorial scan with few angles for the emission and TFM for reconstruction. Firing all the elements at the same time sends more energy into the part leading to better sensitivity.

The results of using PWI with a 35 to 85° sectorial scan and a step of 3° to inspect the 35-mm (1.4-in) HDPE sample have been presented with the gain used and scanning speed achieved. Figure 26 compares TFM and PWI for a side drilled hole while Figure 27 compares these methods for a notch.

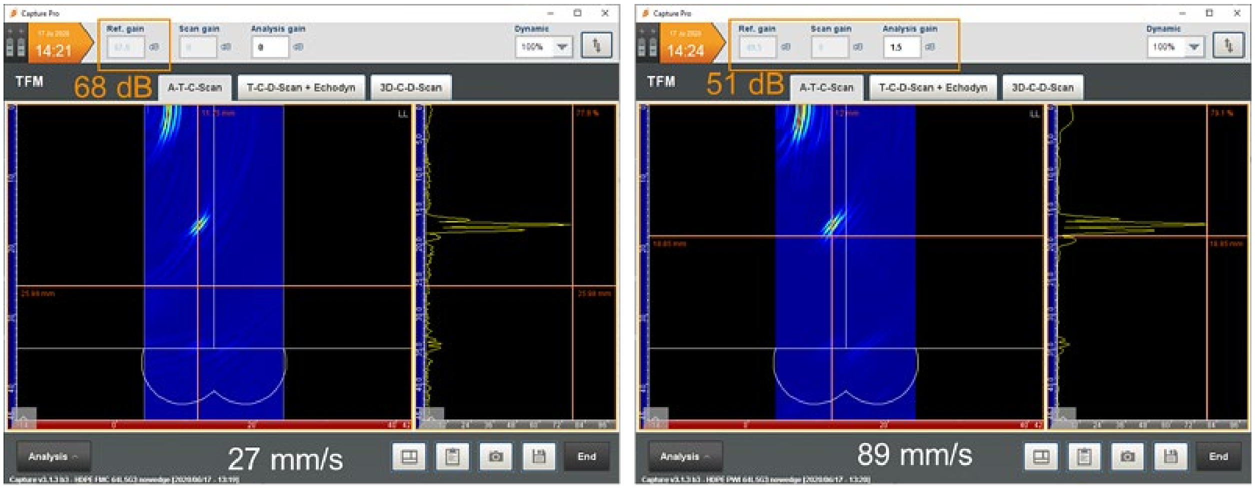

Figure 26. TFM (left) vs. PWI (right) imaging of SDH

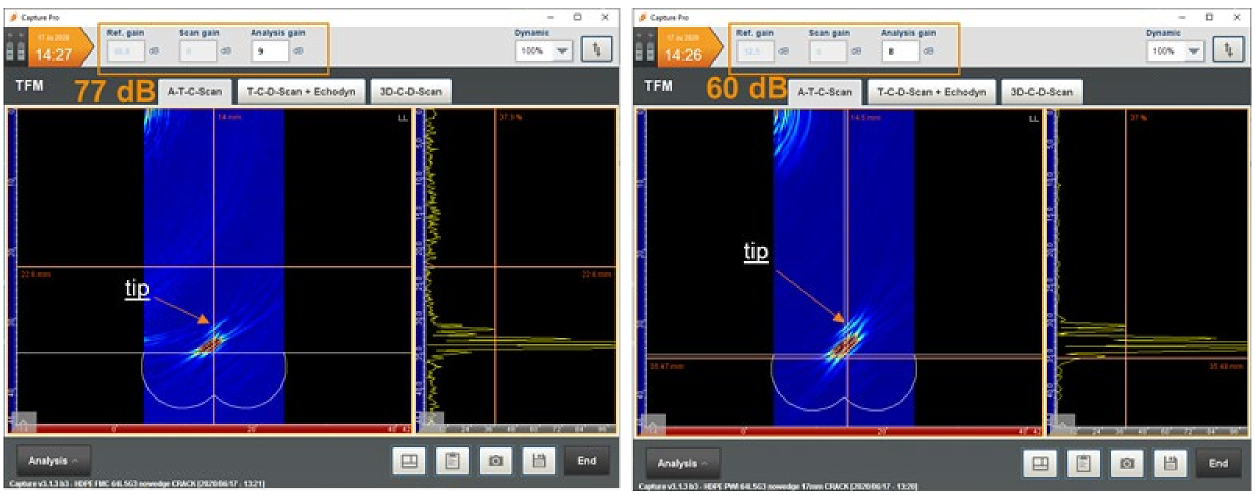

Figure 27. TFM (left) vs. PWI (right) imaging of a notch

The gain required for PWI is 17 dB less compared to FMC/TFM. The electric noise starts to appear when looking at the notch. The SNR measured for the tip diffraction is 13 dB while it is 28 dB with PWI. This is particularly important when dealing with thick HDPE components. The overall energy level, thus sensitivity, depends on the number of angles used during the PWI/TFM process. It is therefore possible to improve even more by using more angles for the emission. The scanning speed was also improved by a factor greater than three times.

Several standards and code documents provide useful guidance for inspection of PE weld joints. ASTM standard E3044 describes an approach to use either or both TOFD and PAUT on butt fusion joints (ASTM 2016). ASTM E3170/E3170M-18 is a Standard Practice for Phased Array Ultrasonic Testing Of Polyethylene Electrofusion Joints (ASTM 2018). ASME BPVC, Section 5, Mandatory Appendix X describes the requirements for the examination of butt fusion welds in HDPE pipe using encoded pulse echo, phased array, or TOFD ultrasonic techniques (ASME 2021). These documents will be referred when EWI develops the laboratory inspection procedures in Task 3 of this program.

NDE techniques with a focus on ultrasonic technology applied to HDPE BF joints uses, limits, and codes acceptance criteria has been reviewed (Svetlik 2019). This review is useful as a convenient reference for code acceptance requirements for HDPE inspection. These requirements can provide a baseline for the initial inspection procedure development efforts to be used in this program.

Prowant et al. investigated UT of butt fusion joints on 12-in. diameter PE4710 pipe. Thermal butt fusion joints were made with the weld bead left in place. A TRL mode was used with two 128 element PAUT probes in a side-by-side arrangement. A 2 x 128 2D matrix probe (2 MHz) was used with elements in a 32x4 arrangement and beam angles between 25 and 85 degrees. Apertures of 32, 64, and full 128 elements were evaluated. Flaws were implanted using stainless steel discs in the pipe wall at various depths. An integrated water column was used. The 64 and 128 element apertures had similar detection capability with 128 element apertures having the best SNR. The 32-element array SNR was worst. Flaws near the OD were most difficult to detect.

Sheng determined that the attenuation coefficient of PE had an approximately linear relation with frequency and that phase velocity rose logarithmically with frequency. The effects of attenuation and dispersion on amplitude spectrum and waveform in time domain of the target signal were investigated. Frequency downshift and time delay shift had an influence on image resolution and focus capability and were believed to be a restriction of current inspection technology. This work also theoretically proved that lower testing frequencies (less than 2.5 MHz) could improve the inspection effectiveness of the applied inspecting systems for HDPE pipes.

When a broadband ultrasound pulse passes through PE pipe, the waveform of the pulse changes as a result of the attenuation and dispersion of PE causing different arrival times of the sound energy. As an example, over an inspection distance of 80 mm, the acoustic signal with an original center frequency of 5.0 MHz drops to 3.5 MHz - a decrease of 1.5 MHz, while that with 2.5 MHz drops to 1.65 MHz or a decrease of 0.85 MHz. Hence, lower frequency has a better inspection stability when acoustic attenuation is considered, which is consistent with the results of other field inspection data.

Zhu, et al. 2014 investigated active infrared thermography for defect detection in PE pipes. Their experimental setup is shown in Figure 28.

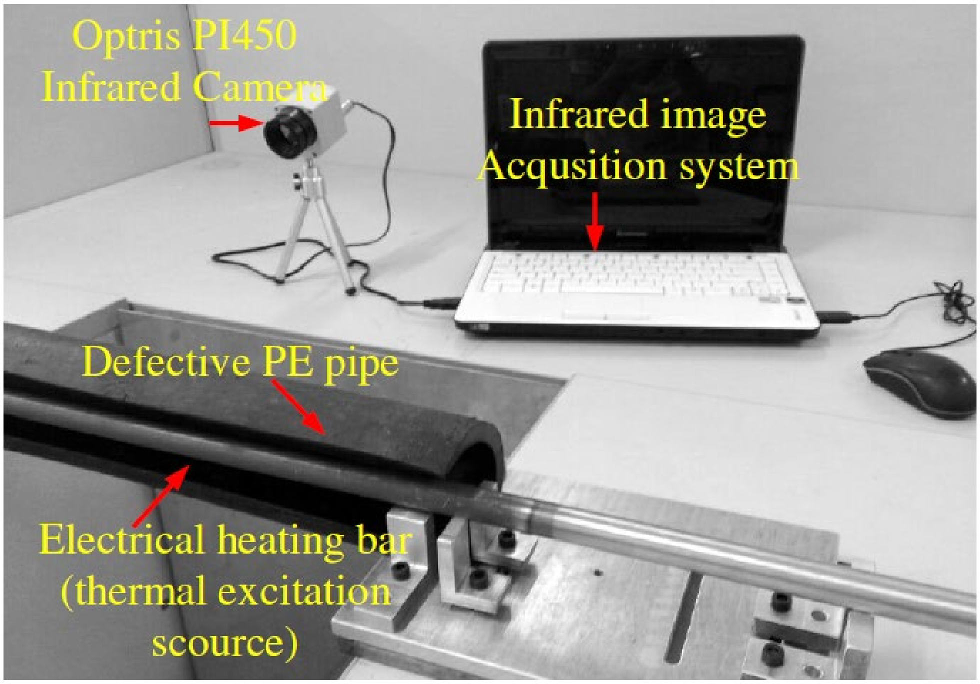

Figure 28. Active thermography setup used by Zhu et al.

The pipe defect pattern and corresponding thermography scans are shown in Figure 29 (a) and (b).

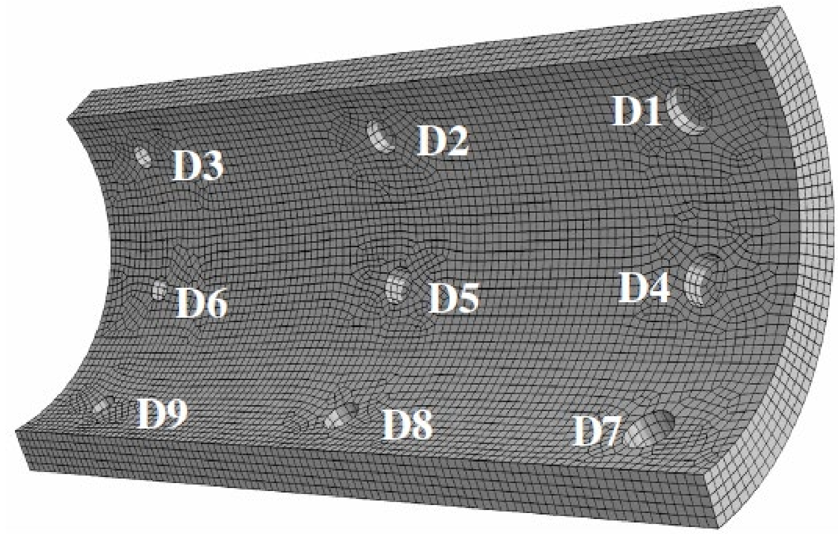

(a)

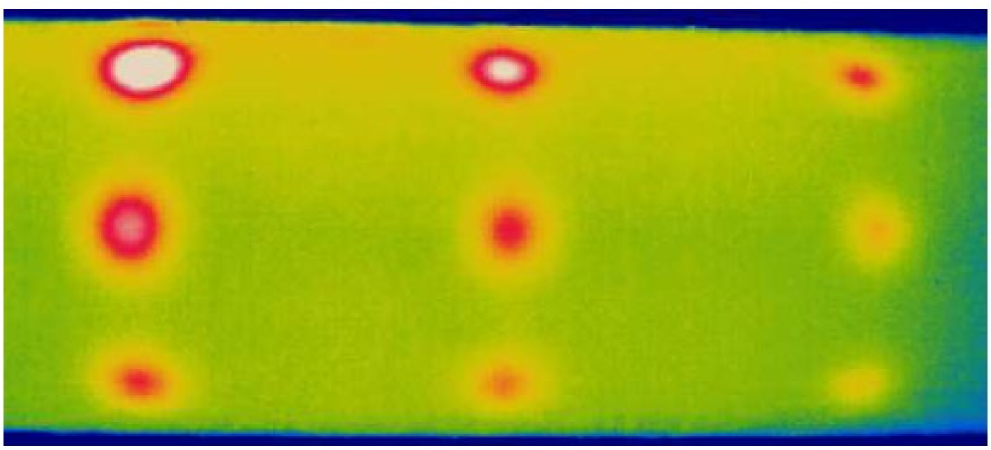

(b)

Figure 29. (a) Defect layout in pipe section (b) Thermography image of defect pattern

Zhu et al. performed a similar set of trials on intentional defects in BF joints HDPE pipes. Figure 30 (a) and (b) show the BF joint and corresponding scan results. These results illustrate the potential of active thermography for both pipe body and joint defect characterization.

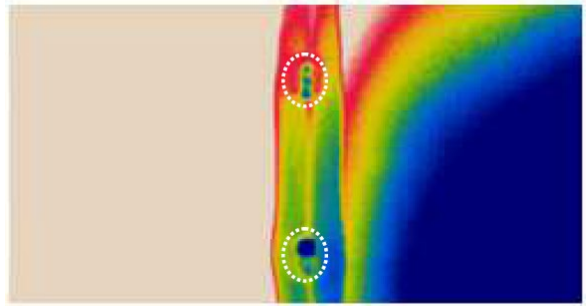

(a) View of the BF joint bead (b) Thermography scan

Figure 30. Active thermography inspection of defects in BF butt joints in HDPE pipe

Sham et al. 2019 examined active and passive thermography for inspecting HDPE liners in underground sewer systems. They found that active thermography methods were best for finding unbonded or disbanded features (using hot air to heat pipes) while leaks (water seepage) were more easily found with passive methods. In addition, the paper documents that the minimum detectable size of defects depends on the spatial resolution of the infrared camera lens and the distance between the infrared camera and the target area. The minimum detection size of an infrared camera lens is determined by multiplying the instantaneous field of view (IFOV) by the distance in meters from the lens to the inspection surface.

Pan et al. 2013 examined microwave methods for cold weld defects in HDPE fusion welds. The paper describes the microwave principal for non-metallic materials as follows:

> *"The basic operating principle of microwave NDT for nonmetallic pipes is based on the backscattering of microwaves as they travel from one medium to another with different dielectric constant. A defect in a nonmetallic pipe can be regarded as a new medium with a different dielectric constant from the surrounding material. Hence it scatters the microwaves at a different rate and phase from the surrounding media."*

By measuring the reflection coefficient of an HDPE weld sample at varied frequency points within a certain range, the most sensitive frequency at which the reflection coefficient exhibited biggest differences among the weld samples can be determined.

The microwave test system used in this study includes a vector network analyzer (Agilent E8357A, maximum frequency = 20 GHz), rectangular waveguide, with a horn antenna. Figure 31 shows the setup.

Cold weld defects in the weld were sensitive to microwave at the frequency of 9.9 GHz, where the reflection coefficient S11 showed most significant differences between the good weld and the defect-containing welds.

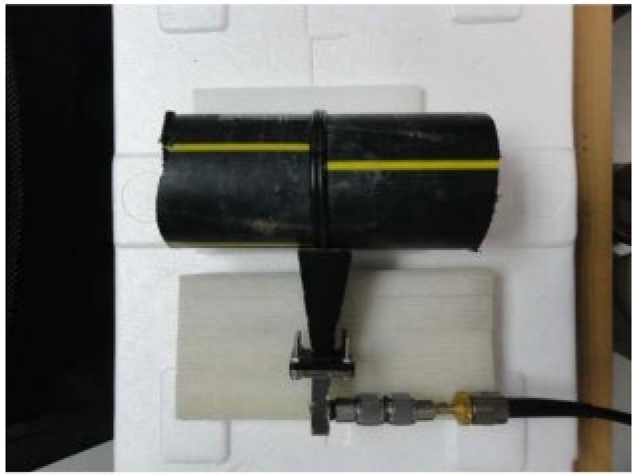

Figure 31. Setup for microwave inspection of fusion welds in HDPE pipe

<u>Key Findings from Recent Research on Filament Wound Glass Reinforced Epoxy Pipe</u>

An ultrasonic conventional technique using a commercially available system having a 5-MHz broad band dual/twin crystal contact probe with the frequency characteristic of the flaw detector receiver–amplifier set to 2 MHz was used successfully to assess impact damage in filament wound glass reinforced epoxy pipe subjected to seawater at the rated internal pressure, 20 bar (2 MPa) at ambient temperature (Ashton et al. 2003).

The ultrasonic method developed has been used to quantitatively examine impact damaged on pipes by three different nose-shaped indenters, both before and after exposure to seawater. Ultrasonic measurements of the extent of the damage have been compared with measurements taken from micrographs of sections of the damaged regions. See Figure 32 for examples of ultrasonic amplitude based and visual imaging of impact damage. Figure 33 shows ultrasonic time of flight imaging results of impact damage. These results demonstrate good ability to quantify this type of damage.

The test results showed that impact damaged pipe exposed to seawater at the rated pressure for up to 6 months displayed no increase in the extent of the damaged region. Ultrasonic measurements of the extent and distribution of the damage through the pipe wall agreed well with measurements taken from micrographs.

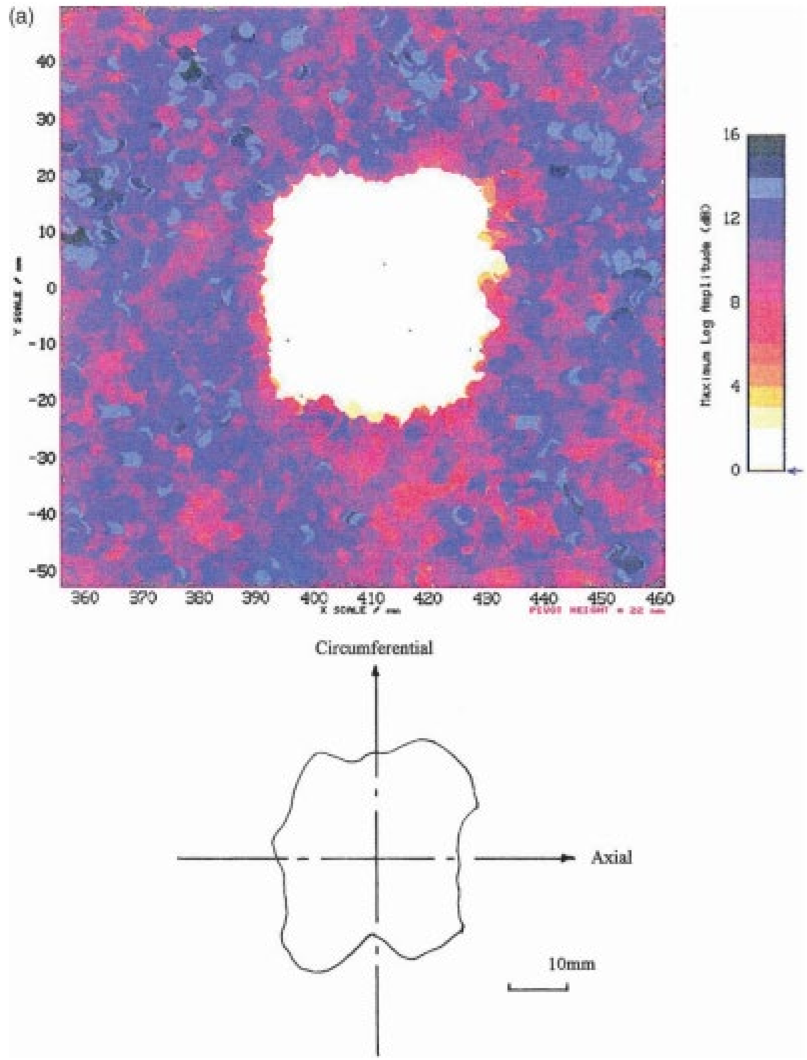

(a)
Maximum Log Amplitude (dB)
X SCALE / mm
Y SCALE / mm
PIVOT HEIGHT = 22 mm
Circumferential
Axial
10mm

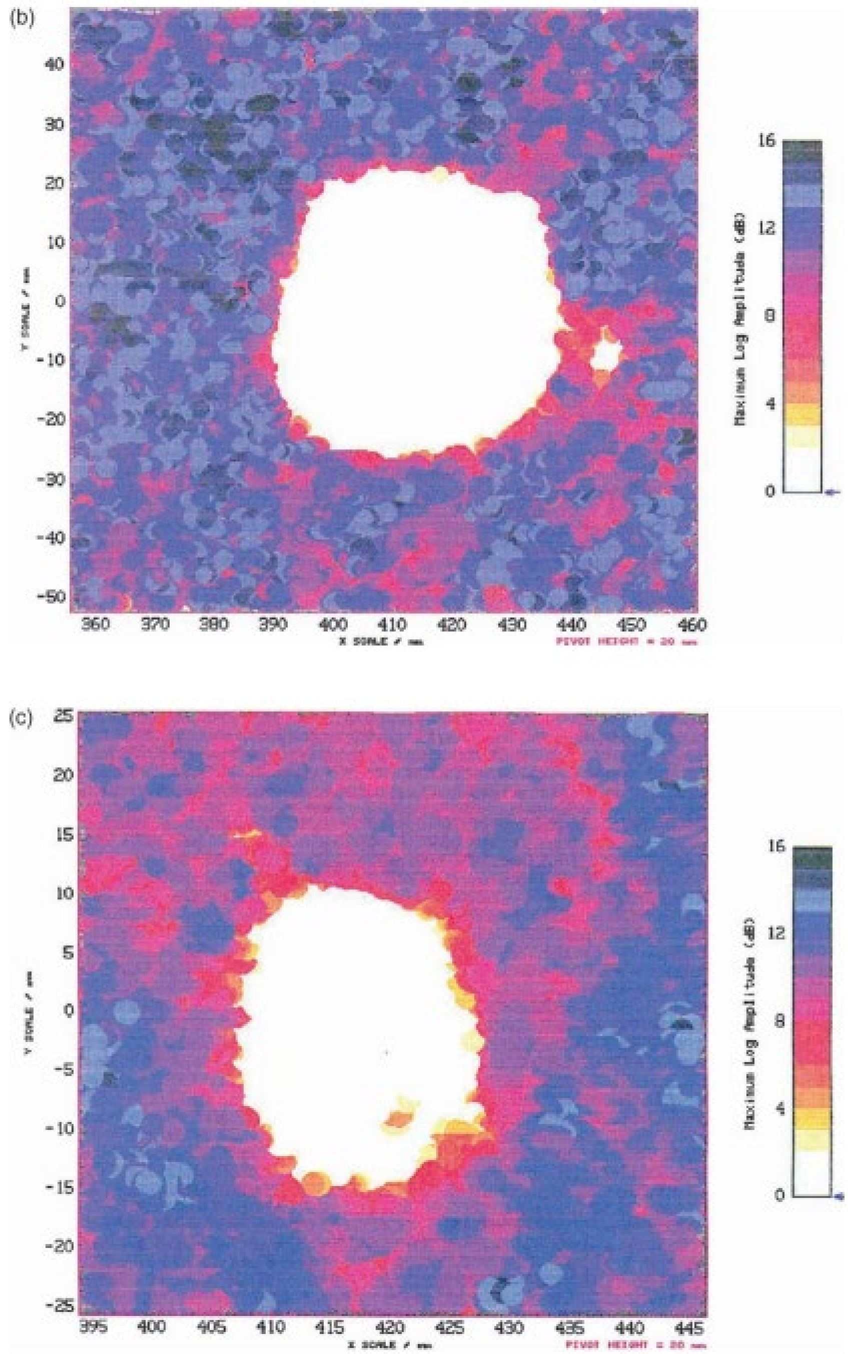

(a) Ultrasonic and visual record of damage produced by the hemispherically-nosed indenter. (b) Ultrasonic record of damage produced by a flat-nosed indenter. (c) Ultrasonic record of damage produced by the conically-nosed indenter.

Figure 32. Ultrasonic amplitude based and visual imaging of impact damage

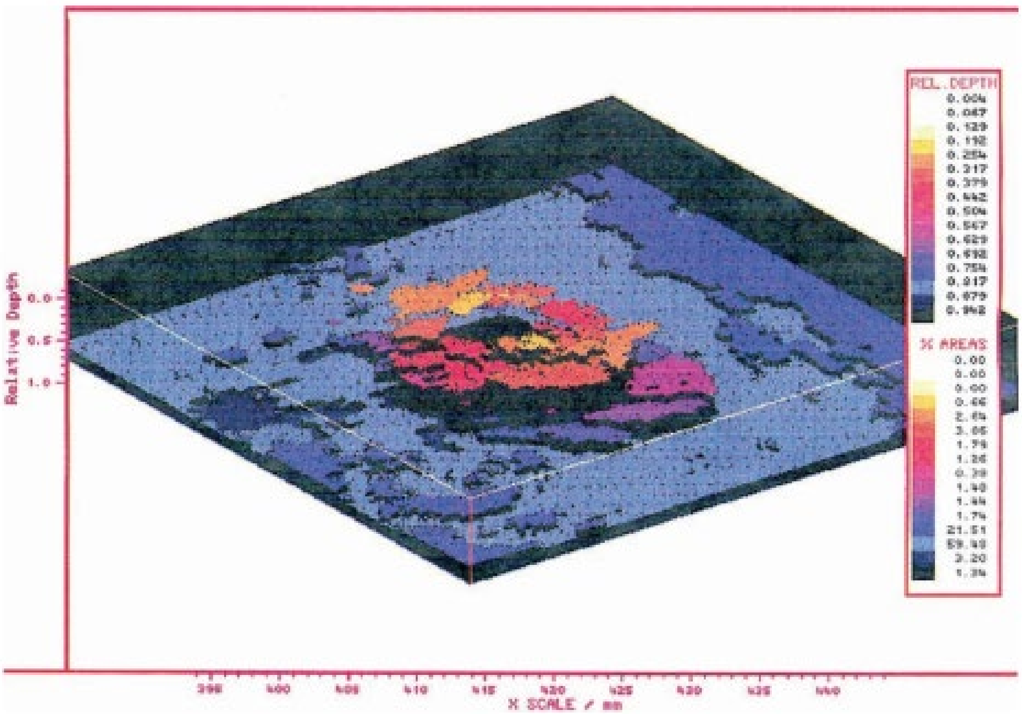

Figure 33. Time of flight based imaging of damage by a conical-nosed indenter

<u>Key Findings from Recent Research on Filament Wound Glass Reinforced Epoxy Pipe</u>

A similar ultrasonic method as described on the previous page has been used to detect and quantify lack-of-bond defects in adhesively bonded couplings.

Good agreement was achieved with the ultrasonic measurement of the lack-of-bond defects in the adhesively bonded couplings. The results have demonstrated that the ultrasonic method developed is an effective technique for the evaluation of impact damage in pipes and for the detection of lack-of-bond defects in couplings. Figure 34 illustrates the pipe coupling configuration while Figure 35 shows relative locations of buried defects between the coupling and pipe.

These results suggest similar results may be possible for inspection underneath connectors on RTP and SCP pipe.

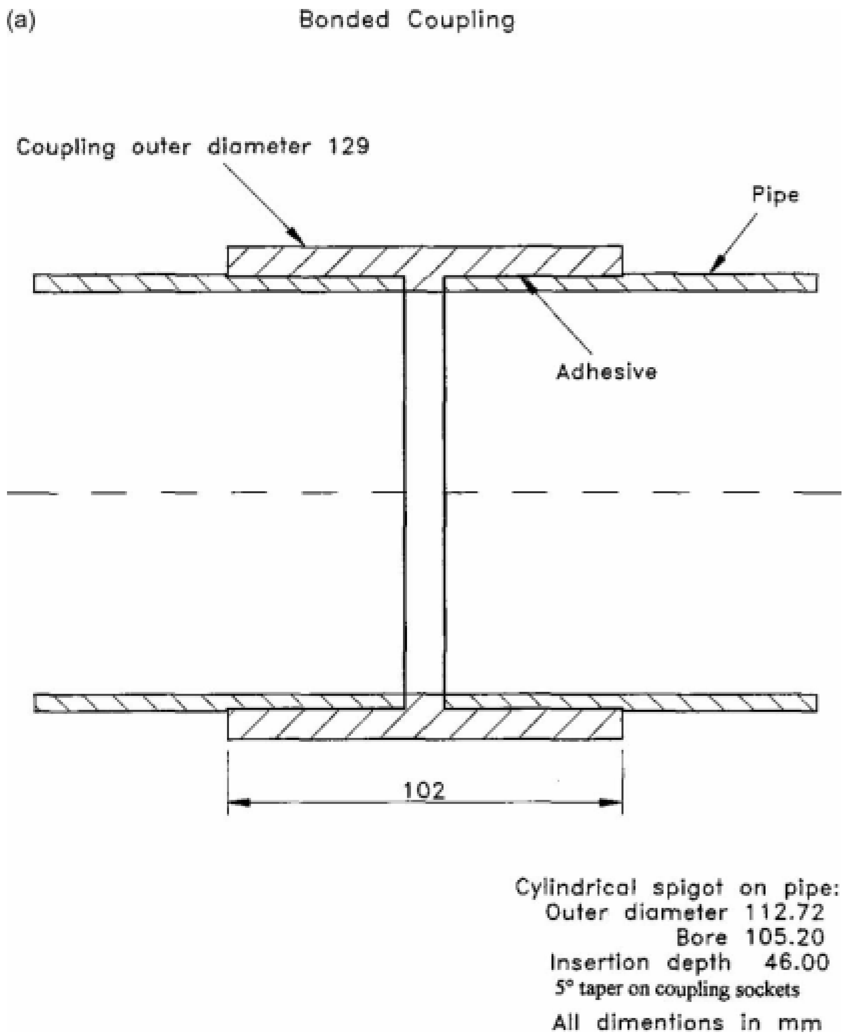

Figure 34. Schematic showing an adhesively bonded pipe coupling configuration

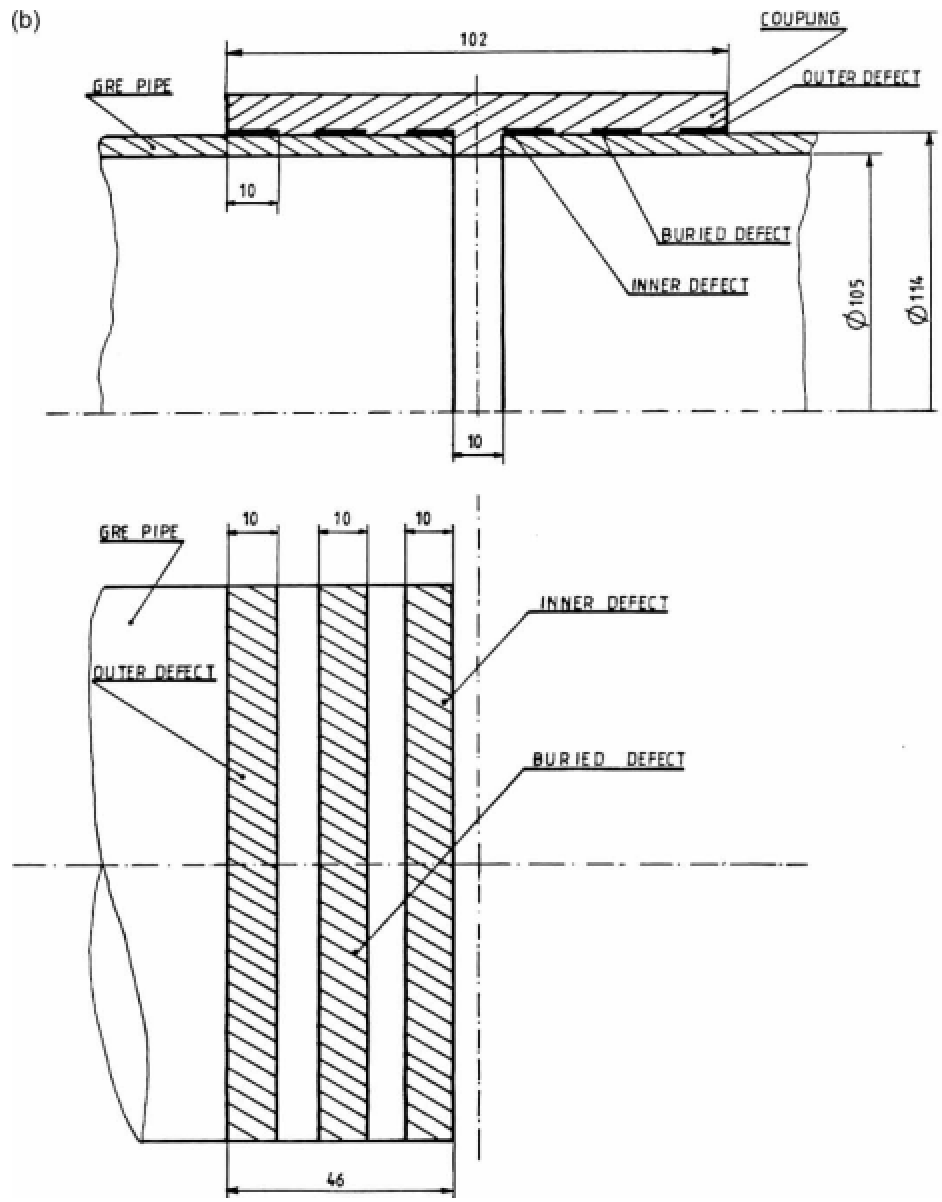

Figure 35. Schematic showing buried defects in an adhesively bonded pipe coupling

Key Findings from Recent Research on Carbon and Glass Fiber Reinforced Polymers (CFRP and GFRP)

The fatigue properties of carbon fiber reinforced polymers (CFRP) have been investigated using linear and nonlinear ultrasonic and microwave techniques as reported in Backe et al. 2012. Nonlinear ultrasonic spectroscopy is a technique with special sensitivity to incipient damage (micro-cracks, delamination etc.) and weak joints. This technique exploits the increase in nonlinearity of forces transferring ultrasound with a decrease in bond strength. The nonlinearity in sound propagation causes higher and sub-harmonic generation as well as mixing of the excitation frequencies and a shift of resonances to lower frequencies with increasing excitation amplitude. The spectra of subsequently measured ultrasonic signals will allow observation and evaluation of damage development and progress. Figure 36 shows an example setup and amplitude response for a nonlinear UT system.

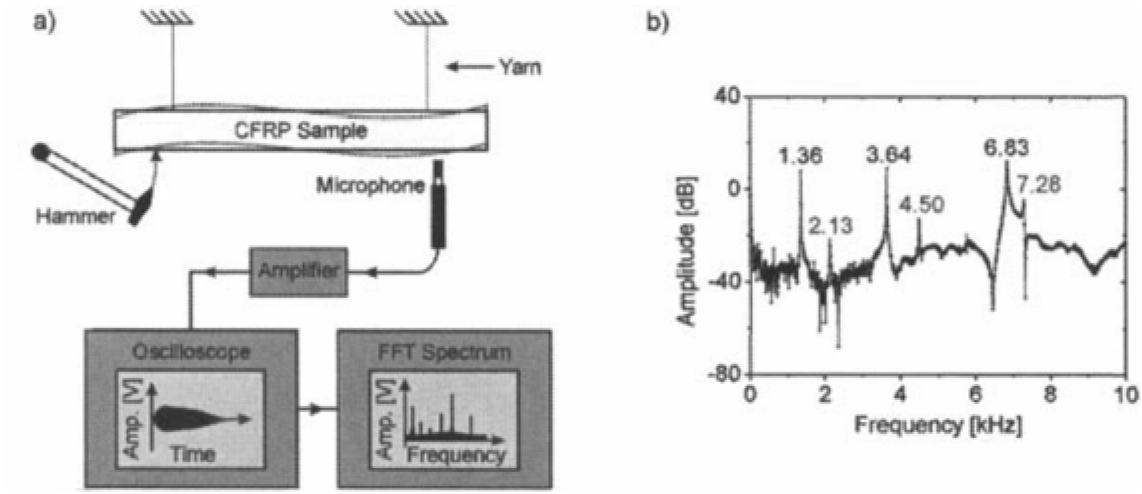

a) Schematic sketch of a sound testing system, b) FFT spectrum of the vibration of a CF-PPS sample (135.5 x 20 x 4 mm^3) indicating transverse bending (1.36, 3.64, and 6.83 kHz) and torsional (2.13, 4.5, and 7.28 kHz) resonances

Figure 36. Schematic sketch of nonlinear ultrasonic spectroscopy system

The reflection and transmission behavior of microwaves (wave lengths in the range of decimeter to millimeter) is determined by the specimen geometry and its complex permittivity. Following the basic equations of the interaction between electromagnetic waves and conducting and nonconducting (dielectric) materials (Fresnel equations), the electric conductivity determines the imaginary part of the permittivity: Decreasing conductivity increases reflection and decreases transmission of microwaves. Figure 37 illustrates the setup for a microwave reflection technique.

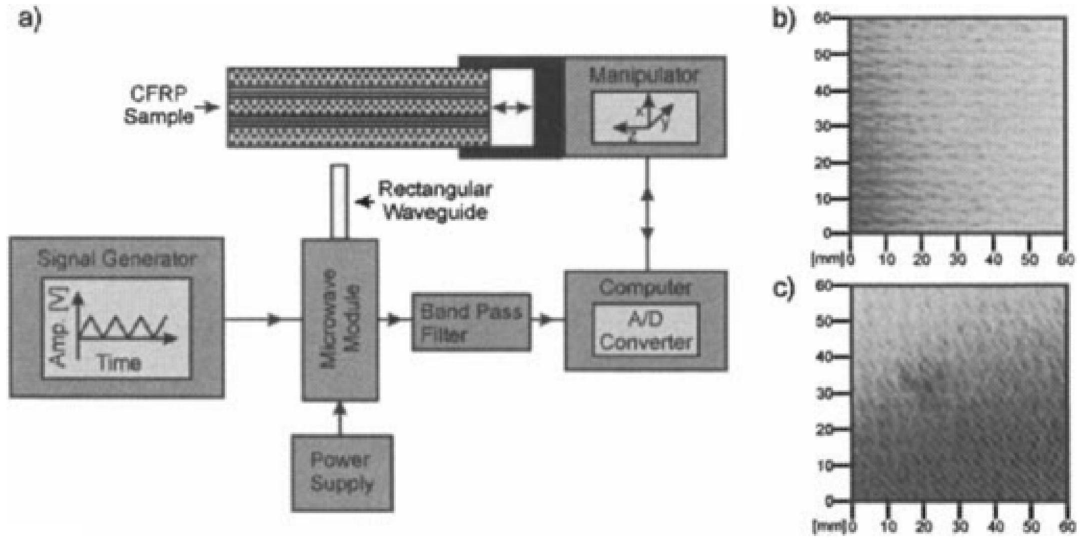

a) Microwave measurement set-up in reflection technique; results on a 3 mm thick carbon fiber reinforced epoxy plate with orthotropic fiber fabric layout (twill 2/2) and a defect induced by an impact of 31 J energy from the impact b) front side and c) back side, respectively

Figure 37. Microwave measurement set-up using reflection technique

The evaluation of impact damage in 2.5-mm thick CFRP composite structures based on fusion of results of ultrasonic testing and x-ray CT has been published in Katunin et al. 2020. In order to determine the estimation error a comparative analysis has been performed on NDT results obtained for artificially damaged carbon fiber-reinforced composite structures using two UT methods and x-ray CT. The latter method was considered here as the reference one, since it gives the best spatial resolution and estimation accuracy of internal damage among the available NDT methods. Fusing the NDT results for a set of pre-damaged composite structures with various energy values of impact and various types of impactor tips applied for introducing damage, the evaluation of estimation accuracy of UT was possible. The performed analysis provided a comparison between UT and x-ray CT NDT results and lead to a proposal of a correcting factor for UT results for impact damage in the analyzed composite structures.

Air-coupled ultrasonic testing (ACUT) has been used to estimate internal defects (e.g., inclusions, delamination, excess resin or lack of) in composite glass fiber reinforced polymer (GFRP) panels (Quattrocchi et al. 2020). ACUT has been expended as a valid alternative to overcome the strong limitation of conventional ultrasonic testing in achieving an efficient contact between the transducers and the testing surfaces. Figure 38 shows the ACUT setup.

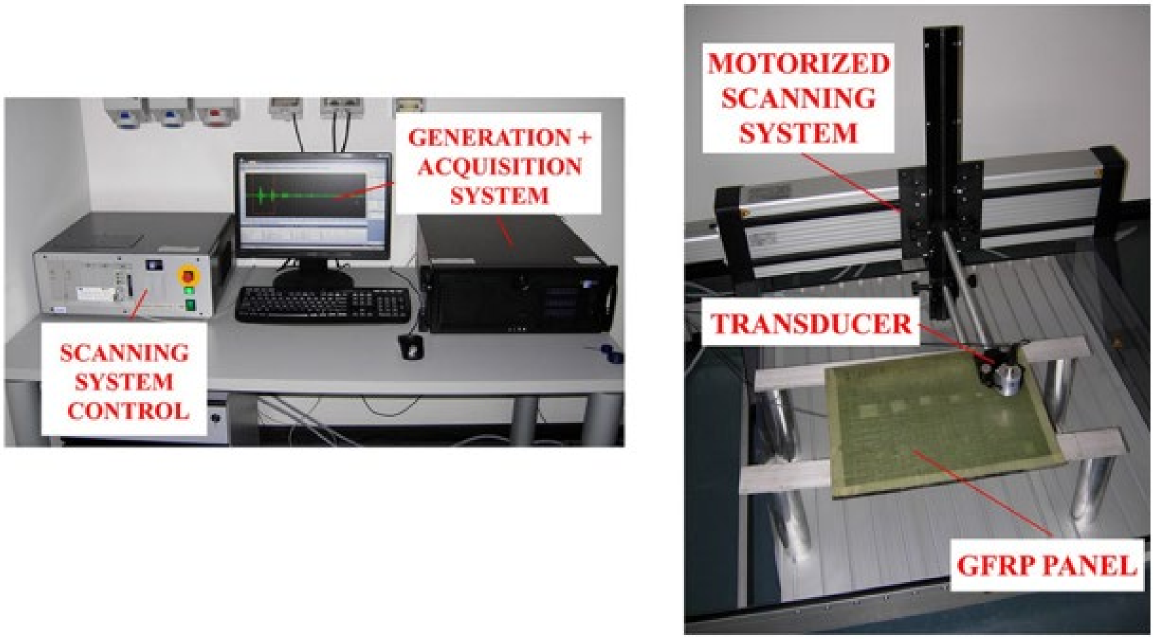

Figure 38. Air-coupled ultrasonic testing setup

Simulated delamination of different sizes was analyzed as well as excess and lack of resin. Results highlighted that a good signal-to-noise ratio can be achieved for delamination greater than 15 mm with correct defect shape recovering, hence making ACUT an appropriate choice for the interactive engineering design and manufacturing of boats. Figures 39 through Figure 42 illustrate some of the results from this study.

Based on these results, ACUT may be promising for interrogating disbonding or delaminations and damage to reinforcement layers in RTP and SCP pipe.

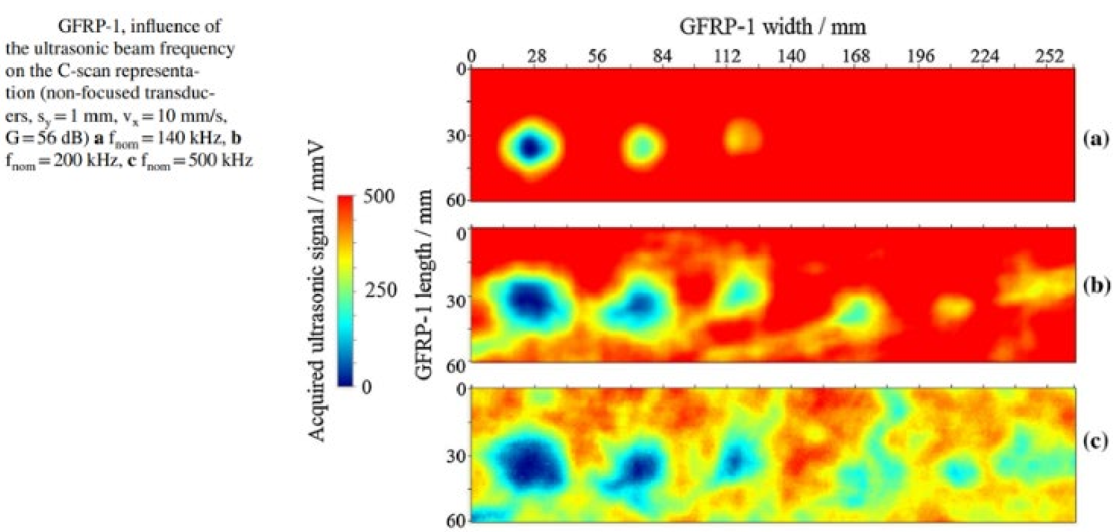

Figure 39. Influence of frequency on Air-coupled ultrasonic testing detection and imaging

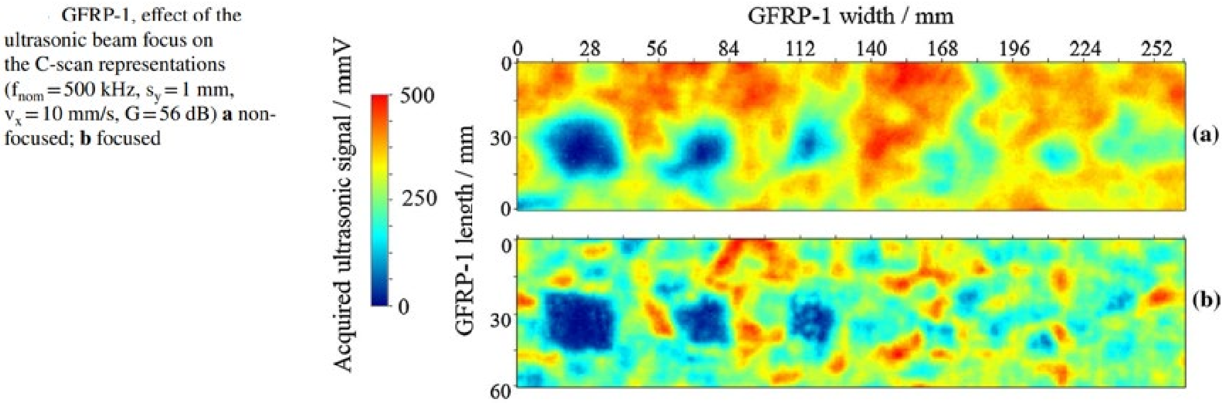

Figure 40. Effect of beam focusing on Air-coupled ultrasonic testing detection and imaging

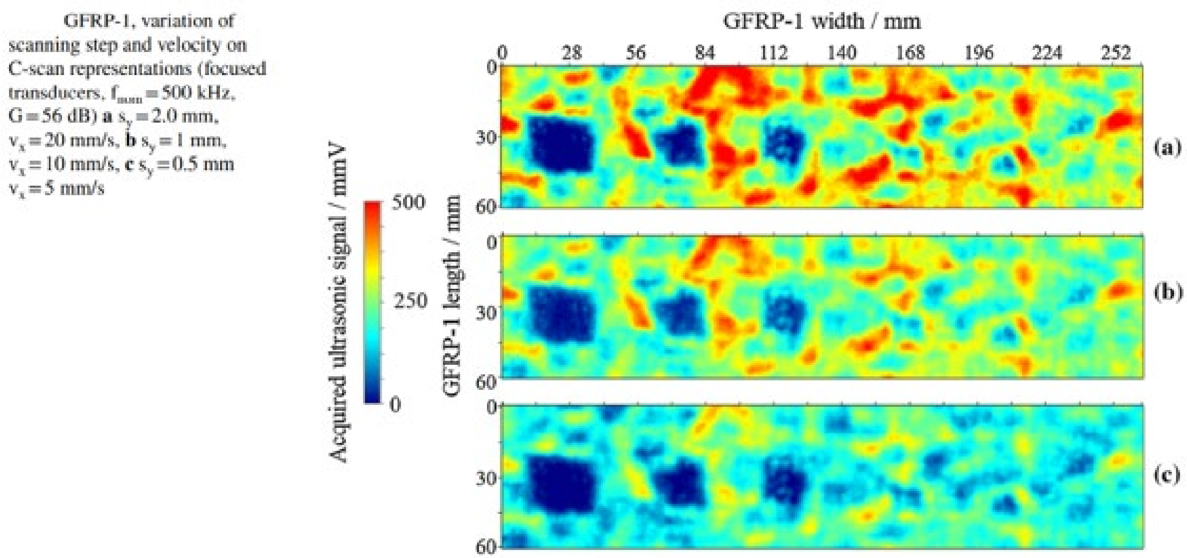

Figure 41. Effect scanning steps and speed on Air-coupled ultrasonic testing detection and imaging

GFRP-1, evaluation of the gain of the acquired ultrasonic signal on the C-scan representations (focused transducers, $f_{nom} = 500$ kHz, $s_y = 1$ mm, $v_x = 10$ mm/s) **a** G = 56 dB, **b** G = 70 dB, **c** G = 84 dB

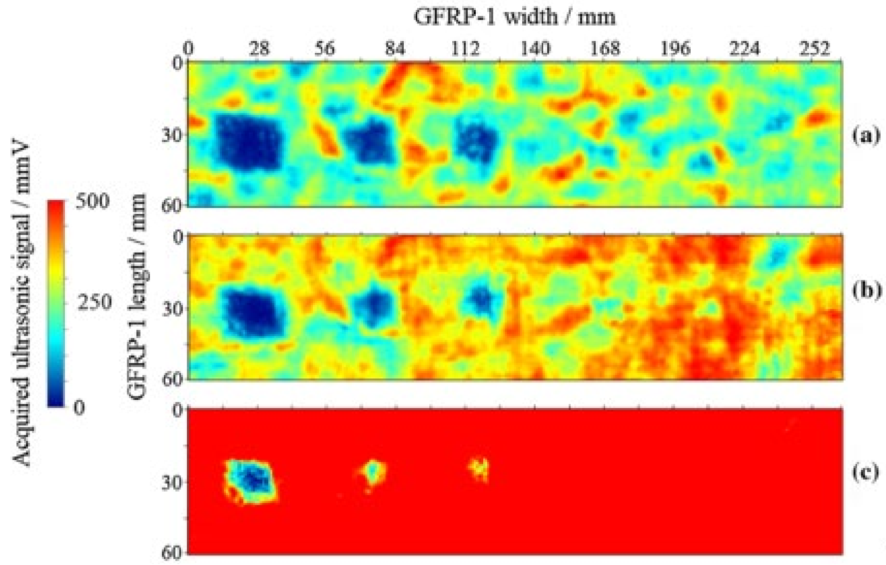

Figure 42. Effect of acquired ultrasonic signal gain on Air-coupled ultrasonic testing detection and imaging

ACUT and active infrared thermography (AIRT) have been compared by performing experimental tests on two reference glass fiber-reinforced polymer (GFRP) composite panels (10 and 2 mm thick) with synthetic defects (Quattrocchi et al. 2021). Polytetrafluoroethylene (PTFE) and aluminum inserts with different sizes and located at various depths were used as artificial defects. The relative merits and drawbacks of the two techniques were highlighted in terms of defect size sensitivity, maximum depth that can be detected, and thermo-physical properties of the reflector. Figure 43 43 (a) and (b) illustrate the inspection setup.

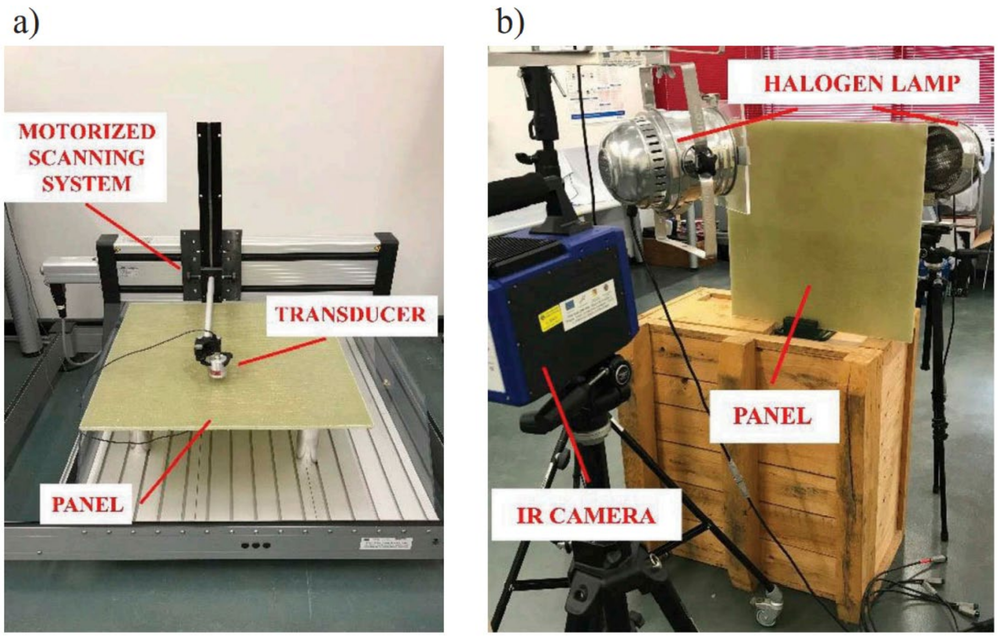

Figure 43. Images showing the experimental setup of the ACUT (a) and AIRT (b) equipment

ACUT were carried out in transmission mode using a control system (SecondWave™ M510, The Ultran Group) and two GMP™ transducers (NCG500-D25-P76, The Ultran Group), one working as a transmitter and the other as a receiver. A dedicated two-axis motorized stage was used for scanning the target surface with a defined scan rate, moving the transducers continuously along the x-axis and in a step-by-step mode along the y-axis. The control system used a tone burst coupled to a transducer with a matched frequency (narrow band). The transmitter had an active diameter of 25 mm and employed a focused ultrasonic beam. It was supplied at 375 V, with three bursts at a nominal frequency of 500 kHz. The receiver was amplified with a gain (G) of 70 dB and its output signal low pass filtered at 100 kHz and high pass filtered at 600 kHz.

The infrared thermography was carried out using a cooled IR camera (Titanium SC7600, Flir Systems Inc.), equipped with a 640 × 512 pixels InSb focal plane array detector working in the mid wave infrared radiation (MWIR) (3.6–5.1 μm) spectral band (noise equivalent differential temperature (NEdT) < 20 mK at room temperature). The IR camera was coupled to a control unit (Edevis GmbH) used for lock-in synchronization and step-heating management. Thermal stimulation was carried out by means of a 1-kW halogen lamp. Tests were performed both in transmission mode and in reflection mode. The distance between the IR camera and the target panel was set to about 100 cm for the GFRP-1 panel and to about 75 cm for the GFRP-2 one, while the halogen lamp was positioned at about 30 cm from the panel. To exploit all the spatial resolution of the IR camera, the field of view was chosen to image four defects at a time, acquiring two images for the GFRP-1 panel and four images for the GPRP-2 one. For locki-in thermography (LT), the halogen lamp was driven using a sinusoidal signal with a lock-in frequency (flock-in) between 0.01 and 1 Hz. Input powers ranged from 0.7 to 1.0 kW. Three cycles of heating, one of which was used for preconditioning, were employed. Tests were always performed at 100% power (i.e., 1 kW), heating the target surface for either 30 s (GFRP-1) or 15 s (GFRP-2). For all the IR tests, the region of interest was about 170 × 140 mm^2. Pulse thermography (PT) with flash excitation (both in transmission and in reflection mode) was also investigated, but since the results were particularly unsatisfactory, especially for the high thickness GFRP-1 panel, they will not be further discussed here.

To make a comparison between ACUT and AIRT, the resulting images were evaluated both qualitatively and quantitatively, measuring the sizes of the defects, see Figure 44 and Figure 45.

For measuring defect size, all the images were preliminary processed using a calibration procedure, consisting of a 20% increase in contrast and brightness of the raw image. Then, a segmentation algorithm was employed to define the edges of each defect and measure its size. Such an algorithm is based on a legacy filter, able to detect the defect extension by means of discrimination of the image grey levels. It works with a specific tolerance (20% threshold of the grey level) to calculate the number of consecutive pixels. A qualitative and quantitative analysis has been carried out to evaluate the ability of the two techniques in retrieving the actual size of the subsurface defects.

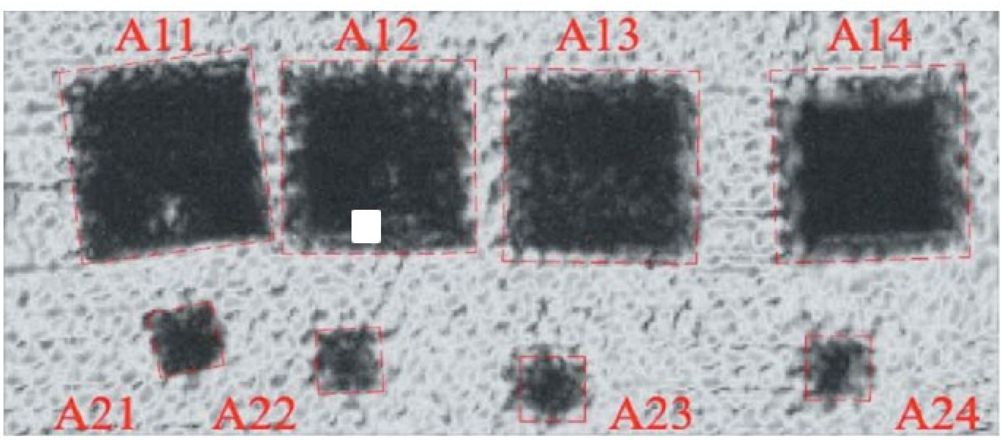

ACUT C-scan of the GFRP-1 panel, focused ultrasonic beam, f_{nom} = 500 kHz, V_x = 10 mm/s, S_y = 1 mm, G = 70 dB. The dashed lines show the actual edges of each defect.

Figure 44. ACUT imaging of GFRP panels

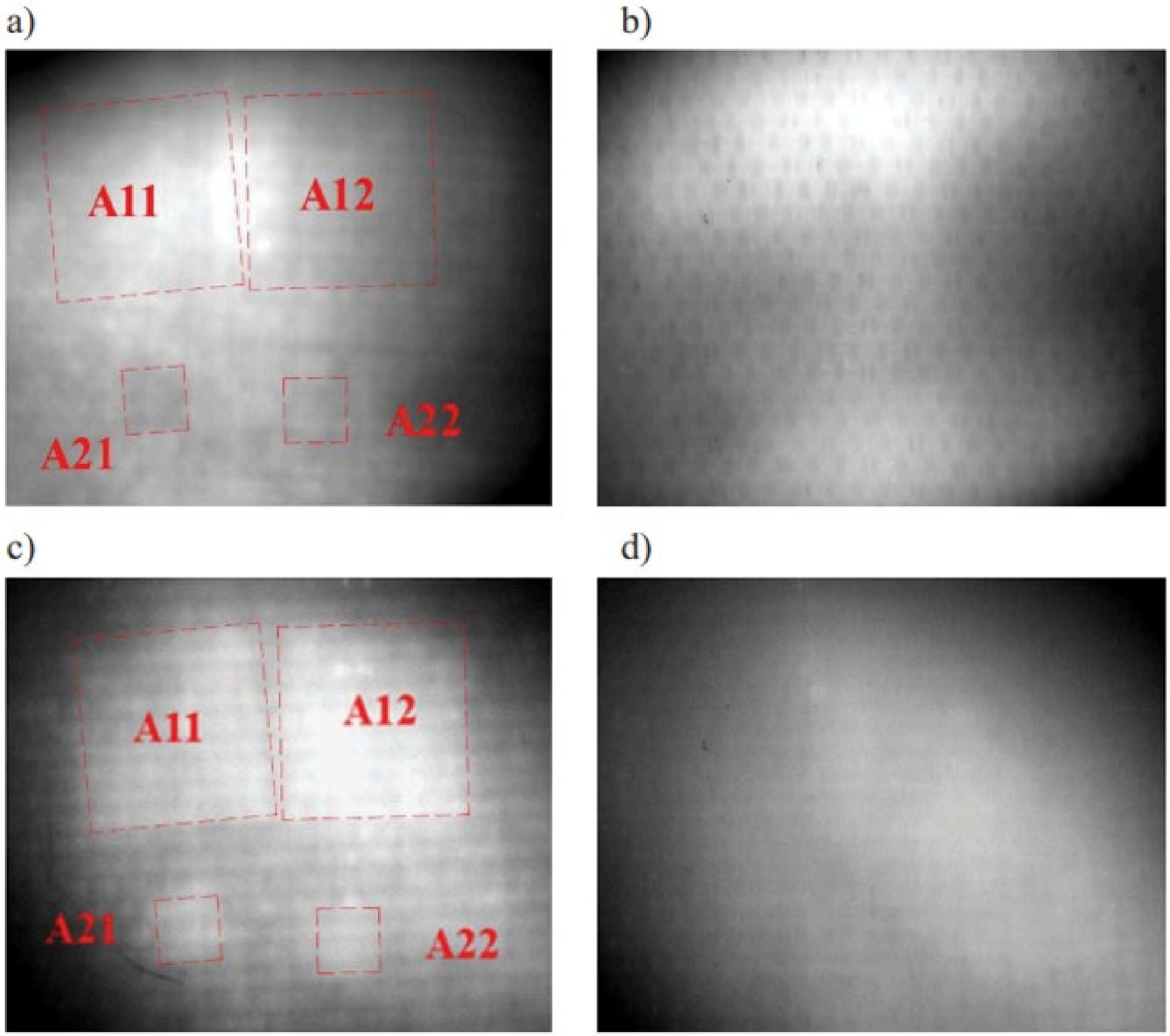

IR images of the GFRP-1 panel at the beginning of the cooling step (after 30 s of heating): (a) left part of the panel (ST, transmission mode), (b) right part of the panel (ST, transmission mode), (c) left part of the panel (ST, reflection mode), (d) right part of the panel (ST, reflection mode). The dashed lines show the actual edges of the defects.

Figure 45. IR imaging of GFRP panels

A quantitative analysis was carried out to assess the accuracy of ACUT and AIRT in recovering the actual sizes of the artificial defects. The results are summarized for two defect sizes in tabulated format for the GFRP-1 panel as shown in Figure 46. ACUT had sizing accuracy within +/- 20 percent, but with most measurements within +/- 12 percent of actual size. The scatter in ACUT sizing results were similar for both defect sizes, giving some indication of the reliability of this technique. AIRT had more scatter in sizing results, particularly in LT transmission and reflection modes.

Quantitative analysis of subsurface synthetic defects (GFRP-1 panel)

Defect	Material	Defect size [mm^2]					
		Real size	ACUT	ST transmission	ST reflection	LT transmission	LT reflection
A11	PTFE	3600	3310 (−8%)	3960 (+10%)	3370 (−6%)	3275 (−9%)	3648 (+1%)
A12		3600	3270 (−9%)	3854 (+7%)	3438 (−5%)	3050 (−15%)	3468 (−4%)
A13		3600	3170 (−12%)	-	-	2730 (−24%)	1624 (−54%)
A14		3600	2940 (−18%)	-	-	2229 (−38%)	-
A21		400	408 (+2%)	451 (+13%)	406 (+2%)	362 (−10%)	485 (+21%)
A22		400	380 (−5%)	432 (+8%)	414 (+1%)	339 (−15%)	421 (+5%)
A23		400	410 (−8%)	-	-	291 (−27%)	-
A24		400	355 (−11%)	-	-	272 (−32%)	-

Figure 46. Accuracy analysis of ACUT vs AIRT imaging

The detection of multiple artificial inclusions in filament-wound glass epoxy composite pipe using the A0 Lamb wave mode, generated and received using non-contact air-coupled ultrasonic transducers, has been studied by Padiyar and Balasubramaniam 2014. A system using the proposed Lamb wave technique has been demonstrated using the setup shown in Figure 47.

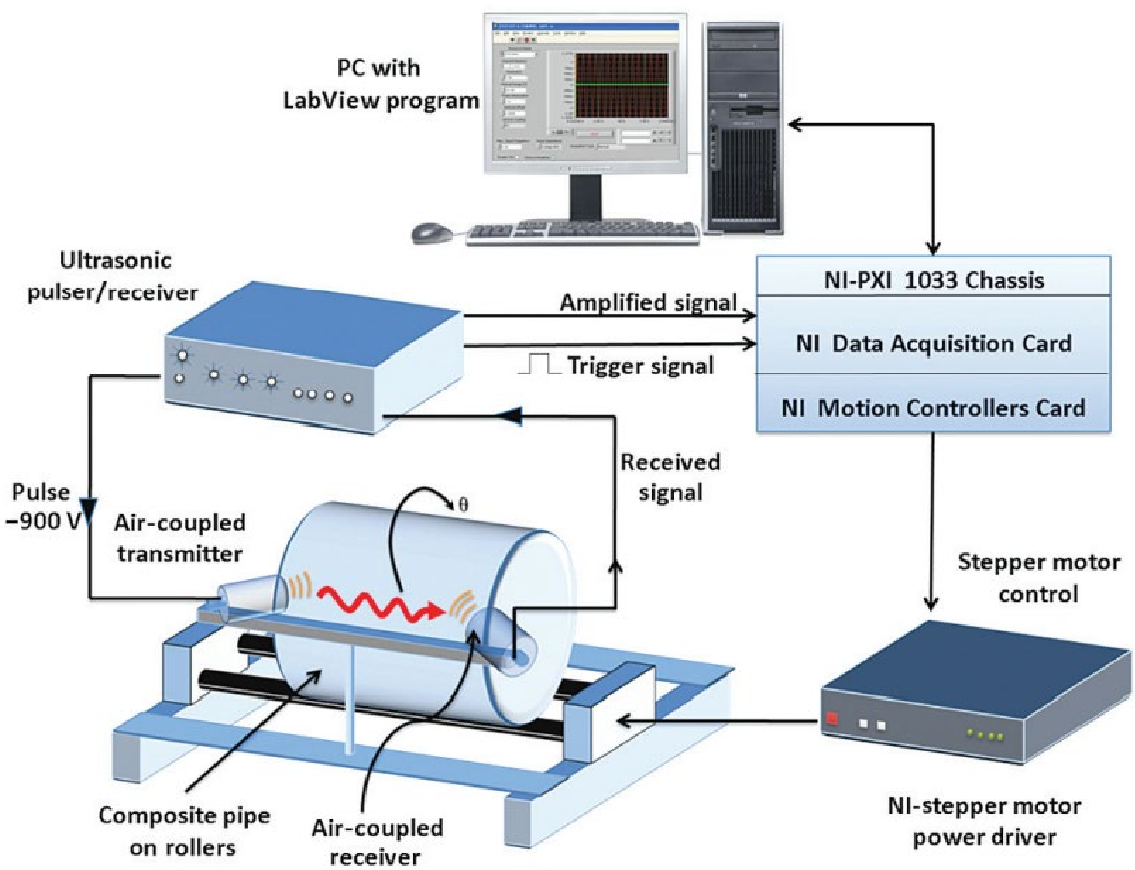

Figure 47. Lamb wave technique system

A two-step inspection technique was proposed based on this work. The first step consists of a single-sided global screening in the axial and radial directions of the pipe using the A0 mode for rapidly locating the defects. In the second step, a limited-area point-to-point air-coupled through transmission inspection for sizing the defects has been proposed. Figure 48 shows the transducer positioning approach.

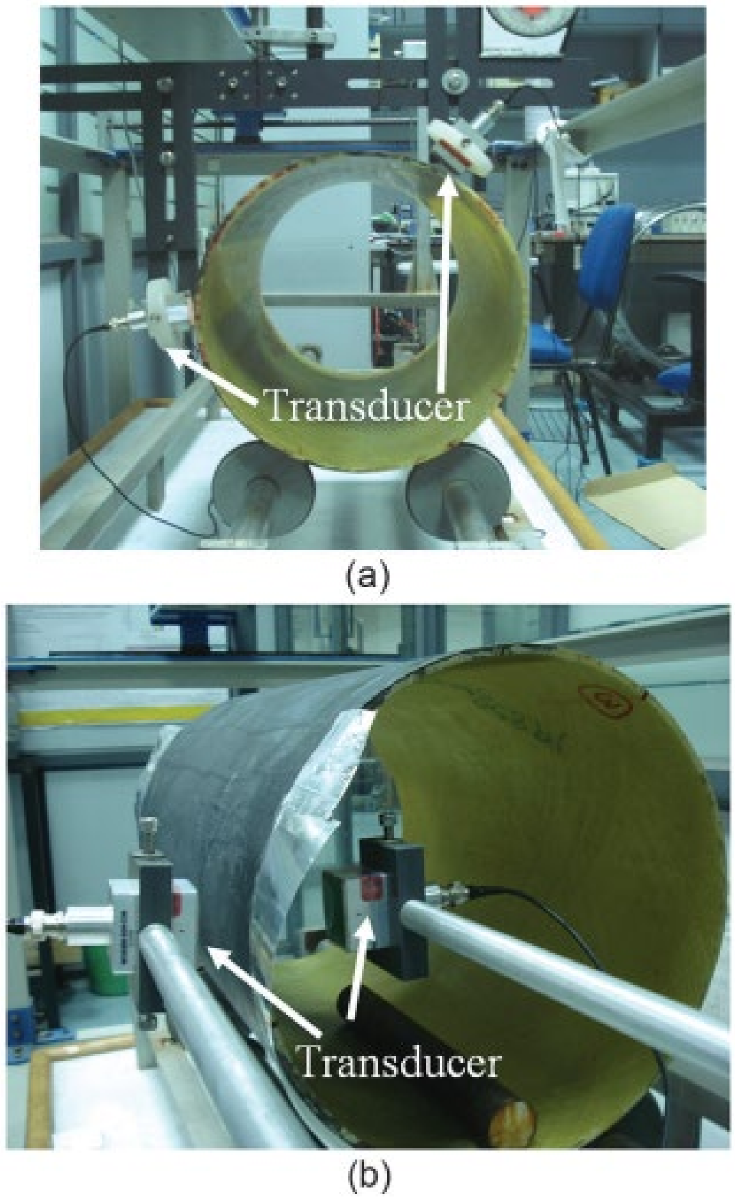

Figure 48. Air-coupled transducer configuration (a) radial (b) normal incidence through-transmission

Lamb wave-based inspections have been interpreted using a two-dimensional intensity profile (B-scans), which satisfactorily indicated the approximate locations of defective regions. Figure 49 provides examples of the Lamb wave scan results.

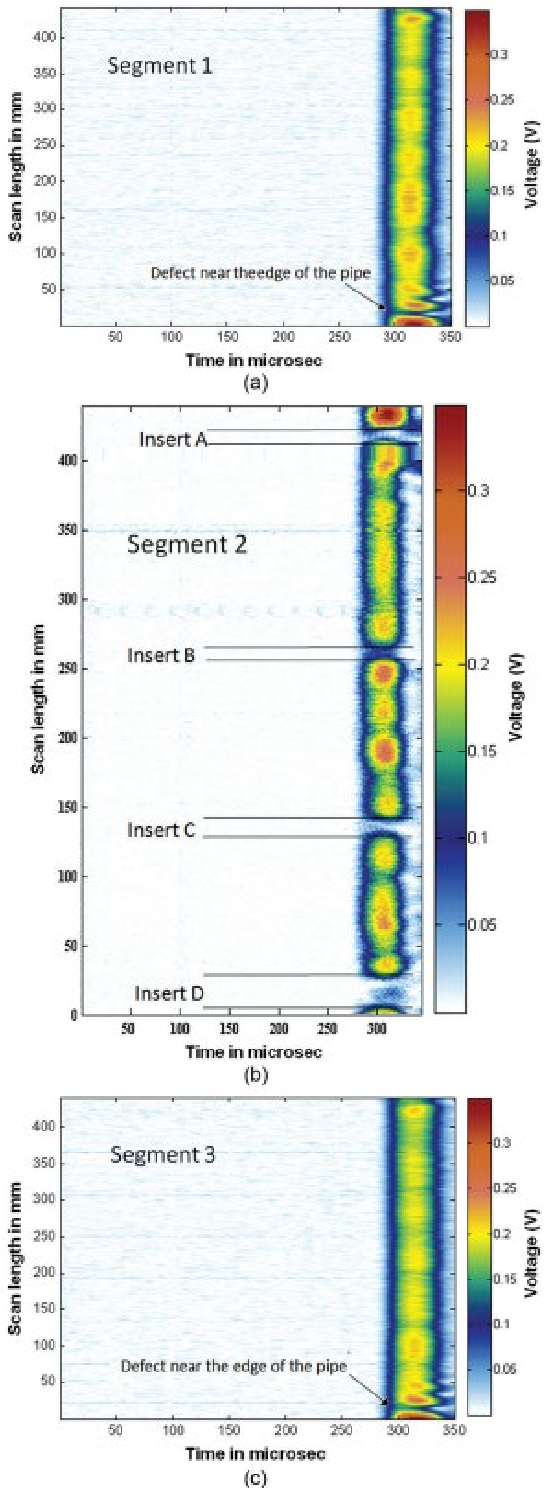

Figure 49. B-scan results (a) segment 1; (b) segment 2; (c) segment 3

A conventional immersion pulse-echo ultrasonic C-scan has been carried out on the pipe, using a 2.25-MHz immersion transducer, to validate the results from the air-coupled C-scan inspection system. See Figure 50 and Figure 51.

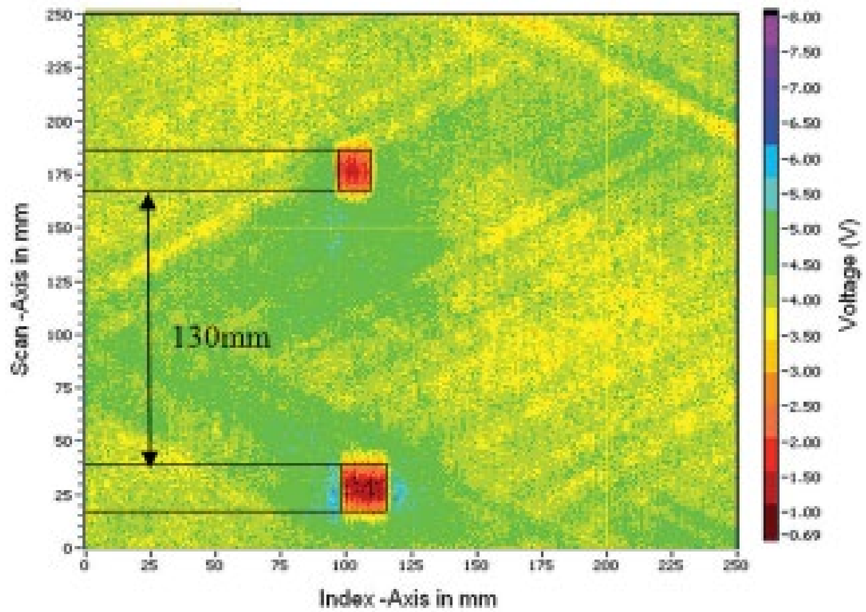

(a)

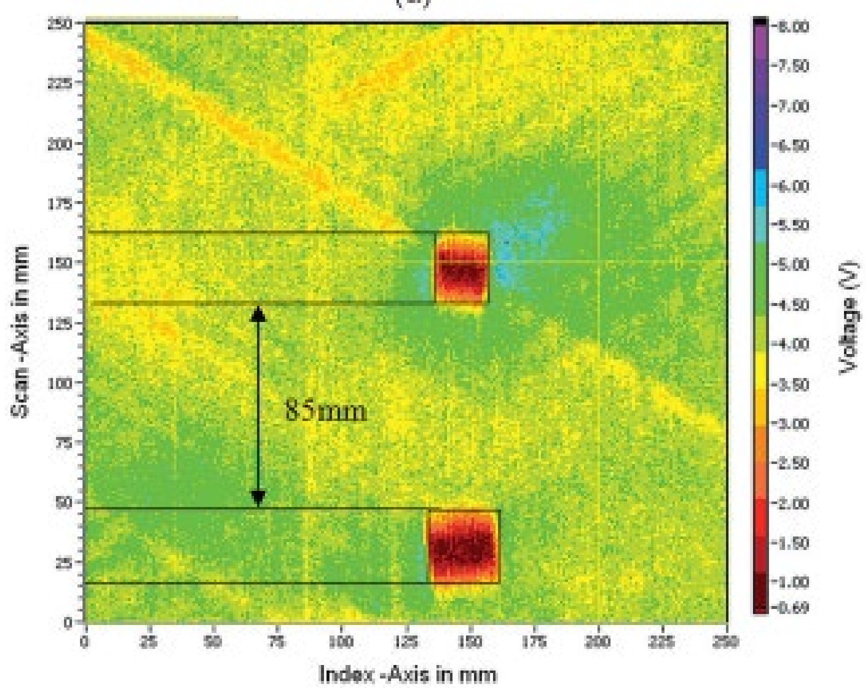

(b)

Figure 50. Normal incidence through-transmission C-scans using a 100 kHz air-coupled ultrasonic transducer (a) region 1; (b) region 2

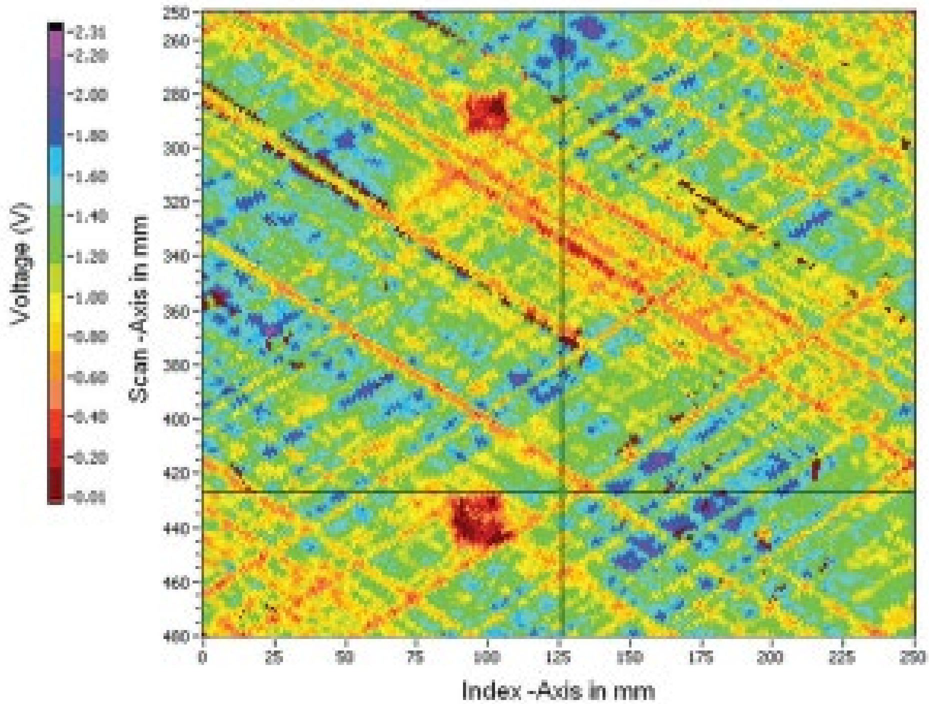

(a)

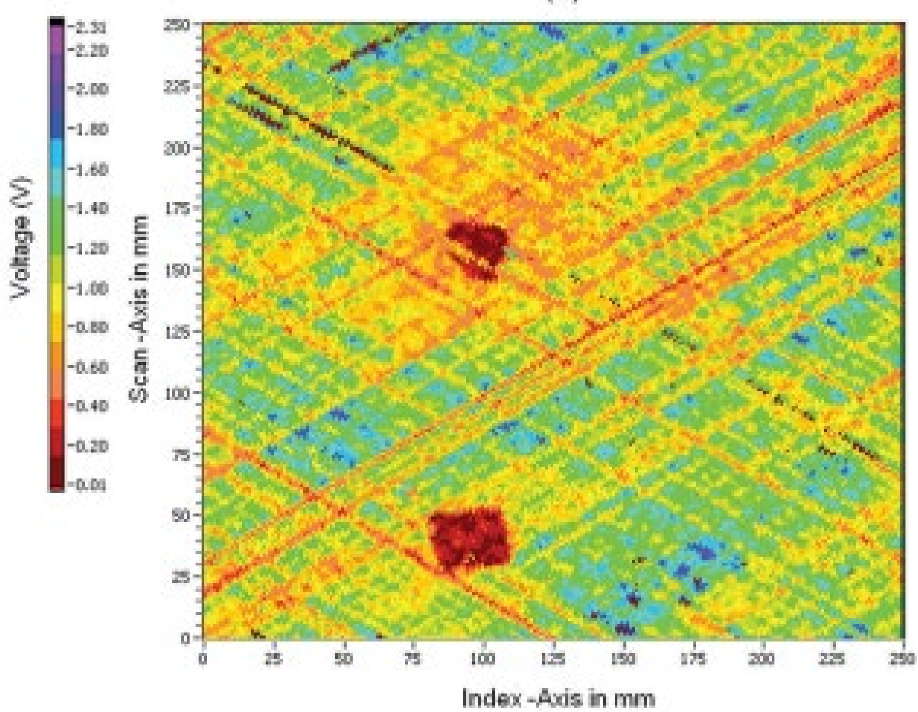

(b)

Figure 51. Pulse-echo C-scans using a 2.25-MHz immersion transducer (a) region 1; (b) region 2

The inspection techniques (ultrasonic testing (UT), radiographic testing (RT), computed radiography (CR), digital radiography (DR), infrared (IR), microwave (MW), AE- acoustic emission) for GFRP repairs in oil and gas industry were reviewed and examples presented in Soares 2022. Figure 52 shows examples of some applications that were considered. Figure 53 provides a histogram from one inspection trial giving a good correlation between AE signal amplitude and the number of features detected.

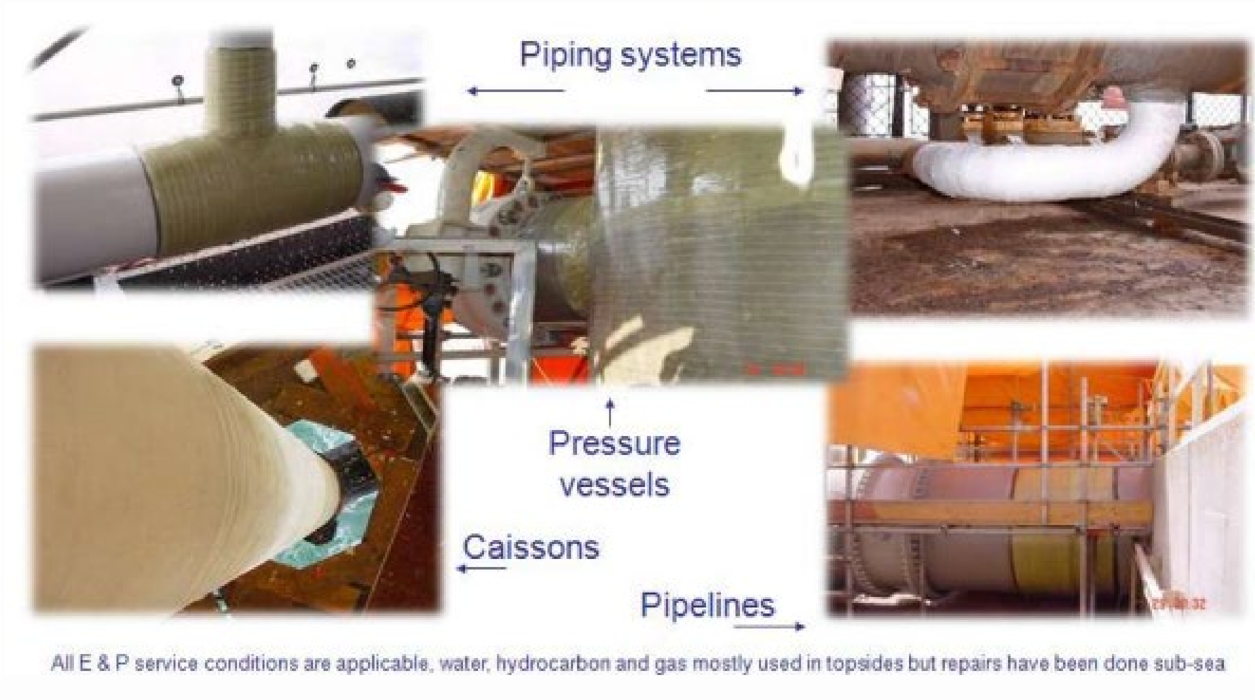

Figure 52. GFRP repair examples

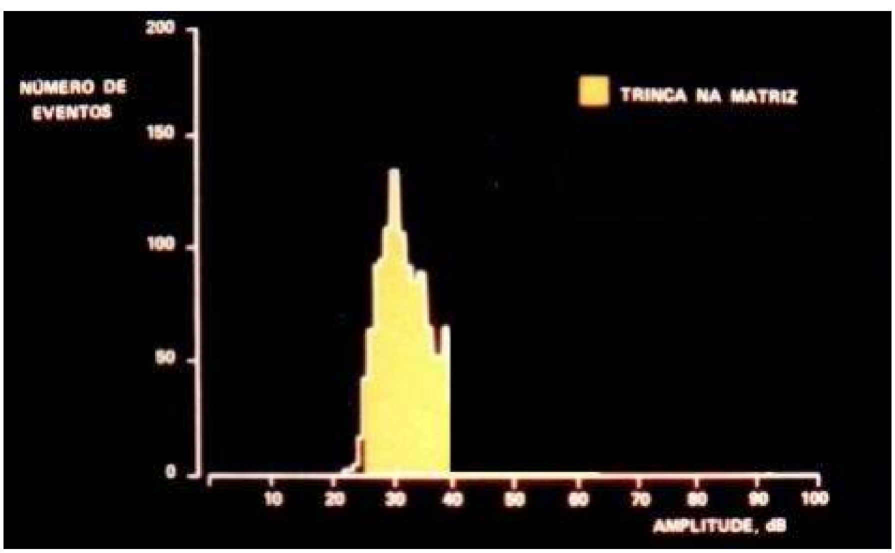

Figure 53. GFRP repair and AE inspection/monitoring showing amplitude vs number of events

Hassen et al. provided a summary of the detectability of features in glass fiber – polypropylene (PP) composites. Figure 54 identifies the type of artificial defects that were examined in this study while Figure 55 shows an example of one defect.

Defect #	Shape	Area (mm^2)	Thickness (mm)	Location in Z-direction	Defect Material
A1	Square	105.2	0.15	Between ply No. 14 and 15	Kapton
A2	Square	104.1	0.12	Between ply No. 34 and 35	Teflon
A3	Circle	172.7	2	Between ply No. 40 and 41	Steel sheet
A4	Triangle	107.8	0.12	Between ply No. 48 and 49	Teflon
A5	Square	349.1	0.6	Between ply No. 60 and 61	Aluminum sheet
A6	Fiber-waviness	N/A	N/A	Oversize cut of ply No. 68 to 80	-

Figure 54. Artificial defects examined in PP composites

Figure 55. An example of an embedded defect that also produced fiber waviness

A listing of various inspection methods and their suitability for detecting flaws in fiber reinforced PP materials is given in Figure 56 where it was shown that PAUT, one of the methods of interest in this PHMSA program, shows good promise for detecting fiber discontinuities, both in terms of shape and size. These capabilities will be important for inspection of the reinforcement layers in RTP and SCP pipe.

		NDE/T characterization method			
		Conventional X-ray	X-ray CT-scan	PA UT	TT UT
Fiber texture	2-D	X	X		X
	3-D		X		
Fiber waviness			X	X	
FOI with comparable density				X	X
Through the thickness detection			X	X	
Accurate FOI shape detection		X	X		X
Accurate FOI size detection		X	X		
In field inspection				X	X
Single sided scan				X	

Figure 56. Comparison of various NDE methods for detecting defects in fiber reinforced PP composites

Walaszek 2013 examined NDE methods for composite and metallic components. This was a broad study, but some elements have relevance to this program. One aspect is thermography of metallic components as it relates to some types of reinforcement in RTP or SCP pipe. One outcome of the Walaszek work evaluated different forms of heating for characterizing partial depth holes having differing depths and diameters in a metal plate as shown in Figure 57. The heating source was on the non-drilled surface (i.e., the surface opposite the holes).

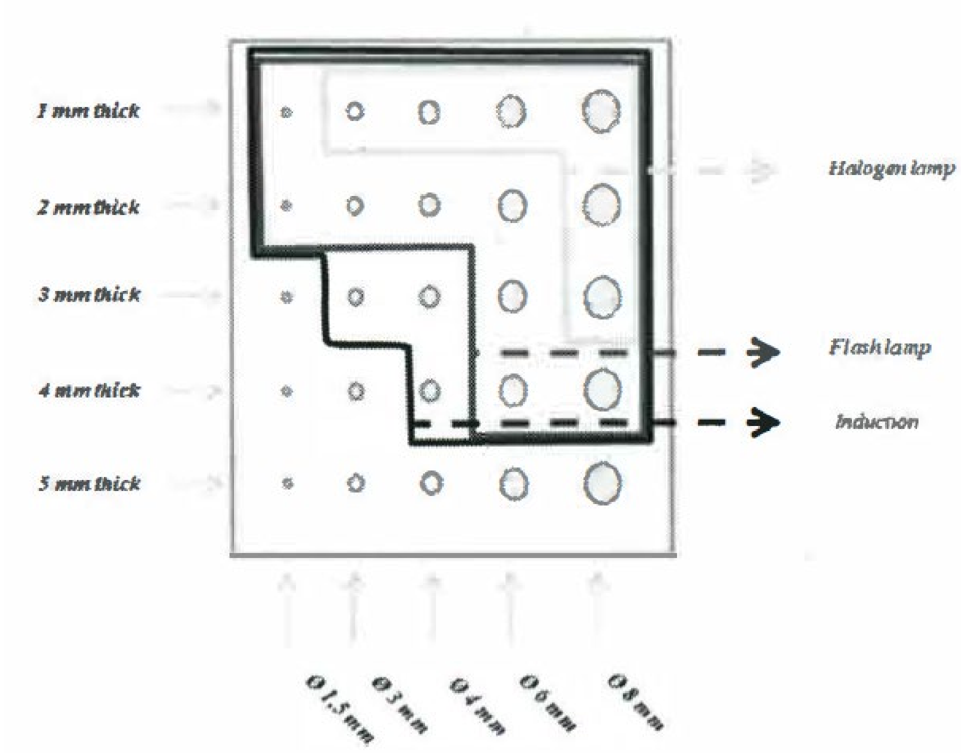

Figure 57. Thermography experiments on drilled holes in a metal plate

The results of this study were mixed as quoted by the author:

"Thermal infrared testing is very sensitive to delamination on composite parts and needs some industrial validation on metallic parts to complete the promising results obtained by CETIM. The method gives a fast and noncontact global view of the surface and subsurface material compacity. Given the novelty of the application of thermography on metallurgical products, there is no normative text on the subject as yet."

Bouteille et al. 2012 examined the effect of induction heating for active thermography inspection of steel ball joints. This study also assessed the influence of the amplitude and phase of the thermographic response and found that the phase parameter was less susceptible to inhomogeneity of heating and geometric variability of the inspected part. Fine-tuning the phase response improved flaw detection.

Meola et al. 2014 used flash thermography to evaluate porosity in carbon fiber reinforced polymers (CFRP). They found thermography viable as an alternative to UT for detection of porosity. This was effective with both unidirectional and symmetrical fiber orientation. Thermography was also found to be insensitive to surface finish, which can be a problem with UT depending on roughness. Results were validated by immersion UT and destructive sectioning.

Grosso et al. 2013 examined active thermography for inspecting adhesive joints in GFRP pipe. The samples were joined through concentric adhesive-bonds, on which some defects (lack of adhesion and lack of adhesive) were introduced in the adhesive area. Using a FLIR SC640 IR imager and external heat sources (two 1.5-kW halogen lamps or a heat blower), each sample was positioned 500 mm away from the camera-heaters set. Inspection of inner and outer surfaces of pipe were carried out to evaluate defect resolution and noise contrast limitations. It was found that if only the outer surface can be accessed, the depth of inspection had a limitation of 8 mm into the pipe wall. Furthermore, detection or resolution sensitivity decays exponentially with GFRP section thickness. Thus, for thicker pipes, it may be necessary to inspect from both the outside and inside surfaces. Obviously, for small diameter pipe, this will present limitations.

Qu et al. 2020 presented a thorough review of a variety of thermography inspection techniques as shown in Figure 58 and Figure 59. This summary suggests that there is not one single thermography technique that is likely to be suitable for inspection of all three primary layers of RTP and SCP pipe (i.e., the inner liner, reinforcement layer and outer jacket). Different thermography methods may be required to fully interrogate RTP and SCP pipes if this method were to be widely adopted. However, thermography may have good capability for inspecting a particular region of these pipes (i.e., the interface between the outer jacket and reinforcement, or the reinforcement layer itself depending on outer jacket thickness).

Method	Advantage	Disadvantage	Application
Flash	High power, high efficiency and high detection accuracy	Cumbersome volume, depth of detection	Metals, nonmetals and composites
Laser	High energy density, very uniform light intensity and high detection accuracy	Large volume, complex system and image time correction	Metals, nonmetals, composites and crackle
IR-Lamp	Wide wavelength range, stable power and portable	The depth of detection is low	Metals, nonmetals and composites
Hot air	Small size, easy to carry, cheap	The depth of detection is low and the energy is low	Less material for light absorption coefficient

Figure 58. Comparison of various pulse thermal excitation techniques

Method	Advantage	Disadvantage
Infrared Pulsed Thermography Testing	The heating mode is simple, fast detection speed and high efficiency	Not suitable for the detection of complex structural components, only for the detection of flat components. In addition, the uniformity of the heat source is very high and the detection depth is limited
Infrared Lock-in Thermography Testing	Large area for one-time detection; provide certain depth information; continuous thermal excitation modulation requires only a small amount of thermal load. Strong ability to suppress noise	For a specific defect depth, a specific frequency is required for detection, with low efficiency; the phenomenon of blind frequency, which is easy to be missed
Infrared Ultrasonic Thermography Testing	Strong penetration and high detection depth; high detection sensitivity and safe operation	Not easy to check the workpiece with complex shape, and the surface finish of the tested object is required to be high; couplant should be filled in the test piece
Infrared Laser Thermography Testing	High power density; high detection accuracy	The method of laser point heat source is limited by the small area of single detection and the longtime of detection process; the laser line scanning method requires higher signal sensitivity; the high-power laser may cause surface damage
Grating Infrared Thermal Wave Scanning Testing	Simultaneous detection of horizontal and vertical cracks; localizable detection; low requirement for sampling frequency of thermal imager	Lack of experimental verification; the existing heat sources are not satisfactory

Figure 59. Advantages and disadvantages of various thermography testing techniques

Gomathi et al. 2022 characterized internal pitting and wall-loss defects in curved GFR components using a Pulsed Thermal NDE technique. This work investigated the ability of Pulsed Thermography to estimate wall-loss defects at various depths and sizes using simulations and experimental validation. The Pulsed Thermal and UT scans imaging results were compared, and a good agreement was reported.

Haryono et al. 2018 compared microwave methods to PAUT for defect detection in glass reinforced epoxy (GRE) pipe and PVC pipe. An open-ended circular probe operating in K-band (18-26.5 GHz) was used. A series of pipe defects were examined with both techniques. The comparison was poorest in the GRE pipe where microwave methods were able to find all defects, but several were missed using PAUT.

Rahman et al. 2020 examined three different microwave probes for inspecting GRFP and HDPE pipes and compared results with PAUT and ultra-high frequency (UHF) UT. The objective was to quantify the relative sensitivity to detecting holes and notches in pipe.

The near field imaging probe for UHF consisted of a small, printed circuit board loop antenna, with images produced at 508.8 MHz. For microwave, the signal was a set frequency (24 GHz for K-band and 33.5 GHz for Ka-band) with the K-band used in a circular or rectangular wave guide. It was found that the rectangular wave guide had higher signal-to-noise ratio. The PAUT equipment consisted of a Omniscan MX2 with linear PA probe operating at frequency of 3.5 MHz (3.5L64-NW1) with 64 elements and an Aqualene wedge (SNW1-0L-AQ25).

All the external defects were detected by the PAUT. The notches and holes are evident and distinguishable. However, the internal defects were not detected.

The results are summarized in Figure 60 where it can be seen that in general the three microwave methods gave similar performance as PAUT and UHF methods, although PAUT was very slightly more sensitive overall. All the external defects were detected by the PAUT. The notches and holes are evident and distinguishable. However, the internal defects were not detected by any method.

#	Defect location	Type	Probe type			PAUT	UHF
			Ka band Rect	K band Rect	K band Cir		
1	External	Notch	√√	√√	√√	√√	√√
2	External	Notch	√√	√√	√√	√√	√√
4	External	Hole	√√	√√	√	√√	√
5	External	Hole	√√	√√	√√	√√	√
6	External	Hole	√√	√√	√√	√√	√
7	External	Hole	√	×	×	√√	√
8	External	Hole	√√	√√	√	√√	√√
9	External	Hole	√√	√√	√√	√√	√√
10	External	Hole	√√	√√	√√	√√	√√
3	Internal	Notch	×	×	×	×	×
11	Internal	Hole	×	×	×	×	×
12	Internal	Hole	×	×	×	×	×

√√ Strong indication, × no indication, √ faint indication

Figure 60. Comparison of microwave with PAUT and UHF UT in GRFP and HDPE pipe

Amineh et al. 2020 presented results for wideband microwave imaging of nested piped PVC pipes (pipe-in-pipe-in-pipe) as illustrated in Figure 61.

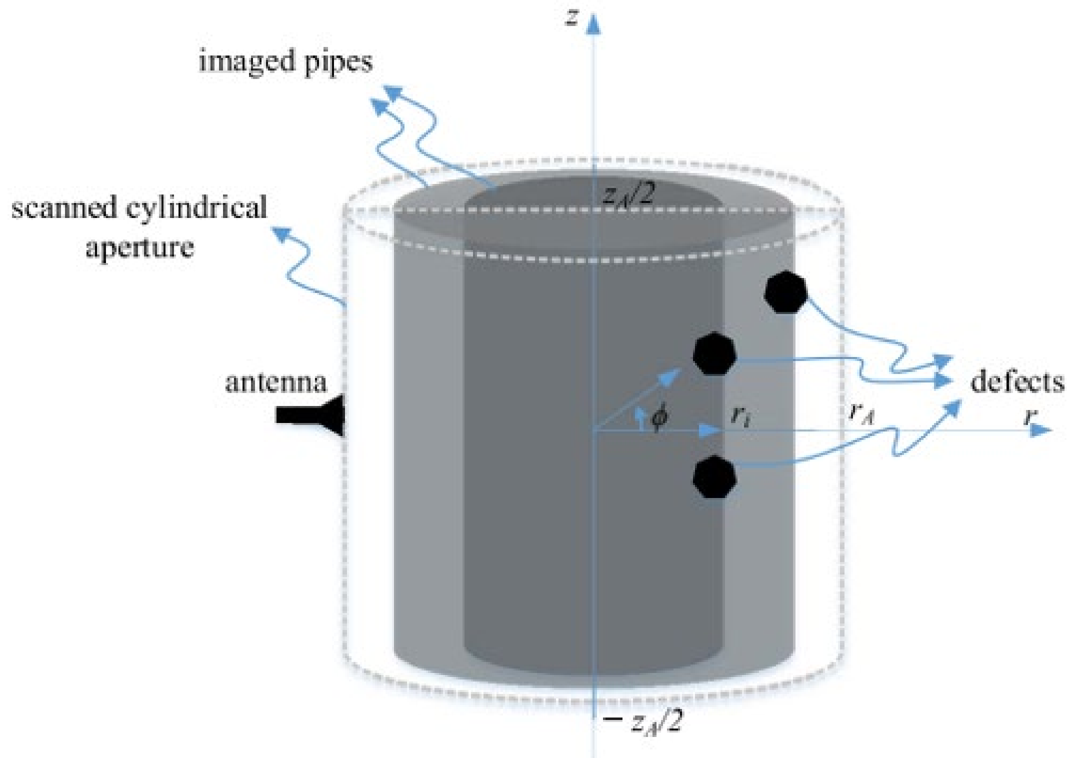

Illustration of the microwave imaging setup. An antenna scans a cylindrical aperture and the images are reconstructed over the cylindrical surfaces with radii $r = r_i$.

Figure 61. Showing the concept for nested pipe inspection

Near field microwave holographic imaging was used, which is similar to the microwave holography used in airports to screen passengers. The microwave frequencies were 6 to 14 GHz with a commercial ultrawide band (UWB) antenna from SMAKN. A complex-valued S11 parameter was measured with a Keysight E5063A vector network analyzer and an antenna positioned 1.5 mm from outer pipe.

Beamspace transformation was necessary to distinguish defects from background noise. Linear transformation was also used to suppress effects of interferences (defects on the other pipes) that are outside each specific region when processing that region. This gave increased gain in the focused area of pipe with lower gain in surrounding areas. Figure 62 provides a scan image for two nested pipes showing reasonable resolution.

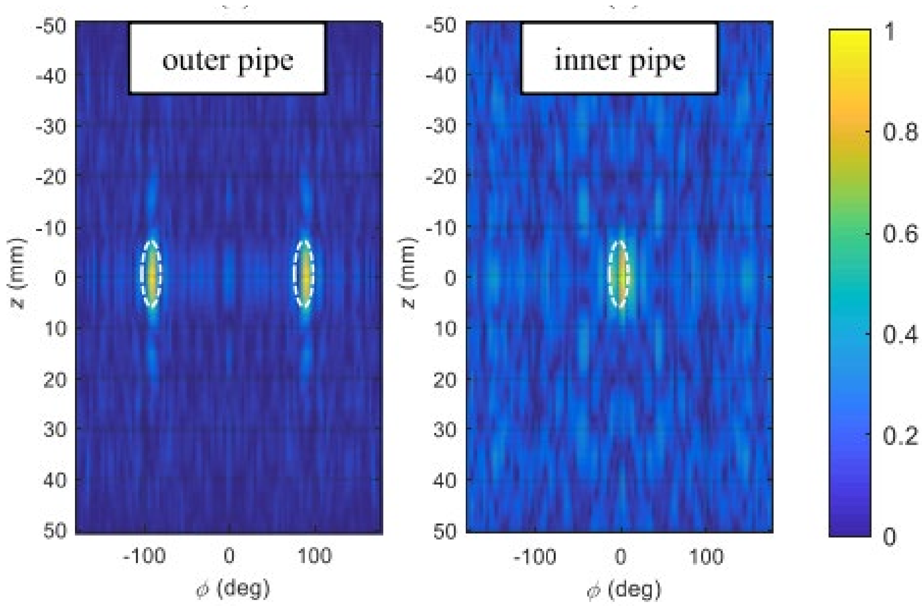

Figure 62. Wideband microwave scan for two nested PVC pipes

Sutthaweekula et al. 2019 studied a microwave open-ended waveguide for detecting and characterizing flat bottom holes (FBHs) in coated GFRP pipes. The technique used principal component analysis (PCA) and synthetic aperture radar (SAR). PCA is a statistical approach extracting principal components as a set of eigenvectors from a multivariate dataset. SAR-tomography or tomographic SAR is an imaging technique for reconstructing reflectivity profiles in the elevation (depth) by using several responses acquired with different probe positions.

The method used in this study applied PCA to decompose the sampling data into various principal components (PC) to overcome the influence of gap variation caused by pipe curvature. A K-band (18–26.5 GHz) frequency was used. It was found that long pulse tomography was not as effective at resolving FBHs. PC feature and SAR tomography can be verified and give location and size of the defect, while the depth of the FHBs is estimated from relative time-of-flight of the FHB reflected signals. Figure 63 illustrates the probe position relative to the FBH along with the physical parameters associated with pipe configurations.

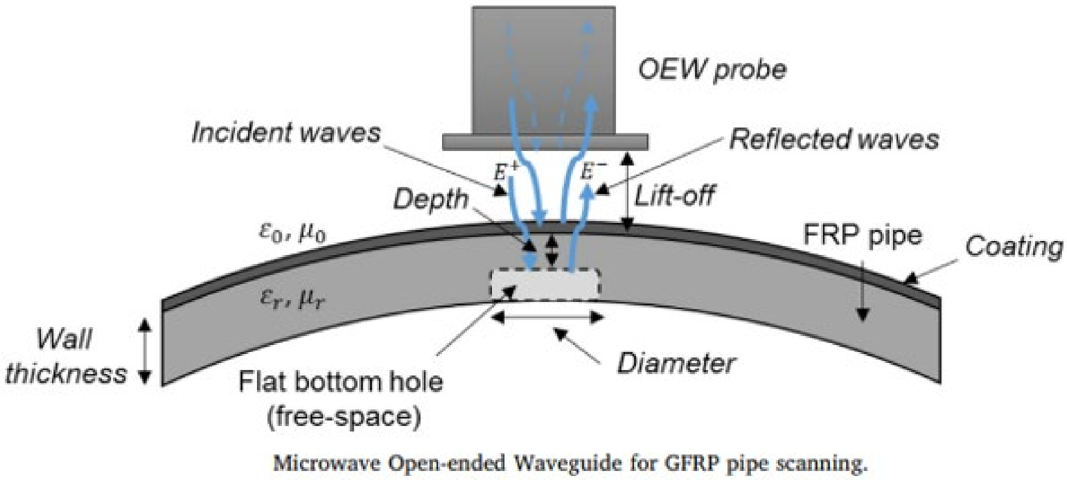

Figure 63. Setup for sizing a FBH using microwave techniques on GFRP pipe

Key Findings from Recent Research on SCP and RTP Pipe

Ultrasonic papers published in the open literature for ultrasonic inspection of SCP and RTP, bonded and unbonded, are very limited. However, the following summary provides a close correlation for inspection trials on similar pipe configurations.

An investigation of the effect of higher attenuation coefficient of polyolefin materials to the ultrasonic inspection was reported in Miao et al. 2015. The interference of a steel mesh skeleton embedded in plastic pipe reinforced by cross helically wound steel wires was considered. EF lap joints with reinforcement steel plate were tested. This type of pipe is termed plastic-steel-plastic (PSP) for an inner plastic pipe adhesively joined to a steel reinforcement layer which is adhesively bonded to an outer plastic pipe. Figure 64 shows a schematic of the pipe construction.

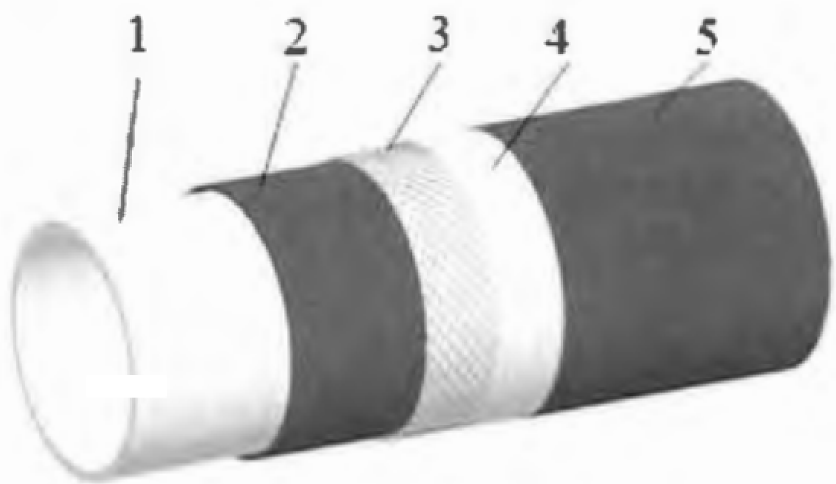

1-Ultrahigh molecular polyethylene lining layer, 2-Inner HDPE,
3- Reticulate steel wire framework, 4-Hot melt adhesive,
5-Outer HDPE

Figure 64. Structure of PSP Pipe

PAUT focused and steered beam generated by customized 2-MHz, 32-element and 4-5-MHz, 64-element probes were used for better detection of possible flaws in PSP pipe welded joints. Both 4-MHz and 2-MHz probe procedures were able to detect the electric wire while the ultrasonic waves pass through a circular hole in the steel plate, which can eliminate the interference of the steel plate. The 4-MHz probe procedure provided better imaging results. Figure 65 provides an example of linear and sector scan images.

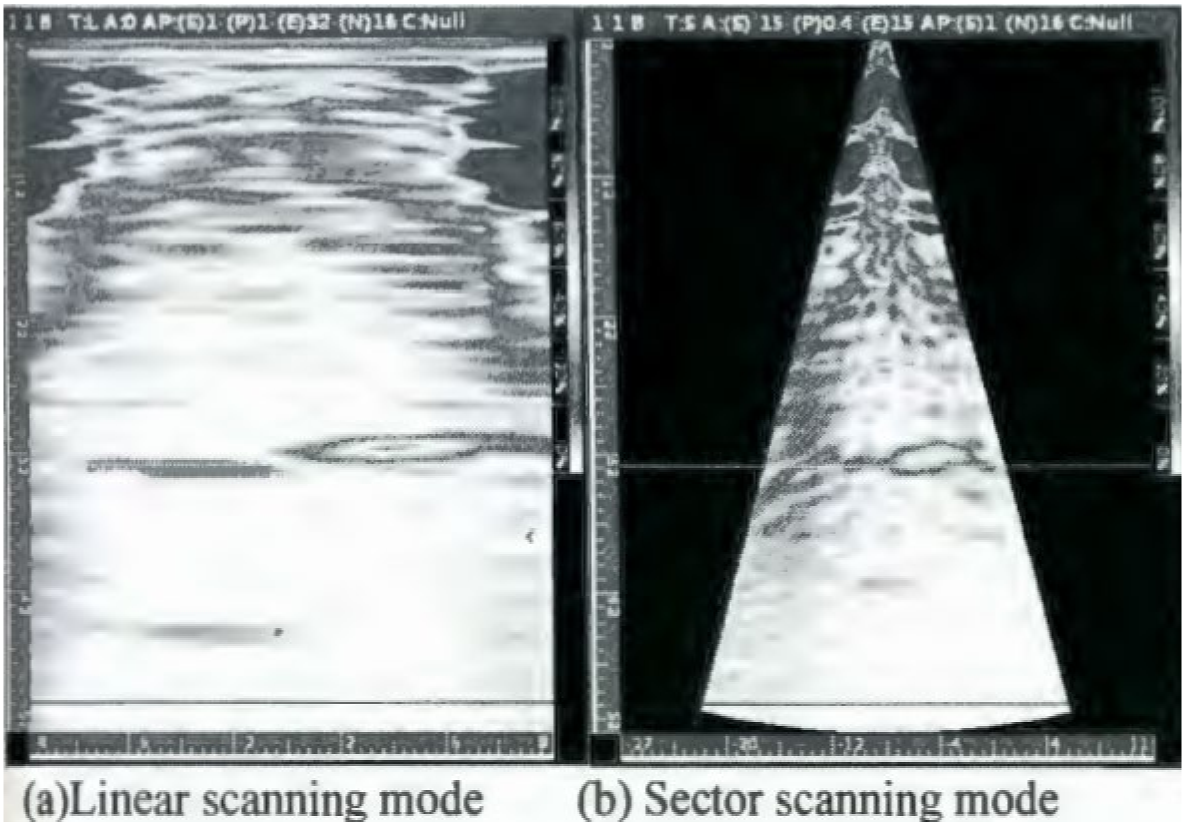

Figure 65. PAUT detection results for a 2-MHz probe used in EF joint imaging through a circular hole

7.0 Conclusions

The results of the literature review strongly indicate that there will not be just one chosen NDT method that can be used for anomaly and damage detection in SCP and RTP pipe. The multi-layered structural composition of these pipes combined with the variety of types of damage and anomalies that can occur will likely require multiple NDE methods to be used to fully interrogate and quantify damage through the entire RTP or SCP pipe system.

The use of each NDE method is associated with limitations and restrictions not only due to the material properties and geometrical constraints but also with flaw type, damage or failure mode type and location. An awareness of the nature and location of potential flaws and damage modes present in the pipe should provide some insight for selecting of the best tailored NDT solution for each scenario. It is the goal of this program to develop and validate that insight and guidance.

While limited literature exists that specifically addresses inspection of RTP and SCP pipe, some insights can be distilled from this literature search effort. The PAUT for EF joint inspection procedures developed during EWI previous project work along with other published work are promising and can be used with some optimization for inspection of bonded SCP and RTP pipe base material if the liner and structural layers are mechanically and acoustically reliably bonded. PAUT probably will be able to detect planar fabrication flaws or erosion damage as small as 1 mm. POD a90/95 = 6-10mm and 95% LUS=8-10mm may be achievable by an experienced PAUT operator. PWI is a promising new approach.

Also, the PAUT for BF and SF joints procedures developed in previous EWI projects and other published work are promising and can be used with some optimization for inspection of pipe-to-connector assemblies. Air-coupled ultrasonic testing (ACUT), active infrared thermography (AIRT) and microwave (MW) are promising techniques for unbonded SCP and RTP pipe base material where the liner and structural layers are mechanically and acoustically not reliably bonded. AE may be a promising technique for short/long term monitoring of composite repairs. Thermography shows much promise for SCP and RTP pipe inspection, but use may be limited by material thickness and composition depending on pipe wall thickness. Microwave inspection will show defect size and shape accurately, but resolution may be difficult if density of features is similar to the base material.

8.0 References

Amineh, R. K., Ravan, M., Sharma, R., Nondestructive Testing of Nonmetallic Pipes Using Wideband Microwave Measurements, IEEE TRANSACTIONS ON MICROWAVE THEORY AND TECHNIQUES, VOL. 68, NO. 5, MAY 2020

Ashton, J.N., Reid, S.R., Soden, P.D., Peng, C. and Heaton, M., 2003, “Non-destructive evaluation of impact damaged composite pipes and pipe couplings with bond line defects”, Nondestructive Testing and Evaluation, Vol. 19, No. 4, December 2003, pp. 165–186.

ASME BPVC.V-2021, Section 5, Mandatory Appendix X.

ASTM E3044-16, Standard Practice for TOFD and PAUT of Polyethylene Butt Fusion Joints.

ASTM E3170/E3170M-18, Standard Practice for Phased Array Ultrasonic Testing of Polyethylene Electrofusion Joints.

Backe, D., Balle, F., Helfen, T.B., Rabe, U., Hirsekorn, S., Sklarczyk, C., Eifler, D. and Boller, C., 2012, “Ultrasonic fatigue testing system combined with online nondestructive testing for carbon fiber reinforced composites”, Supplemental Proceedings: Volume 2: Materials Properties, Characterization, Bergman, M. and Jacobson K., 2016, Digital radiography of PE joints, Plastic Pipes (plasticpipesconference.com)

BOUTEILLE, P., LEGROS, G., MAILLARD, S., CADITH, J., BODNAR, J.L., Induction Active Thermography as an alternative to Magnetic Particle Inspection, 11th International Conference on Quantitative InfraRed Thermography, 11-14 June 2012, Naples Italy

Canada's Oil & Natural Gas Producers (CAPP), "Use of Reinforced Composite Pipe (Non-Metallic Pipelines), Best Management Practice", April 2017, J. Baron Project Services Inc., Calgary, Alberta, Canada

Caravaca, D., C. Bird and D. Kleiner, 2007, "Ultrasonic phased array inspection of electrofusion joints in polyethylene pipes", Insight Vol 49 No 2, pp 83-86.

Crawford, S., Denslow, K., Prowant, M., Moran, T., Jacob, R., Hartman, T., Neil, K. and Nove, C., 2017, "Evaluation of Ultrasonic Phased Array for Detection of Planar Flaws in High-Density Polyethylene Butt-Fusion Joints", NRC-Industry Technical Information Exchange (TIE) Public Meeting Rockville, MD, USA.

Egerton, J., 2018, "ULTRASONIC INSPECTION OF HIGHLY ATTENUATING MEDIA", A thesis submitted to the Imperial College London for the degree of Doctor of Engineering.

Gomathi, R., M. Ashok, M. Menaka and B. Venkatraman, 2022, "Characterization of Wall-Loss Defects in Curved GFRP Components using Pulsed Thermography, Materials Evaluation, Vol. 80, Number 3, pp 32-42.

Grosso, M., Marinho, C.A., Nesteruk, D.A., Rebello, J.M., Soares, S.D., Vavilov, V.P., "Evaluating quality of adhesive joints in glass-fiber plastic piping by using active thermal NDT," Proc. SPIE 8705, Thermosense: Thermal Infrared Applications XXXV, 87050T (22 May 2013); doi: 10.1117/12.2016762

HAGGLUND, F., ROBSON, M., TROUGHTON, M., SPICER, W. and PINSON, I., 2014, "A Novel Phased Array Ultrasonic Testing (PAUT) System for On-Site Inspection of Welded Joints in Plastic Pipes", National Seminar & Exhibition on Non-Destructive Evaluation, NDE 2014, Pune, December 4-6, 2014 (NDE-India 2014) Vol.20 No.6 (June 2015) - The e-Journal of Nondestructive Testing - ISSN 1435-4934 www.ndt.net/?id=17861

Haryono, A., Rahman, M., Abou-Khousa, M., "Inspection of Non-Metallic Pipes Using Microwave Non-Destructive Testing (NDT)", Proceedings of 2018 IEEE International RF and Microwave Conference

Hassen, Taheri, Vaidya, “Non-Destructive Investigation of Thermoplastic Reinforced Composites”, DOE contract DE-AC05-00OR22725

Katunin, A., Wronkowicz-Katunin, A. and Dragan, K., 2020, “Impact damage evaluation in composite structures based on fusion of results of ultrasonic testing and x-ray computed tomography”, Sensors 2020, 20, 1867.

Kim, T., Lim, H., Choi, J. and Lee J., 2016, “Application of ultrasonic NDT technique for butt fusion joints of plastic pipes”, Transactions of the Korean Nuclear Society Spring Meeting, Jeju, Korea.

Lozev, M., A. Savitski and V. Thygarajan, 2005, “Nondestructive Evaluation of Electrofusion Lap Joints in Polyethylene Pipes Using Ultrasonic Phased Array Technique”, EWI Project No. 47134CAP, Northeast Gas Association, New York, NY.

Lozev, M., and R. Spencer, 2007, “VALIDATION OF ULTRASONIC PHASED-ARRAY CAPABILITIES FOR INSPECTION OF BUTT FUSION JOINTS IN POLYETHYLENE PIPES”, IBP1161_07, Rio Pipeline Conference and Exposition.

Lozev, M., and R. Spencer, 2008, “Ultrasonic Phased Array Inspection of Polyethylene Pipe Joints, AGA OPERATING SECTION PROCEEDINGS, Phoenix, Arizona, USA.

Lozev, M., R. Spencer, P. White, E. Todorov, S. Flowers, M. St. John and N. Porter, 2008, “Define, Optimize, and Validate Detection and Sizing Capabilities of Phased-Array Ultrasonic Technique to Inspect Joints in Polyethylene Pipes”, EWI Final Report Project No. 49336GTH, Agreement No. DTPH56-06-T-0002, USDOT-PHIMSA, Washington, D.C.

(TWI, Doosan, PNL etc et al. 2008+)

MacLennan, D., J Allen, I G Pettigrew and C R Bird, 2012, “Phased Array Inspection Solution for HDPE Butt Welds”, https://www.bindt.org/downloads/NDT2012_4B5.pdf

Meola, C., and Toscano, C., “Flash Thermography to Evaluate Porosity in Carbon Fiber Reinforced Polymer (CFRPs)”, Materials 2014, 7, 1483-1501; doi:10.3390/ma7031483

Miao, X., Shi, J. and Zheng, J., 2015, “A method of ultrasonic phased array inspection of middle-high pressure Plastic pipe reinforced by cross helically wound steel wires electro-fusion joint”, Proceedings of the ASME 2015 Pressure Vessels and Piping Conference, July 19-23, 2015, Boston, Massachusetts, USA.

Murata, H., Okuda, T., and Hazama, M., 2018, “Nondestructive infrastructure measurement using microwave guided-mode propagation and reflection along fiber-reinforced plastic mortal pipe wall in underground pipeline”, IEEE Conference on Antenna Measurements and Applications.

Pan, J., Zhu, X., Tan, L., Experimental study on microwave test of cold weld defects in HDPE piping thermal fusion welds, Applied Mechanics and Materials Online, ISSN: 1662-7482, Vols. 433-435, pp 895-899, 2013, doi:10.4028/www.scientific.net/AMM.433-435.895

Padiyar, M.J. and Balasubramaniam, K., 2014,” Lamb wave-based air-coupled ultrasonic inspection technique for filament-wound composite pipes”, Insight, Vol. 56, No. 4, pp 195-202.

Pettigrew, I.G., 2014, “Advanced ultrasonic inspection of HDPE welds “, Proceedings of the Annual Offshore Technology Conference, Houston, TX, USA, pp 3259-3272.

Prowant, M. S., Denslow, K. M., Moran, T. L., Jacob, R.E., Hartman, T. S., Crawford, S. L., Mathews, R. and Neill, K. J., “EVALUATION OF ULTRASONIC PHASED-ARRAY FOR DETECTION OF PLANAR FLAWS IN HIGH-DENSITY POLYETHYLENE (HDPE) BUTT-FUSION JOINTS”, ASME 2016 Pressure Vessels and Piping Conference, PVP 2016, July 17-21, 2016, vol 6B-2016

Qin, Y., Shi, J., Zheng, J., Hou, D. and Guo, W., 2019, “An Improved Phased Array Ultrasonic Testing Technique for Thick-Wall Polyethylene Pipe Used in Nuclear Power Plant “, Journal of Pressure Vessel Technology, Vol. 141.

Qu Z., Jiang P., and Zhang, W., “Development and Application of Infrared Thermography Non-Destructive Testing Techniques”, Sensors 2020, 20, 3851; doi:10.3390/s20143851

Quattrocchi, A., Freni, F. and Montanini, R., 2020, “Air-coupled ultrasonic testing to estimate internal defects in composite panels used for boats and luxury yachts”, International Journal on Interactive Design and Manufacturing, vol. 14, pp 35–41.

Quattrocchi, A., Freni, F. and Montanini, R., 2021, “Comparison between air-coupled ultrasonic testing and active thermography for defect identification in composite materials”, NONDESTRUCTIVE TESTING AND EVALUATION, VOL. 36, NO. 1, pp 97–112.

Reverdi, F., 2020, “How to Optimize High Density Polyethylene (HDPE) Ultrasonic Inspections”, How to Optimize High Density Polyethylene (HDPE) Ultrasonic Inspections (eddyfi.com)

Rahman, M., Haryono, A., Abou-Khousa, M., “Microwave Non-destructive Evaluation of Glass Reinforced Epoxy and High Density Polyethylene Pipes”, Journal of Nondestructive Evaluation (2020) 39:26 https://doi.org/10.1007/s10921-020-00669-2

Searfass, C., Milligan, J. and Lashley, M., 2015, “Ultrasonic evaluation of inclusions and surface-breaking defects in high density polyethylene (HDPE) butt fusion and mitered joints”, Proceedings of the ASME 2015 Pressure Vessels and Piping Conference, July 19-23, 2015, Boston, Massachusetts, USA.

Sham, J., Lai, W., Chan, W., Koh, C. L., “Imaging and condition diagnosis of underground sewer liners via active and passive infrared thermography: A case study in Singapore”, Tunnelling and Underground Space Technology, 84, 2019, 440-450

Smith, C., Den Boer, P., Corley, L., 2009, “The use of TOFD for enhancement of HDPE pipe fusion inspection”, Proceedings of the 17th International Conference on Nuclear Engineering, July 12-16, 2009, Brussels, Belgium.

Soares, S., 2022, “Glass Fiber Reinforced Plastic Inspection”.

Sutthaweekula, R., Tian, G., Wang, Z., Francesco Ciampa, “Microwave open-ended waveguide for detection and characterisation of FBHs in coated GFRP pipes”, Composite Structures, Volume 225, 1 October 2019, 111080

Svetlik, H., 2019, “Ultrasonic Technology Applied to Polyethylene Pipe Butt-Fusion Joints Uses, Limits, Acceptance Criteria”, Svetlik paper (4spe.org)

Tatarov, A. and Gareau, F., 2014, “Different Failure Modes of Non-Metallic Pipelines at Connections”, Proceedings of the 2014 10th International Pipeline Conference, Paper IPC2014-33741, September 29 – October 3, 2014, Calgary, Alberta, Canada

Troughton, M., Spicer, M. and Hagglund, F., “Development of Ultrasonic Phased Array Inspection of Polyethylene Pipe Joints”, PVP 2012 Pressure Vessel and Piping Conference, Toronto, Canada, 15-19 July 2012. Paper no. 78860.

Walaszek, H., 2013, “Impact of new imaging nondestructive methods in testing and monitoring of composite and metallic components”, Proceedings of the ASME 2013 Pressure Vessels and Piping Conference, July 14-18, 2013, Paris, France.

Xiong, S., Dongsheng, H., Jinyang, Z., Investigation on acoustic propagation of ultrasound in polyethylene pipe used in nuclear power plant, ASME 2017 Pressure Vessels and Piping Conference, PVP 2017, July 16-20, 2017, vol 3A-2017

ZHENG, J., ZHANG, Y., HOU D., QIN Y., GUO W., ZHANG C. and SHI J., 2018, “A review of nondestructive examination technology for polyethylene pipe in nuclear power plant”, Front. Mech. Eng., 13(4): pp 535–545.

Zhu, Qiu, Zhong, Fu, Yang, “Active Infrared Thermography for Defect Detection of Polyethylene Pipes”, Advanced Materials Research, Vols. 1044-1045, pp 700-703, 2014

9.0 Disclaimer

EWI disclaims all warranties, express or implied, including, without limitation, any implied warranty of merchantability or fitness for a particular purpose.

Under no circumstances will EWI be liable for incidental or consequential damages, or for any other loss, damage, or expense, arising out of or in connection with the use of or inability to use the report delivered under this engagement. This report may not be reproduced or disseminated to individuals or entities outside of your organization without the prior written approval of EWI.